GENETIC AND MOLECULAR ANALYSIS OF LETHAL HYBRID RESCUE, A MAJOR-EFFECT GENE IN D. MELANOGASTER -D. SIMULANS HYBRID INCOMPATIBILITY

A Dissertation

Presented to the Faculty of the Graduate School

of Cornell University

In Partial Fulfillment of the Requirements for the Degree of

Doctor of Philosophy

by

Nicholas Joseph Brideau

May 2010

GENETIC AND MOLECULAR ANALYSIS OF LETHAL HYBRID RESCUE, A MAJOR-EFFECT GENE IN D. MELANOGASTER-D. SIMULANS HYBRID INCOMPATIBILITY

Nicholas Joseph Brideau, Ph. D.

Cornell University 2010

Post-zygotic hybrid incompatibility (HI) refers to barriers such as sterility and inviability that affect the reproductive success of zygotes from interspecies matings. Although the genetic basis for HI has been studied for decades, very few major-effect genes have been identified. Crosses between *Drosophila melanogaster* and its sibling species *D. simulans* produce incompatible hybrids. In the cross of *D. melanogaster* females to *D. simulans* males, the F1 daughters are semi-viable but sterile, and the sons are inviable. The *D. simulans* gene *Lethal hybrid rescue* (*Lhr*) was identified as contributing to these incompatibilities, on the basis that loss-of-function mutations suppress hybrid male inviability.

I have investigated several properties of *Lhr* in order to understand how it causes HI. I found that LHR physically interacts with another HI protein, Hybrid male rescue (HMR), as well as heterochromatin proteins HP1 and HP6. Furthermore, LHR directly binds to the chromo-shadow domain of HP1 through a potentially novel HP1-interacting motif. Consistent with binding to HP1, LHR localizes to heterochromatic regions of polytene chromosomes. I have discovered that the pericentric localization of LHR depends on both HP1 and HP5, and that this localization may not be critical for causing hybrid male

inviability.

It was previously reported that *Lhr* is evolving rapidly in a manner consistent with positive selection. To understand how the divergence of *Lhr* affects its functions and interactions, I investigated the properties of other *Lhr* orthologs. First, I found that the yeast two-hybrid interactions with HMR, HP1 and HP6 are conserved for six additional LHR orthologs, and despite the extensive sequence divergence among LHR orthologs, that the properties of the HP1-interacting domain are also conserved. Second, three LHR orthologs co-localize with HP1 at heterochromatic regions of polytene chromosomes when expressed in *D. melanogaster*. And finally, I also found that the ability to induce hybrid male lethality, that was previously attributed to only *D. simulans Lhr,* is conserved for *D. melanogaster Lhr*. These results demonstrate that despite the extensive sequence divergence among *Lhr* orthologs, many properties remain conserved. Overall, my work contributes to understanding the function of *Lhr* in both pure species and in hybrids.

BIOGRAPHICAL SKETCH

Nicholas Joseph Brideau was born on November 23, 1981 in Kalamazoo, Michigan to Roger and Vickie Brideau. He always had an interest in science and biology, but this interest was fostered by his parents and their decision to provide microscopes, telescopes, and greenhouse kits instead of video games. Nick graduated from Portage Central High School in 2000, and while there, further developed an interest in biology and started to learn about genetics in an AP Biology course. After high school, Nick continued to study science at the Lyman Briggs School at Michigan State University in East Lansing Michigan. He considers his participation in “LBS 145 - Cell and Molecular Biology” taught by Dr. Douglas Luckie, a big influence on his interest in both molecular biology and Apple products. While at Michigan State, Nick was active in the Pi Kappa Alpha fraternity, as well as other organizations, and was selected to serve the graduating senior class as a member of the 2004 Senior Class Council. In the fall of 2004 he moved to Ithaca, New York to attend graduate school at Cornell University in the field of Genetics and Development. Here he joined the lab of Dr. Daniel Barbash and carried out the work in this thesis. Upon completion of his dissertation, Nick continued on to a postdoctoral position in the lab of Dr. Neil Brockdorff at Oxford University in Oxford, United Kingdom.

To Papere

ACKNOWLEDGMENTS

My experience in graduate school would not be possible without the help of many people. First, I would like to thank my advisor Dr. Daniel Barbash for his support. Dan has a contagious enthusiasm for science, and has taught me how to think both critically and creatively about my work. I also appreciate his willingness to always support my ideas, and the time he spent teaching me how to become a more effective writer. My committee members, Dr. Mariana Wolfner and Dr. Michael Goldberg were also very helpful in both my Ph.D. projects, and in figuring out where to go after Cornell. I would especially like to acknowledge their guidance in helping me decide which of my projects would be the best to pursue after a frustrating year in the lab.

I would also like to thank all the members of the Barbash Lab. I appreciate that the lab was a supportive and fun environment, which is not possible without cool lab mates. I would especially like to thank Shamoni Maheshwari for critical comments and discussions about my projects, and for her friendship and the long list of everything else that goes along with being the first graduate students to join a lab. Heather Flores deserves thanks for helpful discussions, fly work, sharing gossip, and for listening to my cat stories. I would like to thank Dr. Patrick Ferree for his advice on labwork and many of life's challenges as a mentor and long-lost brother. I would also like to thank Satyaki Prasad Rajavasireddy for his ever-sunny disposition and many discussions related to *Lhr*.

Although it may seem like it, not ALL of graduate school is spent in the lab. I would very much like to thank all of my friends here in Ithaca who made my time outside of the lab so much fun. There are too many names to list

here, but in the future when I think back to my times here, I will have many good memories.

It takes a special level of understanding to support a significant other during the many ups and downs of graduate school, especially in the final few months. For her unconditional love and support I would very much like to thank my wife Dr. Chelsea Brideau. She has helped me to enjoy life outside of the lab, but she also served as a sounding board for ideas related to my projects, and even did some fly pushing for me.

And finally, I would like to acknowledge my family. It is through their support that I have been able to accomplish so many things in my life. Even now from across the country (and soon across the world), my family provides their absolute support, for which I am extremely grateful.

TABLE OF CONTENTS

LIST OF FIGURES

LIST OF TABLES

LIST OF ABBREVIATIONS

3’ UTR: 3’ untranslated region

5’ UTR: 5’ untranslated region

AA: amino acid

BESS: boundary element–associated factor 32/Su(var)3-7/Stonewall

bp: base pair

cDNA: complementary deoxyribonucleic acid

CD: chromo domain

CDS: coding sequence

CM-LEU-TRP: complete media lacking leucine and tryptophan

CM-LEU-TRP-HIS: complete media lacking leucine, tryptophan, and histidine

CPRG: chlorophenol red-β-D-galactopyranoside

CSD: chromo-shadow domain

Cy2: cyanine dye

D: Drosophila

DAPI: 4',6-diamidino-2-phenylindole

DNA: deoxyribonucleic acid

D-M: Dobzhansky-Muller

GFP: green fluorescent protein

H3K9: lysine 9 on histone H3

H3K9me2: di-methylated lysine 9 on histone H3

HI: hybrid incompatibility

HMT: histone methyl transferase

HP: heterochromatin protein

kb: kilobases

MADF: myb/SANT-like domain in Adf-1

mel-Hmr: *D. melanogaster Hmr*

mel-Lhr: *D. melanogaster Lhr*

ML: maximum likelihood

mRNA: messenger ribonucleic acid

NLS: nuclear localization signal

NPC: nuclear pore complex

ORF: open reading frame

PAML: phylogenetic analysis by maximum liklihood

PBS: phosphate buffered saline

PEV: position effect variegation

PCR: polymerase chain reaction

rDNA: ribosomal deoxynucleic acid

RFLP: restriction fragment length polymorphism

RNA: ribonucleic acid

RNAi: ribonucleic acid interference

RRX: rhodamine red-x

RT-PCR: reverse transcription-polymerase chain reaction

RFLP: restriction fragment length polymorphism

sim-Hmr: *D. simulans Hmr*

sim-Lhr : *D. simulans Lhr*

UAS: upstream activity sequence

UTR: untranslated region

WT: wild type

YFP: yellow fluorescent protein

I. INTRODUCTION

I.A. Hybrid incompatibilities in Drosophila

I.A.1 Introduction to reproductive isolation

The process of speciation has intrigued biologists for more than a century. A widely accepted definition of species is the Biological Species Concept, in which species are defined as groups of interbreeding populations that are reproductively isolated from other groups (Mayr 1963). The mechanism of reproductive isolation is divided into two categories, pre-zygotic and post-zygotic. Pre-zygotic isolation prevents the formation of a hybrid zygote between members of different populations. Forms of pre-zygotic isolation include ecological, behavioral, temporal and mechanical barriers to mating. Post-zygotic isolation occurs after members of two different species have mated and produced a zygote. Forms of post-zygotic isolation include greatly reduced fitness, sterility, and inviability of the hybrid zygote. The term Hybrid Incompatibility (HI), is often used as a blanket term for these post-zygotic isolation barriers.

I.A.2 The Dobzhansky-Muller model of hybrid incompatibility evolution

An explanation of reproductive isolation and the origin of hybrid incompatibilities even eluded Charles Darwin in his classic work *On the Origin of Species* (Darwin 1859). Darwin questioned how his theory of natural selection would cause the evolution of a maladaptive process such as hybrid sterility (Orr 1995). How does genetic incompatibility between species evolve without causing defects in the pure species? A number of years after Darwin

published *On the Origin of Species*, two *Drosophila* geneticists, Theodosius Dobzhansky (Dobzhansky 1937) and Hermann Muller (Muller 1942), independently developed a model for how hybrid incompatibilities could evolve. The Dobzhansky-Muller (D-M) model proposes that hybrid incompatibilities are a byproduct of divergence of multiple genetic loci.

To illustrate this point, a simple two-locus D-M model is shown in Figure I.A.1. This model begins with two populations with identical genotypes at two loci (*aabb*). As speciation occurs and the two populations begin to diverge, alleles at these two loci change. In population 1, *a* becomes *A* and is fixed. Likewise in population 2, *b* becomes *B* and is fixed. Therefore, the derived alleles are compatible as genotypes *AAbb* and *aaBB* in the separate species. However, when these species mate the derived alleles *A* and *B* are incompatible with each other and lead to sterility or inviability of the hybrid zygote (*AaBb*). The major assumption of this model is that the derived alleles do not cause any incompatibilities in the pure species, and are only deleterious when brought together in the hybrid background.

This simple model demonstrates how the evolution of post-zygotic isolation can be reduced to a genetic incompatibility. For this reason, most of the work to date on hybrid incompatibilities is based on the D-M model (Coyne, Orr 2004).

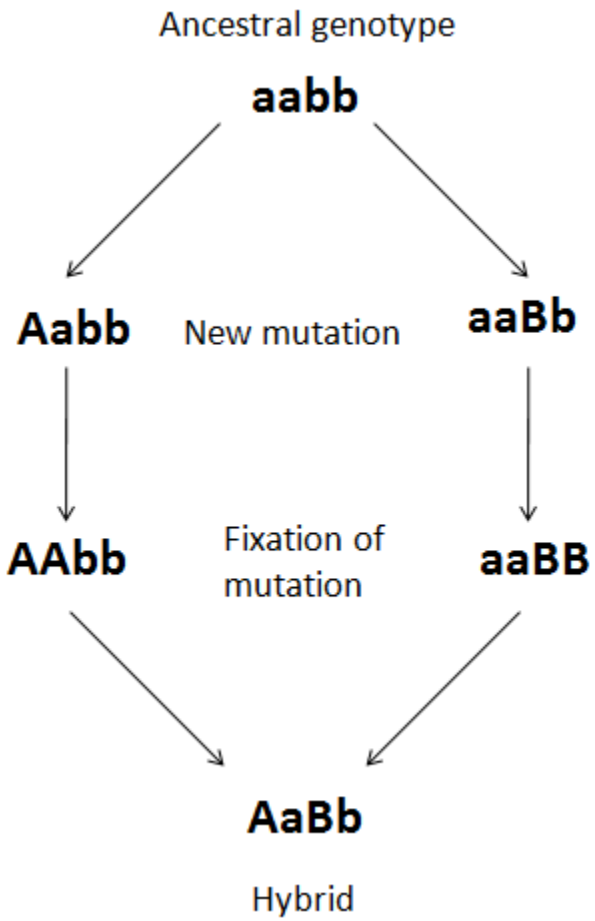

Figure I.A.1 An example of a two-locus Dobzhansky-Muller hybrid incompatibility.

I.A.3 The genetic basis of hybrid incompatibility

Although the D-M model proposes a simple genetic explanation for hybrid incompatibilities, the sterility and inviability of hybrids made classical genetic studies difficult. Early studies on identifying the genes responsible for HI in *Drosophila* relied on chromosome manipulation by mutagenesis (Pontecorvo 1943), naturally segregating mutant alleles (Watanabe 1979), or introgression (Coyne, Charlesworth 1986). Subsequently, many studies have mapped HI genes to small regions of the genome (Naveira, Fontdevila 1986; Pantazidis, Galanopoulos, Zouros 1993; Sawamura, Taira, Watanabe 1993; Hollocher, Wu 1996; True, Weir, Laurie 1996; Naisbit et al. 2002; Presgraves 2003; Tao et al. 2003; Slotman, Della Torre, Powell 2004; Moyle, Graham 2005; Masly et al. 2006; Sweigart, Fishman, Willis 2006; Good, Dean, Nachman 2008; Cattani, Presgraves 2009). Furthermore, recent advances in molecular biology and molecular genetics have allowed researchers to identify and characterize several individual genes that cause HI. Although many of these genes have been discovered in a wide variety of species including yeast (Lee et al. 2008), plants (Josefsson, Dilkes, Comai 2006; Chen et al. 2008), fish (Wittbrodt et al. 1989), and mouse (Mihola et al. 2009), for this thesis I will focus on genes identified in *Drosophila*. Because hybrid incompatibility is a collective term for both sterility and inviability, I will discuss separately the HI genes discovered in *Drosophila* that fall into these categories.

Hybrid sterility genes

Odysseus H (OdsH)

Odysseus was the first HI gene discovered in *Drosophila*, and causes sterility in the *D. simulans* background when co-introgressed with closely linked factors from *D. mauritiana* (Ting et al. 1998). The effects of *OdsH* are species specific, as the reciprocal introgression of *D. simulans OdsH* into a *D. mauritiana* background does not lead to hybrid sterility (Ting et al. 1998). The protein encoded by *OdsH* contains a homeodomain, which is a DNA binding motif characteristic of transcription factors (Hueber, Lohmann 2008). There is a high level of amino acid divergence for OdsH between *D. mauritiana* and *D. simulans*, especially within the homeodomain (Ting et al. 1998). The protein expression pattern is also divergent, as sterile introgression lines accumulate OdsH in the apical part of the testis, which is not observed in fertile or wild-type lines (Sun, Ting, Wu 2004). Both OdsH-sim and OdsH-mau associate with the repeat rich regions of the *D. simulans* X and fourth chromosome. Furthermore, unlike OdsH-sim, OdsH-mau also localizes to the *D. simulans* Y chromosome when expressed in *D. simulans* (Bayes, Malik 2009). *D. melanogaster* OdsH knockout flies have no observable defects in morphology or viability, and only have a subtle effect on male fertility (Sun, Ting, Wu 2004). The function of OdsH remains unknown, but the improper association of OdsH-mau with the *D. simulans* heterochromatic Y chromosome suggests that its effect on hybrid sterility is due to a failure in chromosome packaging (Bayes, Malik 2009).

JYAlpha

Sterility in *D. melanogaster* flies carrying the *D. simulans* fourth chromosome is caused by the transposition of the gene *JYAlpha* (Masly et al. 2006). This gene is present on the fourth chromosome of *D. melanogaster*, but on the third of *D. simulans*. When the *D.simulans* fourth chromosome is introgressed into a *D. melanogaster* background, the resulting hybrid progeny completely lack *JYAlpha*, and are sterile. *JYAlpha* is essential for sperm motility within *D. melanogaster*, and the sterility of the hybrid genotype reflects an absence of a locus that is needed for fertility. Based on molecular analysis of several *Drosophila* species, *JYAlpha* is proposed to have resided on the fourth chromosome ancestrally, and transposed to the third after the split of *D. melanogaster* from the *simulans* clade, but before the split of *D. simulans* from its sister species (Masly et al. 2006). Although *JYAlpha* shows no obvious signs of sequence divergence by positive selection between *D. melanogaster* and *D. simulans*, it represents the discovery of transposition of a gene as a cause of reproductive isolation.

Overdrive (Ovd)

Overdrive causes both male sterility and segregation distortion in F1 hybrids between the Bogota and U.S. subspecies of *Drosophila pseudoobscura* (Phadnis, Orr 2009). The sterile hybrid males contain no functional sperm, and consistent with this finding, *Ovd* is expressed in the testis of both pure subspecies males and in sterile F1 hybrid males. *Ovd* encodes a protein with a Myb/SANT-like domain in Adf-1 (MADF) DNA binding domain. Population genetic analysis revealed that rapid evolution of *Ovd* along the Bogota lineage, and the segregation distortion effects were mapped

to a single-nucleotide substitution. The dual roles of *Overdrive* in both male sterility and segregation distortion suggest that genetic conflict may be an important force in speciation (Phadnis, Orr 2009).

Hybrid inviability genes

Nucleoporin 96kDa (Nup96)

Nup96 was reported to cause inviability between *D. melanogaster* and *D. simulans* (Presgraves et al. 2003). *Nup96* was identified in a screen for recessive lethal interactions between the *D. melanogaster* X chromosome and *D.simulans* autosomes in hybrid males (Presgraves 2003). In this screen, *D. melanogaster* females heterozygous for a deficiency chromosome and a balancer chromosome were crossed to the *D. simulans* hybrid rescue line Lhr^1. This crossing scheme allows hybrid males to first be rescued by the Lhr^1 mutation. The authors then examined hybrid males for a lethal interaction between the hemizygous *D. simulans* autosome and the *D. melanogaster* X chromosome. *Nup96* was the first gene identified with this method.

Barbash (2007) further demonstrated that *Nup96* does not reduce hybrid viability by suppressing the Lhr^1 rescue effect by showing that *Nup96*-dependent lethality occurred when other hybrid rescue mutations were used to create F1 males. The NUP96 protein has a structural role in the nuclear pore complex (Belgareh et al. 2001). Additionally, population genetic analysis revealed that *Nup96* evolved by positive selection along both the *D. melanogaster* and *D. simulans* lineages (Presgraves et al. 2003). Analysis with *D. melanogaster*, *D. simulans* and the sibling species *D. sechellia* and *D. mauritiana* indicates that the genetic basis of *Nup96*-dependent lethality depends on interactions with an unknown number of additional autosomal

genes (Barbash 2007).

Nucleoporin 160kDa (Nup160)

Nup160 was identified in the same screen as *Nup96* (Presgraves 2003) and has many similar properties (Tang, Presgraves 2009). *Nup160* has also experienced adaptive evolution in both lineages. Genetic experiments prove that like *Nup96*, *Nup160* also specifically interacts with the X chromosome of *D. melanogaster* (Tang, Presgraves 2009). NUP96 and NUP160 interact directly as members of the NUP107 subcomplex, a stable component of the nuclear pore complex (NPC). It is unknown whether *Nup96* and *Nup160* form distinct two-locus incompatibilities with the *D. melanogaster* X chromosome, or if they are part of a larger multi-protein incompatibility as part of the NPC.

Hybrid male rescue (Hmr)

Hmr was the first hybrid inviability gene discovered in *Drosophila*, and causes hybrid male lethality in crosses between *D. melangaster* females and its sibling species (Hutter, Ashburner 1987; Barbash et al. 2003). Population genetic analysis revealed that *Hmr* has diverged under positive selection among *D. melanogaster,* its sibling species *D. simulans* and *D.mauritiana*, and along the lineage leading to *D. yakuba* and *D. santomea* (Barbash, Awadalla, Tarone 2004; Maheshwari, Wang, Barbash 2008) In *D.melanogaster*, *Hmr* is required for female viability and fertility (Aruna, Flores, Barbash 2009) and consistent with this requirement, *Hmr* also affects the fertility of F1 hybrid females (Barbash, Ashburner 2003). The protein encoded by *Hmr* contains four MADF domains, which are generally associated with DNA binding. The MADF domains encoded by different *Hmr* orthologs have divergent properties

consistent with binding directly to DNA or to the protein components of chromatin, suggesting that they have potentially divergent binding specificities and functions (Maheshwari, Wang, Barbash 2008). Additionally, *Hmr* has diverged in both its pure species and hybrid lethal functions. *Hmr* from *D. simulans* and *D. mauritiana* both partially complement the fertility defects caused by *Df(1)Hmr* in *D. melanogaster* (Aruna, Flores, Barbash 2009), and only *D. melanogaster Hmr* is lethal to hybrid males (Barbash, Awadalla, Tarone 2004). The relationship between *Hmr* and *Lhr*, another HI gene, is discussed later in this introduction as well as in Chapters II and IV of this thesis.

Lethal hybrid rescue (Lhr)

Lhr causes hybrid male lethality in crosses between *D. melanogaster* females and *D. simulans* males (Watanabe 1979; Brideau et al. 2006). *Lhr* is *Drosophila* specific, and population genetic analyses indicate that between *D. melanogaster* and *D. simulans Lhr* is evolving in a manner consistent with positive selection. *Lhr* encodes a small protein containing a Boundary element–associated factor 32/Su(var)3-7/Stonewall (BESS) domain, which has been shown to mediate protein-protein interactions in other *Drosophila* proteins (Bhaskar, Courey 2002). LHR interacts with HP1, and consistent with this interaction, co-localizes with HP1 at heterochromatic regions of polytene chromosomes (Brideau et al. 2006). *Lhr* is the subject of this thesis, and will be discussed at length in the remaining sections.

Zygotic hybrid rescue (Zhr)

Zhr causes embryonic lethality in F1 daughters from crosses between *D. simulans* females and *D. melanogaster* males (Sawamura, Yamamoto, Watanabe 1993). These hybrid females die due to mitotic defects induced by lagging chromatin (Ferree, Barbash 2009). *Zhr* maps to a heterochromatic region of the *D. melanogaster* X chromosome that contains the 359-bp satellite repeats (Sawamura, Yamamoto 1997). Genetic experiments have shown that the lagging chromatin consists of paternally inherited 359-bp satellite (Ferree, Barbash 2009). Because the 359-bp satellite is not present in *D. simulans*, it is proposed that the hybrid lethality is caused by *D. simulans* mothers not being able to correctly package the satellite block due to a lack or divergence of factors in the maternal cytoplasm (Ferree, Barbash 2009). The study by Ferree and Barbash is a unique demonstration of how divergence in non-coding repetitive sequences between species can directly cause HI.

Conclusions

A number of conclusions can be drawn based on this list of eight HI loci, and are summarized in Table I.A.1. The most obvious is that almost all of these loci are rapidly evolving, and interestingly, many are evolving under positive selection. Second, several of these genes have a function related to fertility in pure species. This latter point seems intuitive, as it seems that the easiest way to cause post-zygotic reproductive isolation between two species would be to disrupt part of the reproductive pathway. However, it is unclear why some of the genes with functions in fertility cause lethality in the hybrids. Third, at least half of these loci are proposed to associate with DNA, either through DNA-binding motifs, binding to chromosomal proteins, or in the case

of *Zhr,* actually being a specific DNA sequence. And finally, it has been proposed that some of these genes have acquired a new function in the hybrid background, which is consistent with predictions of the D-M model.

Table I.A.1 Summary of HI genes

	Rapidly evolving	**Fertility function**	**DNA associated**
Sterility genes			
OdsH	**X**	**X**	**X**
JYAlpha		**X**	
Ovd	**X**	**X**	**X**
Inviability genes			
Nup96	**X**		
Nup160	**X**		
Hmr	**X**	**X**	**X**
Lhr	**X**		**X**
Zhr	**X**		**X**

I.A.4 *Drosophila melanogaster* clade hybrids

The *Drosophila melanogaster* clade is composed of *D. melanogaster* and its sibling species *D. simulans, D. mauritiana,* and *D. sechellia* (Figure I.A.2). Crosses between any two sibling species yields fertile hybrid females and sterile hybrid males (Coyne, Orr 1989). In contrast, *D. melanogaster* is completely reproductively isolated from its sibling species. Matings of *D. melanogaster* mothers to sibling species fathers all produce the same hybrid incompatibility phenotype of semi-viable but sterile daughters and inviable sons (Lachaise et al. 1986). In the reciprocal cross, the F1 males are viable but sterile, and the females are inviable (Sturtevant 1920; Lachaise et al. 1986). The incompatibility of F1 males in the cross between *D. melanogaster* females and *D. simulans* males is suggested to have a different genetic basis than the incompatiblility of the corresponding F1 females (Sawamura, Yamamoto, Watanabe 1993) and each will be described separately below.

Hybrid male inviabilty

Hybrids between *D. melanogaster* and *D. simulans* were first unknowingly described as “unisexual broods” by Quackenbush (Quackenbush 1910), but this situation was later clarified by Sturtevant in his initial description of *D. simulans* as a separate species from *D. melanogaster* (Sturtevant 1920). The male progeny of *D. melanogaster* females crossed to *D. simulans* males die as larvae lacking detectable imaginal discs at the third instar stage of development, or as pseudopupae (Sturtevant 1920; Hadorn 1961; Sanchez, Dübendorfer 1983). Recent analysis of brains from hybrid males indicates a failure of most cells to enter mitosis due to a G1 or G2 cell

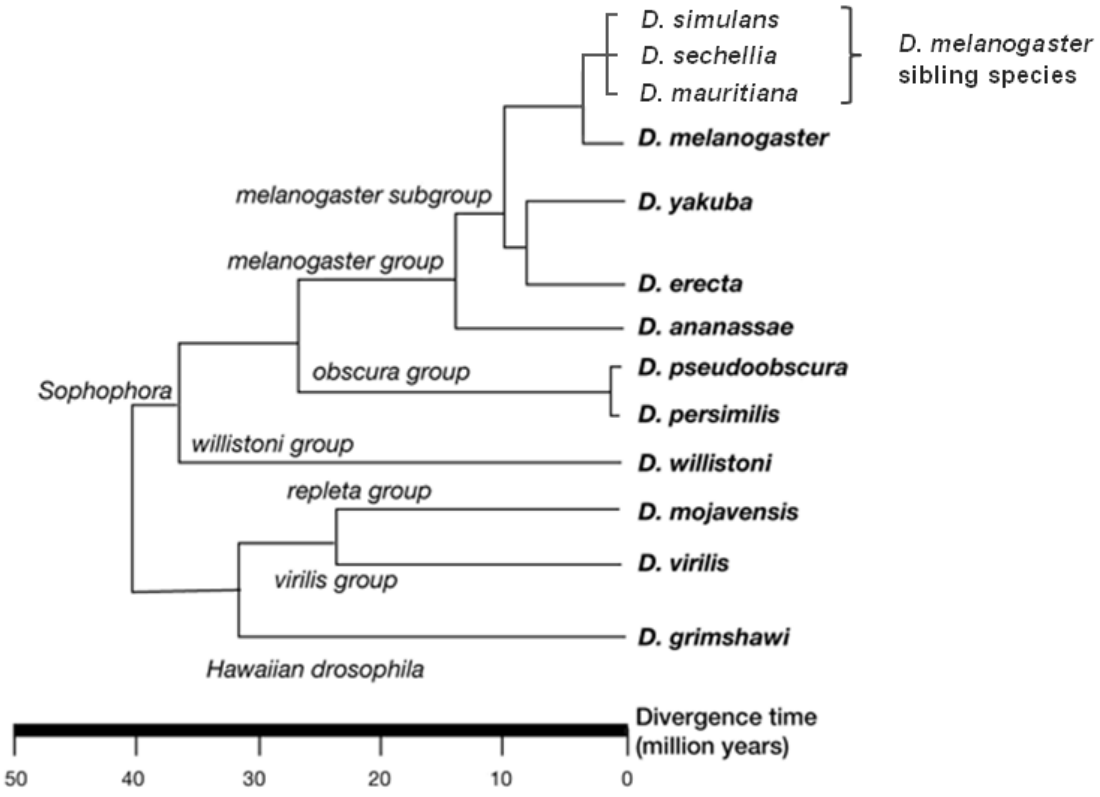

Figure I.A.2 Tree of 13 *Drosophila* species

The relationship between *D. melanogaster* and its sibling species is shown at the top, and additional *Drosophila* species are listed below. LHR from seven of the species listed will be discussed in Chapter III. Figure adapted from Flybase (Crosby et al. 2007).

cycle arrest (Bolkan et al. 2007). This finding is consistent with hybrid male larvae suffering a proliferation defect (Orr et al. 1997), which could explain their small brain size and absent imaginal discs. Additionally, temperature-shift experiments indicate that the lethal developmental defects occur in late second instar stage (Barbash, Roote, Ashburner 2000). Consistent with this result, hybrid male larvae progress slowly through the second instar stage, and many of them die during this stage (Bolkan et al. 2007).

The lethality of hybrid males is due to an incompatibility between one or more genes on the *D. melanogaster* X chromosome and one or more autosomal genes in other species (Sturtevant 1920; Pontecorvo 1943; Hutter, Roote, Ashburner 1990; Yamamoto 1992). Two of these genes have been identified, and some of this work is described in Chapter II. The X-linked *Hmr* gene in *D. melanogaster* and autosomal *Lhr* gene in *D. simulans* have been identified as major-effect genes in this lethality (Watanabe 1979; Hutter and Ashburner 1987; Barbash, Roote, Ashburner 2000; Barbash et al. 2003; Brideau et al. 2006). It has been suggested that gene regulatory differences contribute to the inviability of the hybrid males (Rifkin, Kim, White 2003; Ranz et al. 2004) however, a more recent microarray study comparing the transcriptional profiles of lethal and viable hybrids revealed only small differences between the two classes (Barbash, Lorigan 2007). Additionally, allele specific expression studies of *D. melanogaster*, *D. simulans*, and their F1 hybrids have shown that cis regulatory evolution accounts for a large proportion of differences in expression between the species (Wittkopp, Haerum, Clark 2004; Graze et al. 2009). It has also been suggested that a failure in the dosage compensation pathway contributes to the male lethality (Chatterjee et al. 2007; Rodriguez et al. 2007; Bachtrog 2008). However, the

inviability is X-chromosome specific and is not sex specific, as hybrid females homozygous for the *D. melanogaster* X also die like the males that inherit the *mel*-X (Hutter, Roote, Ashburner 1990; Barbash, Roote, Ashburner 2000; Barbash 2009). While the dosage compensation defect is unlikely to be the primary cause of hybrid lethality, recent genetic testing has shown a viability increase in hybrid crosses with dosage compensation complex mutants, suggesting a role for these proteins in male HI (Barbash 2009).

Hybrid female inviability

In his original description of *D. simulans*, Sturtevant also noted that the cross of *D. simulans* females to *D. melanogaster* males normally produces only male offspring (Sturtevant 1920). The hybrid females are embryonic lethal, and this is proposed to be due to an effect of the maternal cytoplasm (Sturtevant 1920, 1929; Pontecorvo 1943; Hutter and Ashburner 1987; Sawamura, Tiara, Watanabe 1993). In a search for mutations in *D. simulans* that rescued these hybrids from embryonic lethality, Sawamura et al mapped the factor(s) to the second chromosome and named it *maternal hybrid rescue (mhr)* (Sawamura, Taira, Watanabe 1993). Unfortunately, no additional descriptions of finer-scale mapping of *mhr* have been reported. Sawamura and colleagues also recovered a mutation in *D. melanogaster* that rescues the lethal hybrid females. This factor was located on the X chromosome *of D. melanogaster*, and was appropriately named *Zygotic hybrid rescue (Zhr)* (Sawamura, Yamamoto, Watanabe 1993). Initial mapping efforts placed *Zhr* in the pericentric heterochromatin of the X chromosome, which consists primarily of satellite DNA composed of a tandemly repeated 359-bp long monomer. Evidence has recently been reported that the 359-bp satellite block

on the *D. melanogaster* X chromosome causes this female hybrid lethality, as discussed above (Ferree, Barbash 2009). The hybrid females in this cross and the reciprocal cross are genetically similar; however the asymmetry in their viability strongly suggests a maternal effect. It has been proposed that the *D. simulans* mothers lack a factor necessary for proper packaging of the 359-bp satellite block, which causes the mitotic defects and leads to the lethality in early embryos (Ferree, Barbash 2009).

The inviability of hybrid males rather than hybrid females is the better studied of the two phenomena. Although progress has been made to better understand the genetic basis of the incompatibility, much about the mechanism remains unknown. My work in this thesis focuses on *Lhr*, one of the major contributors to hybrid male inviability.

I.B Heterochromatin in Drosophila melanogaster

I.B.1 Introduction to heterochromatin in *D. melanogaster*

Heterochromatin has been studied almost as long as *D. melanogaster-D. simulans* hybrid incompatibility, and was first described more than 80 years ago (Heitz 1928). Cytological experiments with *D. melanogaster* cells showed that the genome was organized into two domains: the lightly staining euchromatin, and the darker staining heterochromatin (Heitz 1930). Euchromatin is generally considered to be gene-rich, transposon-poor, and transcriptionally active. In contrast, heterochromatin is gene-poor, transposon-rich and transcriptionally repressive (Vermaak, Malik 2009). Many of these properties of heterochromatin stem from its compact nature. Heitz's experiments with salivary gland polytene chromosomes further compartmentalized heterochromatin into two domains, α and β. The α-heterochromatin was described as a small region in the middle of the chromocenter, which undergoes little replication, and the β-heterochromatin is the remainder of the chromocenter material more capable of replication (Heitz 1928; Weiler, Wakimoto 1995).

D. melanogaster heterochromatin has been studied extensively. In a typical *Drosophila* cell, 30-35% of the genome is organized into heterochromatic domains. This includes almost the entire Y and fourth chromosome, 40% of the X chromosome, and 25% of chromosomes 2 and 3 (Weiler, Wakimoto 1995). *D. melanogaster* heterochromatin is highly enriched in satellite DNAs and repetitive elements. It is estimated that 11 satellite sequences compose 70-80% of the heterochromatin in diploid cells. Molecularly, these simple repeats range from 100-900 kb in size, and vary in

copy number (Lohe, Roberts 1988; Le, Duricka, Karpen 1995). Despite its compact and repetitive nature, heterochromatin has important roles in many cellular processes. Although the study of heterochromatin has been relatively slow due to technical complications, much progress has been made studying *Drosophila* heterochromatin, and I will briefly summarize such work related to this thesis in the following sections.

I.B.2 Gene expression in heterochromatin

Heterochromatin is usually associated with gene repression and silencing, and this view is likely due to the "heterochromatinization" of loci not normally associated with heterochromatin that is caused by various chromosomal aberrations. The first report of this process was based on the *Bar* eye mutation. Sturtevant noted a difference in expression between two lines containing the same number of mutant *Bar* loci in different arrangements, and named this influence of arrangement "position effect" (Sturtevant 1925). A second example was described by Muller. Muller recovered several mutations of the *white* gene that resulted in a "mottled" eye color. Each of these mutations changed the location of the *white* gene on the chromosome, and this rearrangement-induced phenotype was named "variegated position effect" (Muller 1930). The basic interpretation of position effect variegation (PEV) is that a chromosomal rearrangement creates a novel junction between euchromatin and heterochromatin and induces mosaic phenotypes by silencing the normally euchromatic gene (Weiler, Wakimoto 1995). In the years following Muller's work, the *white* alleles and several other reporters have been used to study PEV extensively (for in depth reviews see: (Lewis 1950; Karpen, Spradling 1990; Weiler, Wakimoto 1995; Zhimulev 1998;

Farkas, Leibovitch, Elgin 2000; Schulze, Wallrath 2007). Some genes reside in heterochromatin despite the repressive effects of heterochromatin on a euchromatic gene. At least 40 heterochromatic loci have been identified in *D. melanogaster* (Gatti, Pimpinelli 1992). Some of these loci are repetitive in nature such as the 18 and 28S rDNAs, while others like *rolled* and *light* have repetitive DNAs located near or within the coding region, and require a heterochromatic environment for proper expression (Devlin, Bingham, Wakimoto 1990; Biggs et al. 1994). Collectively, the results above demonstrate that heterochromatin has both a repressive and an active role in gene expression, and open the door for more detailed study of the genes and proteins associated with it.

I.B.3 *D. melanogaster* heterochromatin-associated proteins

The first heterochromatin protein was discovered due to its predominant localization to pericentric and other heterochromatic regions of salivary gland polytene chromosomes and was named Heterochromatin Protein 1 (HP1) (James, Elgin 1986). HP1 is encoded by the *Su(var)2-5* gene in *D. melanogaster*, and is a classic dose-dependent modifier of PEV (Eissenberg et al. 1990). The discovery of HP1 and the demonstration of its role in heterochromatin provided the basis for additional molecular investigations of heterochromatin (Vermaak, Malik 2009). A large number of proteins have been identified as “heterochromatin-associated” based on their localization, PEV modifying activity, and interactions with other heterochromatin proteins. An exhaustive list of these proteins is not relevant to the purpose of this thesis. I will instead focus on HP1 and some key heterochromatin modifiers, as well as some recently described HP1-associated proteins (Figure I.B.1)

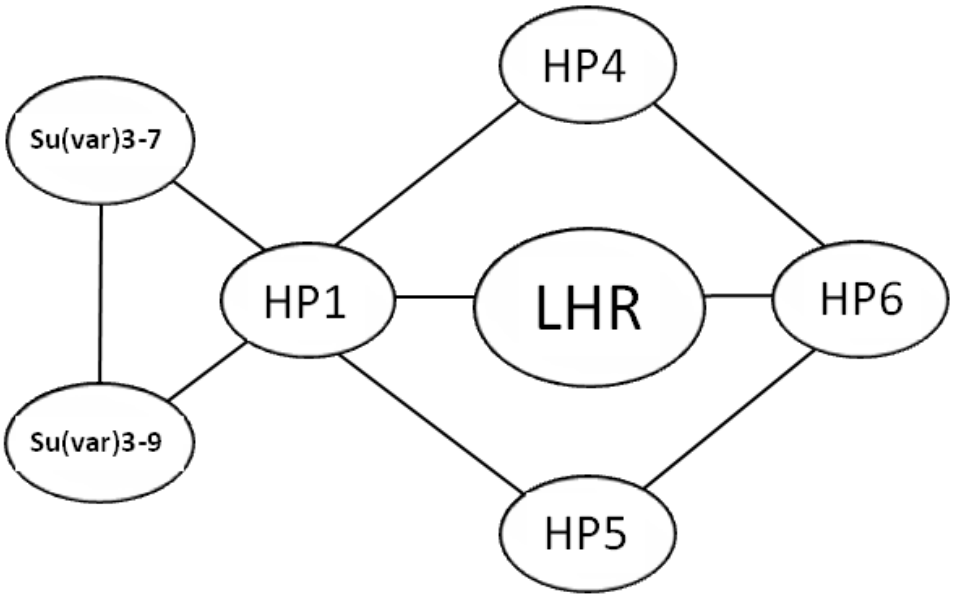

Figure I.B.1 Diagram of several HP1-associated proteins

Seven heterochromatin proteins mentioned in this thesis are shown. The connecting lines represent interaction data (yeast two-hybrid or co-immunoprecipitation) reported in the literature. These proteins are described in more detail in the setions below. Figure is adapted from Greil et al. 2007.

Heterochromatin Protein 1 (HP1)

HP1 is one of the most well-studied non-histone chromosomal proteins, and is conserved from fission yeast to humans (Singh, Georgatos 2002). *Su(var)2-5* encodes HP1, is an essential gene, and is expressed throughout the life cycle of *Drosophila* (Stolc et al. 2004). The HP1 protein is 205 amino acids long and contains two recognizable functional domains, the N-terminal chromo domain (CD) (Paro, Hogness 1991) and the C-terminal chromo-shadow domain (CSD) (Aasland, Stewart 1995). The CD is responsible for the association of HP1 with heterochromatin. The CD of HP1 binds to dimethylated lysine 9 on the N-terminal tail of histone H3 (Bannister et al. 2001; Jacobs, Khorasanizadeh 2002). The CSD mediates protein-protein interactions to proteins containing a degenerate protein motif, PxVxL (Smothers, Henikoff 2000). The CSD is responsible for homodimerization of HP1, as well as heterologous interactions (Brasher et al. 2000).

In addition to localizing to predominantly heterochromatic regions of chromosomes, HP1 is also found at a high number of euchromatic sites (Fanti et al. 2003; de Wit, Greil, van Steensel 2005). Many functions have been associated with HP1, including roles in gene expression and silencing (Dorer, Henikoff 1997; Lu et al. 2000; Liu et al. 2005), telomere capping (Fanti et al. 1998; Oikemus et al. 2004), chromosome segregation (Kellum, Alberts 1995; Kellum, Raff, Alberts 1995; Inoue et al. 2008), and DNA damage response (Luijsterburg et al. 2009); for reviews of HP1 function see: (Fanti, Pimpinelli 2008; Vermaak, Malik 2009). HP1 is also reported to have more than 20 protein interaction partners, including the five proteins described below

Suppressor of variegation 3-7 (Su(var)3-7)

Su(var)3-7 encodes a 1280 amino acid protein that contains seven zinc finger motifs, one BoxA motif, and a BESS domain, and the function of these domains has been investigated (Jaquet et al. 2002). The zinc fingers are responsible for the proteins association with both pericentric heterochromatin and euchromatin, and additionally two of the zinc fingers have strong affinity for the 353 and AATAT satellite sequences (Cleard, Spierer 2001). The BoxA domain is proposed to have a role in mediating interactions with other proteins, and the BESS domain mediates self interaction, and interaction with other proteins. In contrast to HP1 but similar to LHR, SU(VAR)3-7 is a rapidly evolving protein that is *Drosophila* specific. SU(VAR)3-7 predominantly associates with pericentric and telomeric heterochromatin, although it is also found at a variety of euchromatic sites (Reuter et al. 1990; Cleard, Delattre, Spierer 1997). The chromocenter localization of SU(VAR)3-7 appears conserved in other *Drosophila* species despite the lack of conservation of its primary sequence (Jaquet et al. 2002). As its name implies, *Su(var)3-7* mutants strongly suppress position effect variegation in a dose-dependent manner similar to *HP1* (Reuter et al. 1990). The dosage of *Su(var)3-7* also affects the morphology of the X-chromosome in males, as well as the localization of dosage compensation complex proteins (Spierer et al. 2008). SU(VAR)3-7 interacts genetically and physically with both HP1 (Cleard, Delattre, Spierer 1997) and SU(VAR)3-9 (Schotta et al. 2002), and the trio of proteins are considered part of the basic units of heterochromatin.

Suppressor of variegation 3-9 (Su(var)3-9)

Su(var)3-9 encodes a 635 amino acid protein that contains both a SET and a chromo domain, modules also found in some other chromatin proteins (Jenuwein et al. 1998; Jones, Cowell, Singh 2000). Like HP1, *Su(var)3-9* is conserved from fission yeast (Ivanova et al. 1998) to humans (Aagaard et al. 1999). SU(VAR)3-9 colocalizes with both SU(VAR)3-7 and HP1 at predominantly heterochromatic regions (Schotta, Reuter 2000), but it is also present at many sites throughout the genome (Greil et al. 2003). Consistent with this localization data, SU(VAR)3-9 directly interacts with both SU(VAR)3-7 and HP1, and the heterochromatin associations of HP1 and SU(VAR)3-9 are interdependent (Schotta et al. 2002). Mutations in *Su(var)3-9* also dominantly suppress position effect variegation in a dose dependent manner (Tschiersch et al. 1994). SU(VAR)3-9 is a histone methyl transferase (HMT) and it selectively methylates lysine 9 of the N-terminal tail of histone H3 (H3K9) (Rea et al. 2000). The H3K9 methylation by the SET domain of SU(VAR)3-9 is restricted to the chromocenter (Schotta et al. 2002), as other HMTs are responsible for methylation at other chromosomal sites (Seum et al. 2007).

Heterochromatin Protein 4 (HP4)

HP4 was recently identified based on its association with HP1 (Greil et al. 2007) and is also described as HP1- interacting protein, or HIP (Schwendemann et al. 2008). HP4 is non-essential and is well conserved throughout *Drosophila*. The predominant localization pattern of HP4 is at heterochromatic regions of chromosomes, and this localization is dependent on HP1 (Greil et al. 2007; Schwendemann et al. 2008). Consistent with its localization, HP4 also immunoprecipitates with HP1 *in vivo*. HP4 contains

three novel HP1-binding modules, and has been suggested to act as a bridging protein to stabilize higher-order chromatin structure (Schwendemann et al. 2008). The function of HP4 is unknown; however, mutations in HP4 dominantly suppress PEV, suggesting a role in the structure of heterochromatin (Greil et al. 2007, Schwendemann et al. 2008).

Heterochromatin Protein 5 (HP5)

HP5 was also identified by Greil et al. in 2007 and is an HP1-interacting protein. *HP5* is on the X chromosome, is rapidly evolving between *D. melanogaster* and *D. simulans*, and encodes a protein with no identifiable domains (Brideau, unpublished). Similar to many of these other HPs, HP5 predominantly localizes to heterochromatic regions of chromosomes, and this localization is dependent on HP1. Also like many of these HPs, mutations in *HP5* dominantly suppress PEV, suggesting a role in heterochromatin structure.

Heterochromatin Protein 6 (HP6)

HP6 was the last novel protein described in the Greil et al. study (2007), and was independently identified as Umbrea (Joppich et al. 2009; Vermaak, Malik 2009). *HP6* encodes a small 106 amino acid protein that primarily consists of a chromo-shadow domain similar to the CSD in HP1 (Greil et al. 2007; Joppich et al. 2009). The similarity to HP1 is consistent with a recent report suggesting that HP6 is an ancient duplication of the HP1 paralog HP1B in *Drosophila* (Vermaak, Malik 2009). The sequence of *HP6* is not well conserved in *Drosophila*. Several reports disagree on the localization properties and viability of HP6 mutants. Greil et al. (2007) report that HP6 is

uniformly distributed in the nucleus in a pattern not overlapping with HP1, and does not depend on HP1 for localization (2007). In contrast, Joppich et al. (2009) report that HP6 colocalizes with HP1 at the pericentric heterochromatin and telomeres and depends on HP1 for this localization (2009). The discrepancy between these results may be a result of the proteins that were detected (epitope tagged vs native) or the tissue that was examined (Kc cells vs salivary glands). The function of HP6 is also not conclusively agreed upon. Mutations in HP6 do not modify PEV (Greil et al. 2007), but do cause telomere fusions (Joppich et al. 2009) and a low frequency of eggs produced by HP6 homozygous mutant females contain dispersed polar bodies (Mukai et al. 2007). There is also an inconsistency in the literature about the viability of HP6 mutants. Greil et al. (2007) reported that a P-element insertion mutant in HP6 was homozygous semi-lethal, but concluded that this semi-lethality may be in part due to the location of the insertion. HP6 is nested in an intron of *dumpy*, and the P-element may also have affected dumpy expression. Mukai and colleagues used this same P-element to generate an imprecise excision mutation in *HP6*. This mutant deletes the genomic region encoding the chromo-shadow domain, but is viable as a homozygous mutant (Mukai et al. 2007; Brideau, unpublished). In contrast to the report from Mukai and colleagues and my preliminary work, both (Joppich et al. 2009) and (Vermaak, Malik 2009) report that RNAi knockdown of HP6 results in embryonic lethality.

A molecular model for heterochromatin establishment and maintenance

The basic model for heterochromatin assembly is centered around *Su(var)3-9*, dimethylated H3K9 and HP1. In this model, SU(VAR)3-9 associates with heterochromatic sequences and methylates histone H3 at

Lysine 9 (dimeH3K9). This H3K9 mark is then recognized by the chromo domain of HP1, and the association of HP1 then initiates the establishment of HP1/SU(VAR)3-7/SU(VAR)3-9 repressive complexes. These proteins then form a positive feedback loop, where HP1 recruits SU(VAR)3-9 through its chromo-shadow domain to methylate nearby H3K9 residues, which in turn are recognized by HP1, and heterochromatin spreads. Once established, heterochromatin also needs to be maintained, and SU(VAR)3-7 and HP1 are proposed to be partially responsible for this action. The roles of the other HPs mentioned above are not well understood yet; however, the results that many of them dominantly suppress PEV suggest a role in the structure or maintenance of heterochromatin. Genome-wide mapping indicates that while many of these proteins are found together at various sites in the genome, other sites are bound by some proteins and not others (Greil et al. 2003, 2007). These results suggest that heterochromatin is heterogeneous in protein composition. Additionally, the boundaries of heterochromatin are dynamic, and likely vary with respect to tissue type and developmental timepoint (Weiler, Wakimoto 1995). Therefore, better understanding of the structure and function of heterochromatin requires additional study of heterochromatin-associated proteins. In this thesis, I explore the relationship between LHR and several of these HPs in order to understand both the function of LHR and the role of heterochromatin in hybrid incompatibility.

I.B.4 Evolution of satellite DNA in *D. melanogaster* and its sibling species

The satellite DNA profile is different between *D. melanogaster* and its sibling species (Lohe, Roberts 1988). Based on a hybridization assay, most major satellites in *D. melanogaster* are present in its sibling species, except in

D. simulans, which is missing three. Furthermore, only one of the eight satellites in *D. simulans* has identical sequence to satellites in *D. melanogaster*, although at least three are closely related in sequence. The copy number of satellites also varies widely among species, which suggests a rapid quantitative change. The copy number of satellites in *D. melanogaster* is generally reduced in *D. simulans*, and is further reduced in *D. erecta*. Consistent with this observation, the X and Y chromosomes of *D. simulans* and *D. erecta* are shorter than those of *D. melanogaster* due to differences in heterochromatic regions. The last major difference in satellite DNA between *D. melanogaster* and its sibling species is the chromosomal location. For example, in *D. melanogaster*, the most abundant satellite (1.705) is found on all chromosomes. In contrast, the same 1.705 satellite is found on the sex chromosomes in *D. simulans,* and only on the tip of the Y chromosome in *D. mauritiana*. It remains to be examined if the differences in satellite sequence, abundance, and location have a major role in the reproductive isolation of *D. melanogaster* from its sibling species. However, two recent reports suggest this may be the case in two different HI systems, and are discussed in the next section.

I.B.5 Heterochromatin and hybrid incompatibilities

It has been recently suggested that hybrid sterility between *D. mauritiana* and *D. simulans* (Bayes, Malik 2009) and hybrid female inviability between *D. simulans* and *D. melanogaseter* (Ferree, Barbash 2009) are caused by heterochromatic sequences. Each of these cases is briefly discussed above in Chapter I.A.3 as *OdsH* and *Zhr*, respectively. Although one model proposes a gain-of-function interaction and the other proposes a

loss of function as the cause, the proposed mechanisms of lethality are similar in that the resulting defect is the decondensation of heterochromatin. Both models also suggest the possibility that the evolution of the repeat sequences is being driven by genetic conflict. Genetic conflict such as meiotic drive has been suggested as a cause for the rapid evolution of centromeric DNA repeats (Henikoff, Ahmad, Malik 2001). Consistent with this hypothesis, centromeric drive has recently been suggested in *Mimulus* (monkeyflower) where certain centric or pericentric repeat alleles have a selective advantage during meiosis in interspecific hybrids (Fishman, Saunders 2008). One major goal in the study of rapidly evolving HI genes is to connect the rapid evolution by positive selection to the underlying biological cause. Co-evolution between heterochromatic sequences and heterochromatin-associated proteins seems like a good candidate for the biological basis of this rapid evolution. In Chapters II and III of this thesis, the association of the rapidly evolving protein LHR with potentially rapidly evolving heterochromatic proteins is discussed.

I.C Thesis organization

This thesis describes projects aimed at understanding the functions and properties of *Lethal hybrid rescue*, one of the few hybrid incompatibility loci identified to date.

Chapter II is a modified version of a manuscript authored in collaboration with many members in the lab of Dr. Daniel Barbash and published in *Science* on the identification and characterization of *Lhr.* We show that the gene CG18468 is *Lhr*, and causes male hybrid lethality between *D. melanogaster* and *D. simulans*. We further show that *Lhr* is rapidly evolving in a manner consistent with positive selection. We also found that *Lhr*

interacts with *Hybrid male rescue (Hmr)* to form a pair of Dobzhansky-Muller interacting loci and cause HI. Additionally, we found that LHR interacts with HP1 in a yeast-two hybrid assay, and co-localizes with HP1 at heterochromatic regions of polytene chromosomes.

Chapter III is a modified form of a paper we plan to submit in the near future on analyses I have performed with LHR. In this chapter I examine the interaction between LHR and HP1 more closely, show that LHR directly binds to HP1, and investigate the mediating domains in each protein. I also found that LHR depends on two heterochromatin proteins, HP1 and HP5, for proper heterochromatic localization. To study how the divergence of LHR affects its functions and interactions, I also analyzed the properties of *D. simulans*, *D. yakuba*, and *D. virilis* LHR when expressed in *D. melanogaster*. I found that localizing to heterochromatin and interacting with HP1 and HP6 are two conserved properties for LHR orthologs. In conflict with the asymmetry predicted by the D-M model that we found in Chapter II, I also found that *D. melanogaster Lhr* can induce hybrid male lethality.

Chapter IV presents additional analysis of LHR that will not be included in the paper in Chapter III. In this chapter I explore the interaction of *Hmr* and *Lhr*, and show the two encoded proteins interact in yeast two-hybrid. Additionally, I investigate if mutations in HP1 and HP4-6 interact genetically with *Lhr*-dependent hybrid male rescue. I also show data from initial experiments using the mislocalization of LHR in HP5 mutants to test if the hybrid lethal activity of LHR depends on its heterochromatic localization.

Chapter V discusses the data presented in earlier chapters in an effort to synthesize a model for the function of LHR, and how LHR causes hybrid lethality. I also discuss possible areas for further exploration.

The **Appendix** contains data from some initial characterization experiments with an *Lhr* knockout line in *D. melanogaster*, and data from an attempt to quantify the strength of interaction between several LHR orthologs and HP1. I have included data on Lhr^{1} complementation analysis with four *Lhr* orthologs that was meant to be included in Chapter III, but was left out due to technical uncertainties. I have also included a manuscript that was published in *Molecular and Cellular Endocrinology* which contains data I generated in the lab of Dr. Kate Whitlock.

II. TWO DOBZHANSKY-MULLER GENES INTERACT TO CAUSE HYBRID LETHALITY IN DROSOPHILA[1]

This work was published in Science in November of 2006. I was involved in the yeast two-hybrid experiments demonstrating that *D. melanogaster* and *D. simulans* LHR interact with HP1 and created Figure II.C.3A-B. I also contributed to supplementary Figures II.C.S1, II.C.S2 and II.C.S6 which show the alignments of the BESS domain, LHR, and HP1, respectively. In addition, I created the LHR::YFP constructs used in Figures II.C.3D-F and Figure II.C.S7, and helped write the paper.

II.A Abstract

The Dobzhansky-Muller model proposes that hybrid incompatibilities are caused by the interaction between genes that have functionally diverged in the respective hybridizing species. Here, we show that *Lethal hybrid rescue (Lhr)* has functionally diverged in *Drosophila simulans* and interacts with *Hybrid male rescue (Hmr)*, which has functionally diverged in *D. melanogaster*, to cause lethality in F1 hybrid males. LHR localizes to heterochromatic regions of the genome and has diverged extensively in sequence between these species in a manner consistent with positive selection. Rapidly evolving heterochromatic DNA sequences may be driving the evolution of this incompatibility gene.

[1] Brideau, N.J., Flores H.A., Wang J., Maheshwari, S., Wang X., Barbash, D.A. 2006. Two Dobzhansky-Muller genes interact to cause hybrid lethality in *Drosophila*. Science 314:1292-1295.

II.B Materials and Methods

II.B.1 Drosophila crosses and stocks

All crosses were done at room temperature (22-24°). 2-3 replicates were done for each cross in Tables II.C.1 and II.C.S1, each containing ~15-20 female and ~30 male parents for interspecific crosses, and ~8 females and ~8 males for intraspecific crosses. Four collections of 2-4 days each were performed for each replicate. The *Lhr* hybrid rescue mutation of (Watanabe 1979) is designated Lhr^1. The *D. simulans jba* marker is as described (*2*). *Df(1)Hmr–* is described in (Barbash, Lorigan 2007). All other Drosophila stocks used are described on FlyBase (Grumbling, Strelets, Consortium 2006).

II.B.2 Recombination mapping of *Lhr*

The visible marker *jba* has not been identified in *D. melanogaster* , and is estimated to be in region 55A1-55C1 based on noncomplementation of *D. melanogaster* deletions (Yamamoto et al. 1997). Lhr^1/Lhr^1 *D. simulans* females were crossed to *jba/jba D. simulans* males. The F1 *D. simulans* female progeny (Lhr^1 + / + *jba*) were crossed to *jba/jba D. simulans* males, and the F2 *D. simulans* sons collected as potential Lhr^1 *jba/* + *jba* recombinants, which were then typed for Lhr^1 by crossing them to *D. melanogaster* females and looking for rare interspecific hybrid sons. We established about 110 crosses each with 8-10 *D. melanogaster* females and 7-8 potentially recombinant males. This brooding strategy was appropriate due to the close proximity of *Lhr* and *jba*, such that any cross is unlikely to contain more than one recombinant male. Ten of these crosses produced hybrid sons. We developed PCR-based RFLP markers across cytological region 54 (covering approximately 700 kb), and determined that all 10 recombinants occurred

within a region of approximately 475 kb between the genes *Sip1* and *mapmodulin*.

II.B.3 Transgenic constructs

P{w+mC UAS-Dsim\Lhr =UAS-Dsim\Lhr} was made by amplifying the predicted 5'UTR and CDS of *CG18468* by PCR from *D. simulans* strain C167.4 with the forward primer 5'-ccctttagatctaatttccatcgctattagtttgc-3' and the reverse primer 5'-gccttttctagatcatgttctcagcgtaggccg-3', the underlined sequences are *Bgl*II and *Xba*I restriction sites, respectively. Following restriction digestion, the PCR product was cloned into the transformation vector pUAST (Brand, Perrimon 1993). Subsequent sequencing of the insert revealed an internal *Xba*I site (presumably polymorphic in C167.4) in its 5'UTR that failed to digest during cloning and thus is present in the construct. A plasmid containing *D. melanogaster Lhr* was made by PCR from a strain of Oregon- R, cloned into the *Bgl*II and *Xba*I sites of pUAST, and fully sequenced. This *Lhr* clone contains 5 silent changes relative to the *CG18468* reference sequence; these represent either polymorphisms in Oregon-R and/or mutations caused by PCR. The plasmid pENTR-*Lhr* was made by PCR amplification from this progenitor plasmid using the forward primer 5'-caccATGAGTACCGACAGCGCCGAGGAA-3' and the reverse primer 5'-TCATGTTCTCAGCGTAGGCCG-3', followed by cloning of the PCR product into the plasmid pENTR/D-TOPO (Invitrogen). The plasmids *P{w+mC UASVenus::Lhr=UAS-YFP::Lhr}*, an N-terminal fusion of YFP to LHR, and *P{w+mC UASLhr::Venus=UAS-Lhr::YFP}*, a C-terminal fusion of YFP to LHR, were made by performing a Gateway LR clonase-mediated recombination reaction between pENTR-*Lhr* and the plasmids pTVW and pTWV,

respectively. pTVW and pTWV are described at http://www.ciwemb.edu/labs/murphy/Gateway%20vectors.html; Venus is an enhanced version of Yellow Fluorescent Protein (Nagai et al. 2002).

II.B.4 Genotyping of flies.

Genotypes of some flies in Table II.C.S1 were determined by PCR (footnotes *c* - *h*). Presence of *P{UAS-Dsim\Lhr}* was tested using the primers 5'-GCAACTACTGAAATCTGCCAAG-3' and 5'-ATTTTTCGCACTGTGTTTTTCC-3'. Presence of *P{act5C-GAL4}* and *P{tubP-GAL4}* was tested using the primers 5'- AATAAGTGCGACATCATCATCG-3' and 5'-ATAGGGCAGTAGGGGTGAAAAT-3'.

II.B.5 *Lhr*^{1} insertion and *Lhr*^{2} allele

The insertion in the *Lhr1* strain was isolated by PCR using Takara LA polymerase, using the primers 5'-CTCCGCTATCGACAACCAAA-3', and 5'-GCTCAACGCTCTCGTAGCTT-3'. Sequencing of this product from the 3' side of the insertion failed after 23 bp of poly(A) of the insert; this sequence feature suggests that the insertion resulted from retrotransposition. Several hundred base pairs of sequence was obtained from the 5' end of the insertion, which matched to several regions of the *D. simulans* genome. These sequences were deposited to GenBank under accession numbers EF057388 and EF057389. The hybrid rescue strain containing the *Lhr*^{2} allele was discovered by H. Allen Orr, Univ. of Rochester (personal communication), who generously provided it to us. The GenBank accession number for the sequence of the *Lhr*^{2} allele is EF044061.

II.B.6 RT-PCR

RT-PCR was done from 1 µg of total RNA using the SuperScript III First-Strand Synthesis System (Invitrogen). In Figure II.1.D, *Lhr* was PCR amplified with primers 5'- TTGCCCTTCGTGAAATCTCT-3' and 5'-CTAATGCGGAATCCGTCAAT-3', and *CG6546* with primers 5'- GCTGGAAAGTACCTATGCTGGCTA-3' and 5'-ATCATCAGGACTTTGGTTCTGAGC-3'.

II.B.7 Yeast two-hybrid assays

Clontech vectors pGADT7-AD and pGBKT7 DNA-BD, modified to contain the Gateway cloning cassette (Invitrogen), were kindly provided by K. Ravi Ram, A. Garfinkel, and M. F. Wolfner (Cornell University; personal communication). *Lhr* was PCR amplified using wild type DNA from the *D. melanogaster* strain Oregon-R and the *D. simulans* strain C167.4 DNA as templates, with primers 5'-caccATGAGTACCGACAGCGCCGAGGAA-3' and 5'-TCATGTTCTCAGCGTAGGCCG-3' and Accuprime *Pfx* polymerase (Invitrogen). *D. melanogaste HP1* was amplified by RT-PCR (Invitrogen Superscript III) using 1µg of total RNA from *D. melanogaster* strain *w1118* larvae and the primers 5'-caccATGGGCAAGAAAATCGACAACC-3' and 5'-TTAATCTTCATTATCAGAGTACC-3'. Each PCR product was gel purified and cloned into pENTR/D-TOPO entry vector (Invitrogen). The correct structure and sequence of all entry clones were verified by restriction endonuclease digestion and DNA sequencing. Subcloning of each gene from the pENTR/D-TOPO vector into each two-hybrid destination vector was performed via LR recombination according to the manufacturer's instructions (Invitrogen). Yeast strain PJ69-4A was double transformed with both the AD and BD

vectors using a standard LiAc/SS-DNA/PEG procedure (Gietz, Woods 2002). PJ69-4A cultures grown overnight at 30°C in YPD were transformed and then plated on CM-LEU-TRP plates to select for both BD and AD plasmids. Colonies were then grown overnight at 30°C in CM-LEU-TRP. Each culture was serially diluted to densities of 10^6 - 10^2 cells/mL. 10 µL of each dilution was spotted to both CM-LEU-TRP and CM-LEU-TRP-HIS, incubated at 30°C, and growth was assessed after 3 days. Three independent replications of the yeast two-hybrid experiments were performed.

II.B.8 YFP imaging and polytene immunolocalization

For imaging of live YFP, intact glands were fixed for 4% paraformaldehyde and 0.1% Triton-X in 1X PBS for 15 minutes, followed by 3 washes in 1X PBS. Glands were then incubated in a DAPI solution (final concentration of DAPI 1µg/ml in 1X PBS) for fifteen minutes, washed in 10% Glycerol/1X PBS and mounted in 50% glycerol/1XPBS. Immunolocalization of polytene chromosomes was done as described in (Schwartz, Werner, Lis 2003). Anti-HP1 (mouse monoclonal C1A9, Developmental Studies Hybridoma Bank, Univ. of Iowa) was used at a dilution of 1:4 or 1:10, and rabbit anti-GFP (Invitrogen) was used at 1:200 or 1:500 dilution. Cy2 and RRX conjugated secondary antibodies (Jackson Immunoresearch) were used at 1:500 dilution.

II.B.9 *Lhr* gene structure and orthologs

D. melanogaster Lhr (*CG18468*) has been annotated as containing a 334 codon CDS (Grumbling, Strelets, Consortium 2006). We found that all of the *melanogaster* subgroup species contain an ortholog of *CG18468*, but that their first methionine aligned to the methionine at codon 16 of *D. melanogaster.* We

therefore suggest that *D. melanogaster CG18468* likely initiates translation at its second ATG codon and encodes a protein of 319 amino acids. Orthologs to *D. melanogaster Lhr* were identified as reciprocal best Blast hits; in addition at least one flanking gene from *D. melanogaster* was found flanking *Lhr* from the more distant species *D. pseudoobscura*, *D. virilis*, *D. willistoni*, and *D. mojavensis*. *D. mauritiana Lhr* was PCR amplified from strain C164.1 and directly sequenced. *Lhr* orthologs from the following species were identified from trace archives and preliminary assemblies of whole-genome shotgun sequences: *D. simulans* strain w^{501} (and other *D. simulans* strains) and *D. yakuba* (Washington University Genome Sequencing Center, St. Louis, MO); *D. sechellia* (Broad Institute, Cambridge, MA) and *D. erecta, D. ananassae, D. mojavensis* and *D. virilis* (Agencourt Bioscience, Beverly, MA) and *D. willistoni* (J. Craig Venter Institute, Rockville, MD). We annotated *Lhr* orthologs by maximizing similarity to *melanogaster* subgroup sequences. For all species except *D. willistoni* we used the largest single exon ORF. We annotated *D. willistoni Lhr* as containing an intron, positioned to maximize similarity with other species. *D. pseuoobscura Lhr* (*CG14945*) was annotated previously as containing an intron (Richards et al. 2005). We performed RT-PCR on larval RNA using primers 5'-CAGGGACTTGAGTATGGC-3' and 5'-CTTCACCCGAACGATTAG-3', and found that this region is exonic; *D. pseudoobscura* therefore contains a large coding insertion relative to the other species, as shown in Figure II.C.S2. *Lhr* was also previously annotated as initiating translation at a serine; we annotated *D. pseudoobscura Lhr* as starting translation at its fourth in-frame ATG. The GenBank accession number for *D. mauritiana Lhr* is EF044062. GenBank Third-Party Annotation (TPA) accession numbers for the remaining *Lhr* orthologs are BK005905-BK005914.

II.B.10 *Lhr* population sampling, phylogenetic analysis and divergence calculations

12 alleles of *D. melanogaster Lhr* were sequenced from a collection of iso-2 stocks derived from flies collected in State College, PA (Lazzaro, Clark 2001). 11 alleles of *D. simulans Lhr* were sequenced from a collection of inbred iso-female lines collected in Maryland, USA (Dr. C. F. Aquadro, personal communication). None of these strains contain the insertion found in the Lhr^1 allele, nor do the strains w^{501}, C167.4, MD106TS, New Caldonia and Sim4/Sim6 (Washington University Genome Sequencing Center, St. Louis, MO). Population genetic analyses were done using DnaSP (Rozas et al. 2003). Population data was analyzed using the McDonald-Kreitman test (McDonald, Kreitman 1991) The K_A and K_S values of *Lhr* between *D. melanogaster* and *D. simulans* were calculated from the total population data set, using equation 10.20 of Nei (Nei 1987), with Jukes-Cantor correction. We compared these values to a published dataset (Betancourt, Presgraves 2002). Excluding rapidly evolving *Acp* genes, mean values in this dataset are K_A = 0.018 and K_S = 0.125. Among 194 genes K_A of 0.078 for *Lhr* ranks 6th highest while K_S of 0.106 for *Lhr* ranks 105th highest. Similar values of K_A and K_S were obtained using the maximumlikelihood (ML) method in the PAML package (Yang 1997). With PAML and using the reference sequence from *D. melanogaster* and the *D. simulans* w^{501} allele, the ML estimated values were K_A = 0.0801 and K_S = 0.1259, with K_A/K_S = 0.6362 (runmode=2 [pairwise], CodonFreq=3 [estimating frequency for each codon]). The phylogenetic trees in Figure II.C.S5A and B were constructed using MEGA 3.1 (Kumar, Tamura,

Nei 2004) and PAML, respectively. Genbank accession numbers for *Lhr* alleles used in our population sample are EF044038-EF044049 for *D. melanogaster* and EF044050-EF044060 for *D. simulans*.

II.C Results and Discussion

Plant and animal hybrids are often sterile or lethal as a result of interspecific genetic divergence. The Dobzhansky-Muller model proposes that hybrid incompatibilities (HIs), which contribute to speciation, evolve as a consequence of interactions between or among genes that have diverged in each of the hybridizing species (Coyne, Orr 2004). Dobzhansky-Muller incompatibility genes require three criteria: each gene reduces hybrid fitness, has functionally diverged between the hybridizing species, and depends on the partner gene to cause HI (Figure II.C.1A). Major-effect HI genes have been discovered, and functional divergence of single genes has been demonstrated by genetic tests (Ting et al. 1998; Barbash, Awadalla, Tarone 2004) or suggested by patterns of molecular evolution (Presgraves et al. 2003). Although HI systems composed of complementary factors have been described (Hutchinson 1932; Christie, MacNair 1984) and interacting genomic regions of hybridizing species identified (Carvajal, Gandarela, Naveira 1996; Kazianis et al. 1998; Sweigart, Fishman, Willis 2006) no pair of Dobzhansky-Muller genes has been reported. It remains unclear whether HI phenotypes can be explained even in part by two-locus interactions, or alternatively whether HIs require complex multilocus interactions (Cabot et al. 1994; Maside, Barral, Naveira 1998; Tao et al. 2003).

Interspecific crosses of *D. melanogaster* females to *D. simulans* males

produce no sons. The *D. simulans* mutation *Lhr*^{1} suppresses the lethality of these F1 hybrid males (Watanabe 1979). A mutant allele of the X-linked *D. melanogaster* gene *Hmr* similarly suppresses hybrid male lethality (Barbash et al. 2003). *Hmr* encodes a rapidly evolving protein with sequence similarity to the myb/SANT-like domain in Adf-1 (MADF) class of DNA binding proteins (Barbash et al. 2003). Genetic interaction studies (Barbash, Roote, Ashburner 2000; Orr, Irving 2000) suggested that *Hmr* and *Lhr* interact to cause lethality in a manner consistent with the Dobzhansky-Muller model (Figure II.C.1A). *Lhr*^{1} maps 1.7 centimorgans from the visible marker *jba* on chromosome 2R (Yamamoto et al. 1997). We identified recombinants between *Lhr*^{1} and *jba* and typed them using molecular markers that distinguish the *Lhr*^{1} and *jba D. simulans* strains (Figure II.C.1B). On the basis of the distribution of recombinants, *Lhr*^{1} is likely within several hundred kilobases centromere-proximal to *qkr54B*.

Because of the paucity of visible markers in *D. simulans*, we did not attempt to obtain a proximal limit for *Lhr* by mapping. Instead, we searched preliminary assemblies of the *D. simulans* genome for candidate genes on the basis of similarities to *Hmr*, namely higher-than-average divergence between *D. melanogaster* and *D. simulans* and a possible role in DNA or chromatin binding. Among ~37 genes, we first examined *CG18468* because it contains a boundary element–associated factor 32/Su(var)3-7/Stonewall (BESS) domain. The BESS domain is found in 21 *Drosophila* proteins, often associated with MADF domains, and mediates protein-protein interactions (Bhaskar, Courey 2002). *Hmr* is predicted to encode a protein with two MADF domains (Barbash et al. 2003), and we detected a putative BESS domain (Figure II.C.S1), suggesting a possible functional relationship between *CG18468* and *Hmr*.

Figure II.C.1 *CG18468* encodes *Lhr*

(A) Model of *Hmr* and *Lhr* functional divergence and the interaction that causes hybrid lethality. Lethality results from the interaction between the *D. melanogaster Hmr* allele (*Hmr-mel*) and the *D. simulans Lhr* allele (*Lhr-sim*). (B) Map of *Lhr* region in *D. simulans*. Genetic markers and estimated cytological locations in *D. melanogaster* are shown below the line. Ten recombinants between *jba* and *Lhr* were selected and cross-overs mapped within a region of approximately 480 kb; the most proximal recombinant was between *Sip1* and *qkr54B* (diagram not to scale). (C) *CG18468* has a characteristic leucine zipper-like structure in all *Drosophila* species except *D. simulans*, *D. mauritiana*, and *D. sechellia*, which have a 16–amino acid insertion; this insertion is lacking in the *D. simulans* rescue strain Lhr^2.(D) Map of *CG18468* region at 54B7 and insertion in the Lhr^1 strain. Black boxes, coding regions; unfilled boxes, UTRs; arrows, predicted translation start sites. The large triangle represents an insertion of ~4 kb (triangle not to scale) located between nucleotides 11 and 13 of the predicted *CG18468* mRNA in Lhr^1. (E) The insertion in Lhr^1 reduces the level of mRNA of *CG18468* but not of *CG6546*. RT-PCR with larval RNA from a *vermillion* (*v*)–marked *D. simulans* strain and from the Lhr^1 strain.

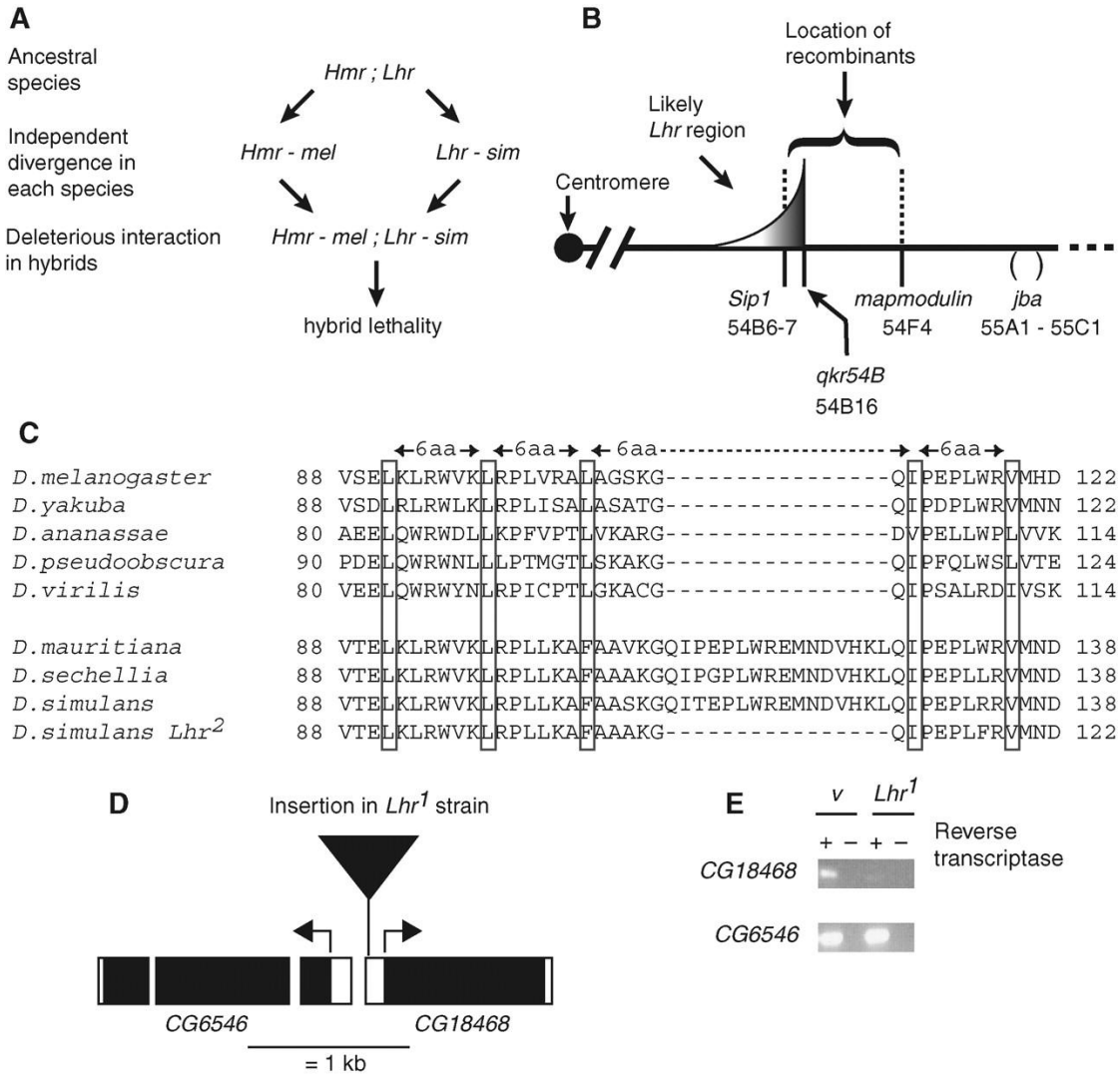
A
Ancestral species
Independent divergence in each species
Deleterious interaction in hybrids
Hmr ; Lhr
Hmr - mel
Lhr - sim
Hmr - mel ; Lhr - sim
hybrid lethality
B
Location of recombinants
Likely Lhr region
Centromere
Sip1
54B6-7
mapmodulin
54F4
jba
55A1 - 55C1
qkr54B
54B16
C
6aa
6aa
6aa
6aa
D. melanogaster 88 VSELKLRWVKLRPLVRALAGSKG----------QIPEPLWRVMHD 122
D. yakuba 88 VSDLRLRWLKLRPLISALASATG----------QIPDPLWRVMNN 122
D. ananassae 80 AEELQWRWDLLKPFVPTLVKARG----------DVPELLWPLVVK 114
D. pseudoobscura 90 PDELQWRWNLLLPTMGTLSKAKG----------QIPFQLWSLVTE 124
D. virilis 80 VEELQWRWYNLRPICPTLGKACG----------QIPSALRDIVSK 114
D. mauritiana 88 VTELKLRWVKLRPLLKAFAAVKGQIPEPLWREMNDVHKLQIPEPLWRVMND 138
D. sechellia 88 VTELKLRWVKLRPLLKAFAAAKGQIPGPLWREMNDVHKLQIPEPLLRVMND 138
D. simulans 88 VTELKLRWVKLRPLLKAFAASKGQITEPLWREMNDVHKLQIPEPLRRVMND 138
D. simulans Lhr2 88 VTELKLRWVKLRPLLKAFAAAKG----------QIPEPLFRVMND 122
D
Insertion in Lhr1 strain
CG6546
CG18468
= 1 kb
E
v
Lhr1
+ − + −
Reverse transcriptase
CG18468
CG6546

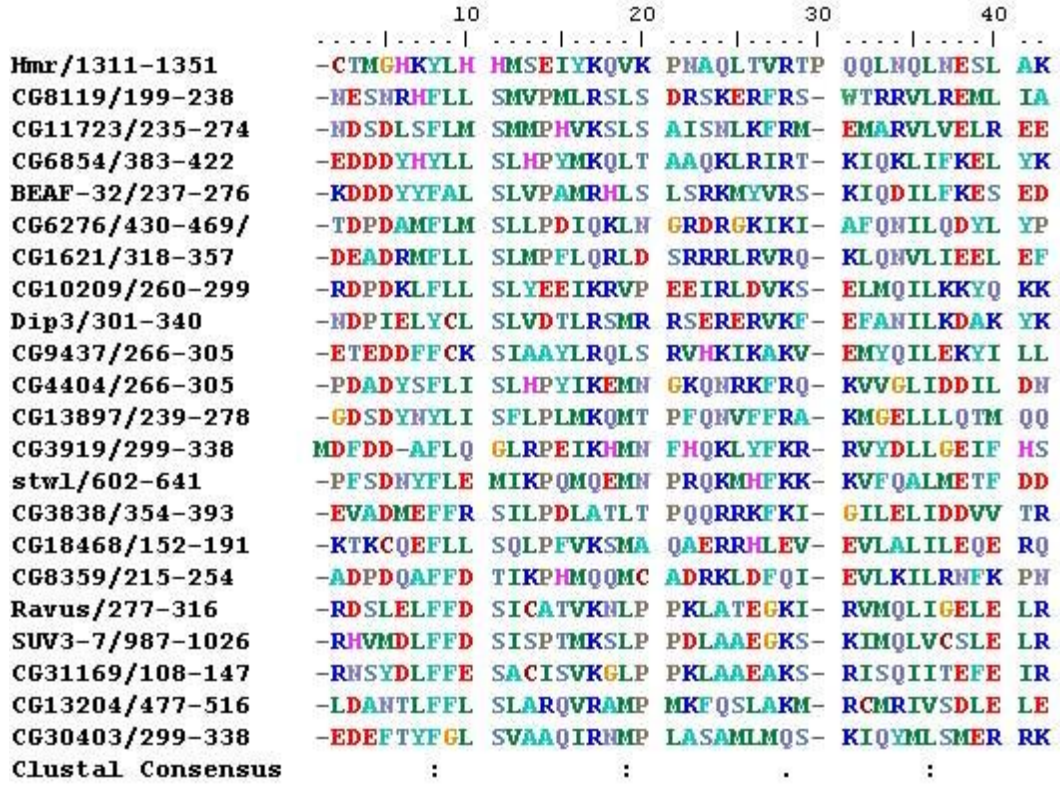

Figure II.C.S1 Alignment of a putative BESS domain from HMR with BESS domains from 21 other *D. melanogaster* proteins.

We discovered that *CG18468* is mutated in the *Lhr*[1] rescue strain, which contains an insertion of ~4 kb in the predicted 5' untranslated region (UTR) (Figure II.C.1D) that appears to be a moderately repetitive retrotransposed sequence.

Most predicted *D. simulans* proteins are >90% identical to their *D. melanogaster* orthologs. In contrast, CG18468 has only ~80% identity, caused by amino acid divergence and by a 16–amino acid insertion in *D. simulans* (Figure II.C.1C and Figure II.C.S2). The estimated average divergence of *CG18468* is similar to *Hmr* (Barbash et al. 2003), measuring 0.078 at nonsynonymous sites (K_A) and 0.106 at synonymous sites (K_S). This K_A value, but not the K_S value, is substantially higher than the average value between *D. melanogaster* and *D. simulans*. Again similar to *Hmr, CG18468* is highly diverged outside the *melanogaster* subgroup (Figure II.C.S2), and both genes apparently lack orthologs outside of *Drosophila*.

This insertion is not found in any of the five strains from which genome sequence is available nor from 11 additional lines we sequenced. *CG18468* is adjacent to and divergently transcribed from *CG6546* (Figure II.C.1D), so the insertion in the Lhr^1 rescue strain could potentially affect the transcription of either or both of these genes. Reverse transcription polymerase chain reaction (RT-PCR) products, derived from RNA from the critical early larval stage (Barbash, Roote, Ashburner 2000), showed that both genes are transcribed in a control strain but that *CG18468* transcription is strongly reduced in the Lhr^1 rescue strain (Figure II.C.1E). These data suggest that the Lhr^1 phenotype is caused by reduced expression of *CG18468*.

We cloned the wild-type *CG18468* gene from *D. simulans* and transformed *D. melanogaster* with *P* element vectors containing a *D. simulans CG18468* cDNA under the control of *Saccharomyces cerevisiae Upstream Activity Sequences* (*UAS*), henceforth referred to as *UAS-Dsim*/*Lhr*.

Figure II.C.S2 Alignment of *Lhr* orthologs

The first six species are in the *melanogaster* subgroup. *D. mauritiana* and *D. sechellia* are sister species of *D. simulans*. Orthologs were identified and gene structures predicted as described in Materials and Methods. Most of these gene structures have not been experimentally verified. The BESS domain is underlined.

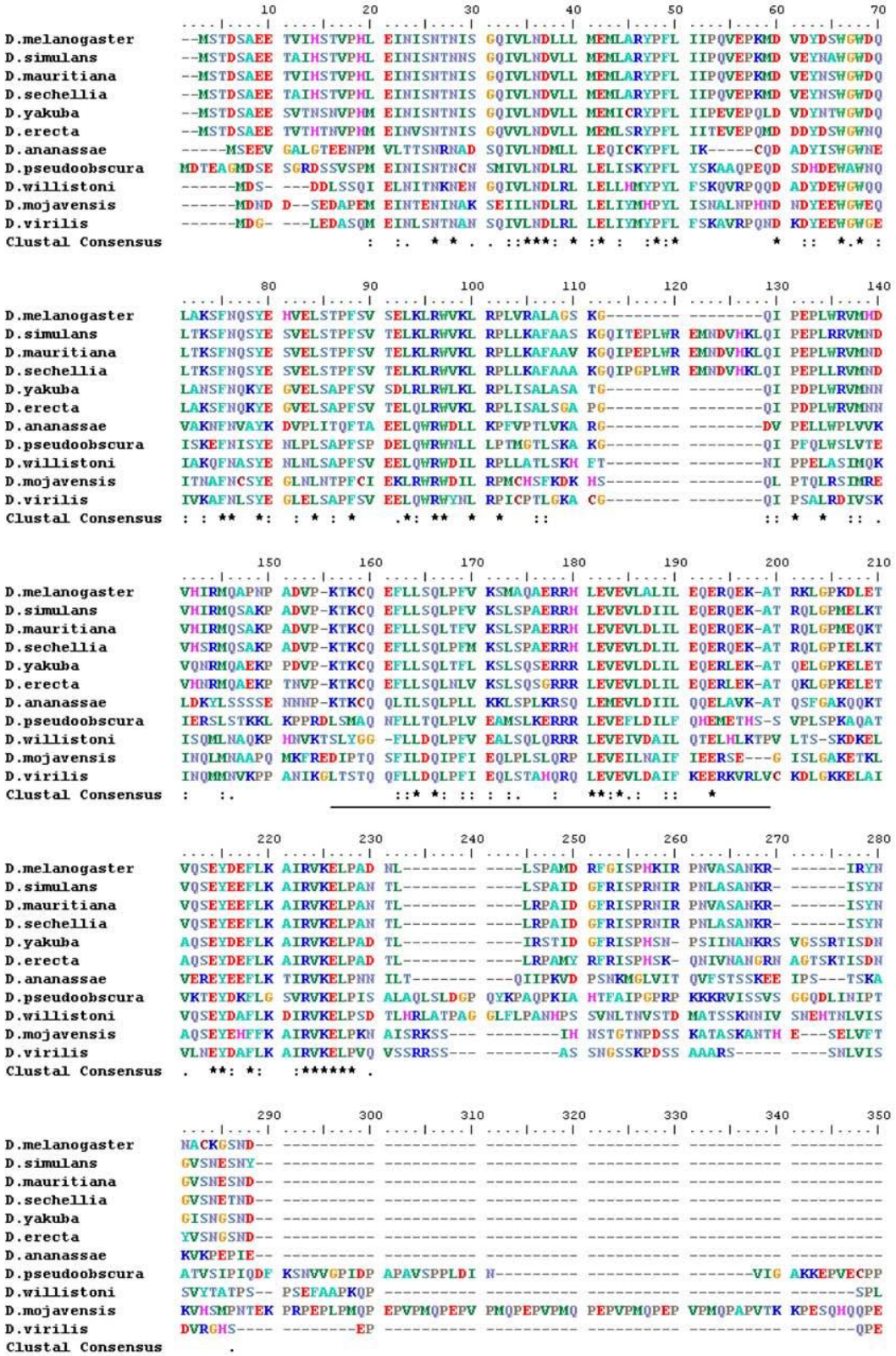
D.melanogaster
D.simulans
D.mauritiana
D.sechellia
D.yakuba
D.erecta
D.ananassae
D.pseudoobscura
D.willistoni
D.mojavensis
D.virilis
Clustal Consensus

Figure II.C.S2 (continued)

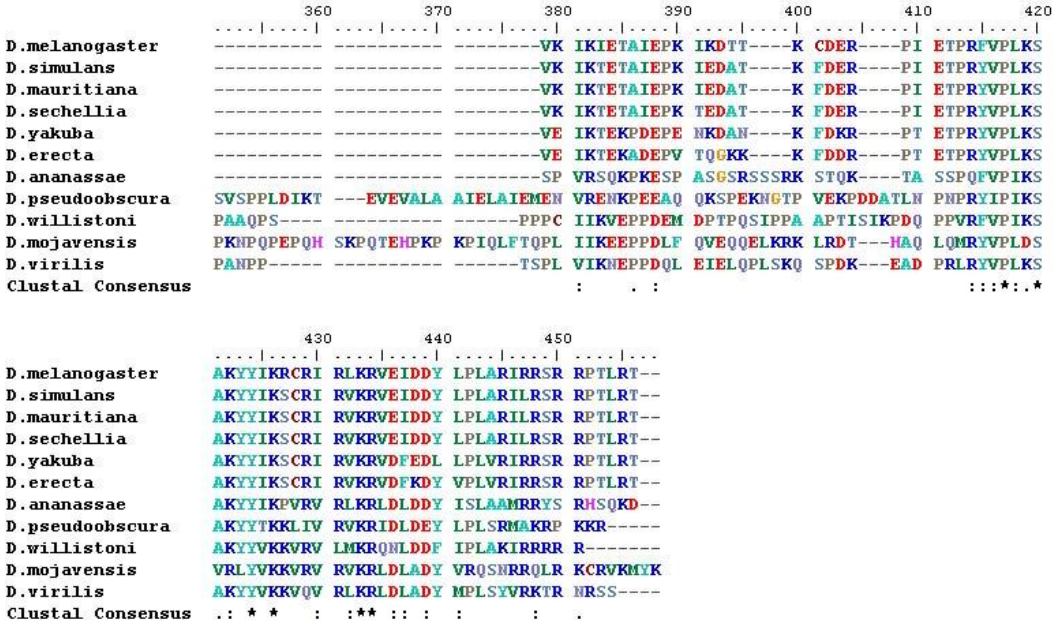

Expression was induced from a second, independently segregating transgene expressing the *S. cerevisiae* transcriptional activator *GAL4* (Figure II.C.2). Control crosses using two different *GAL4*-expressing transgenes suggested that activation of *UAS-Dsim*/*Lhr* does not cause lethality in *D. melanogaster* , as evidenced by the similar numbers of progeny inheriting the *GAL4* driver ("red eyed" in Table II.C.1) compared to those that did not ("orange eyed" and "white eyed") (Table II.C.1 and Table II.C.S1).

This result demonstrated that we could introduce both *UAS-Dsim*/*Lhr* and the *GAL4*-expressing transgenes into hybrids from the *D. melanogaster* parent (Figure II.C.2). In contrast to the intraspecific control cross, when the same *D. melanogaster* females were crossed to *D. simulans* Lhr^1 males, only half of the expected hybrid males carrying the *GAL4*-expressing transgene were obtained (Table II.C.1). PCR-based genotyping confirmed our inference that Lhr^1-rescued males carrying only the *GAL4*-expressing transgene are viable, whereas those carrying both transgenes and thus expressing *UAS-Dsim*/*Lhr* are lethal (Table II.C.S1). The reduced viability in some crosses of Lhr^1-rescued males containing only the *UAS-Dsim*/*Lhr* transgene is likely due to maternal inheritance of the GAL4 protein (Table II.C.S1).

These results suggest that expression of *UAS-Dsim*/*Lhr* complements the Lhr^1 hybrid rescue phenotype. We confirmed that *UAS-Dsim*/*Lhr* expression is not generally lethal to hybrids compared with *D. melanogaster* pure species by testing for effects in hybrid males rescued by a mutation in *Hmr*. We found that both *D. melanogaster* control males and male hybrids rescued by the null mutation $Df(1)Hmr^-$ are fully viable when expressing *UAS-Dsim*/*Lhr* (Table II.C.1).

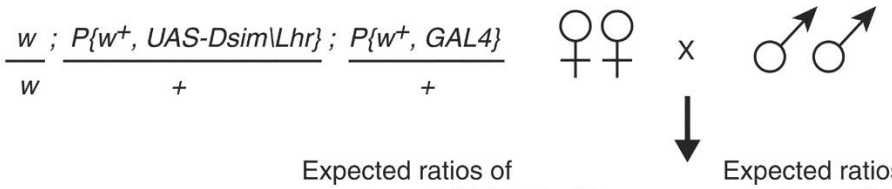

Eye color phenotype:	Expected ratios of genotypes if UAS-Dsim\Lhr expression is viable:	Expected ratios of genotypes if UAS-Dsim\Lhr expression is lethal:
Red	2: UAS/+ ; GAL4/+ and +/+; GAL4/+	1: +/+; GAL4/+
Orange	1: UAS/+; +/+	1: UAS/+; +/+
White	1: +/+; +/+	1: +/+; +/+

Figure II.C.2 Complementation crosses to test for suppression of hybrid male rescue

Female parents are heterozygous for both transgenes, each marked with w^+ producing intermediate levels of eye pigmentation. The *GAL4*-containing transformants have darker eye colors and are epistatic to the lighter-colored *UAS*-containing transformants. The red-eyed class is therefore potentially composed of two distinct genotypes.

Table II.C.1 Number of offspring recovered from complementation tests of hybrid rescue mutations by *UAS-Dsim/Lhr* expression.

Full parental genotypes and female progeny are shown in Table II.C.S1, crosses 9 to 12. UAS indicates *D. simulans Lhr* under yeast UAS transcriptional control; GAL4 indicates yeast GAL4 protein driven by the *Actin5C* promoter. In the absence of viability effects, the ratio of red-eyed:orange-eyed:white-eyed males will be 2:1:1. Deviations from this ratio were tested by X^2 tests. Results for the control cross and the cross with *Df(1)Hmr*$^{-}$ were not significantly different from this ratio ($p > 0.05$). Results for the crosses with *Lhr*^{1} and *Hmr*^{1} were significantly different from this ratio ($p < 0.001$).

Progeny		*D. melanogaster* control	*Lhr*^{1}	*Df(1)Hmr*$^{-}$	*Hmr*^{1}
Phenotype	Genotype				
Red-eyed male	UAS/+;GAL4/+ and +/+;GAL4/+	485	89	169	22
Orange-eyed male	UAS/+;+/+	214	9	82	7
White-eyed male	+/+;+/+	262	94	95	33

Table II.C.S1 Complementation tests of hybrid rescue mutations by D. simulans CG18468 expression

			Female progeny				Male progeny			
Cross	Female parent	Male parent	UAS/+; GAL4/+ and +/+; GAL4/+ (Red eye)	UAS/+; +/+ (Orange eye)	+/+; +/+ (White eye)	Total [a]	UAS/+; GAL4/+ and +/+; GAL4/+ (Red eye)	UAS/+; +/+ (Orange eye)	+/+; +/+ (White eye)	Total [a]
1	*w/w; P{UAS-Dsim\Lhr}3/+; P{tubP-GAL4}LL7/+*	*D. mel. w*^{1118}*/Y* (control)	393	211	177	781 (n.s.)	361	212	183	756 (n.s.)
2	"	*D. sim. Lhr*^{1}				870	210 [c]	225	222	657***
3	*w/w; P{UAS-Dsim\Lhr}13/+; P{tubP-GAL4}LL7/+*	*D. mel. w*^{1118}*/Y* (control)	493	253	225	971 (n.s.)	479	235	232	946 (n.s.)
4	"	*D. sim. Lhr*^{1}				747	202 [d]	170	188	560***
5	*w/w; P{UAS-Dsim\Lhr}3/+; P{Act5C-GAL4} 17bFO1/+*	*D. mel. w*^{1118}*/Y* (control)	130	66	83	279 (n.s.)	145	78	94	317 (n.s.)

Table II.C.S1 (continued)

6	"	*D. sim. Lhr*^{1}				261	72[e]	1[i]	67	140 ***
7[b]	*Df(1)Hmr*$^{-}$*/+; P{UAS-Dsim\Lhr}3/+; P{Act5C-GAL4} 17bFO1/+*	*D. sim.* w^{501}/Y	452	234	244	930 (n.s.)	262	122	138	522 (n.s.)
8[b]	*Hmr*^{1}*/+; P{UAS-Dsim\Lhr}3/+; P{Act5C-GAL4} 17bFO1/+*	*D. sim.* w^{501}/Y	437	206	211	854 (n.s.)	23[f]	19	33	75 ***
9	*w/w; P{UAS-Dsim\Lhr}13/+; P{Act5C-GAL4} 17bFO1/+*	*D. mel.* w^{1118}/Y (control)	541	257	288	1086 (n.s.)	485	214	262	961 (n.s.)
10	"	*D. sim. Lhr*^{1}				404	89[g]	9[i]	94	192 ***
11[b]	*Df(1)Hmr*$^{-}$*/+; P{UAS-Dsim\Lhr}13/+; P{Act5C-GAL4} 17bFO1/+*	*D. sim.* w^{501}/Y	380	190	203	773 (n.s.)	169	82	95	346
12[b]	*Hmr*^{1}*/+; P{UAS-Dsim\Lhr}13/+; P{Act5C-GAL4} 17bFO1/+*	*D. sim.* w^{501}/Y	557	323	296	1176 (n.s.)	22[h]	7	33	62 ***

Table II.C.S1 (continued)

Data from crosses 9 - 12 are summarized in Table 1.
Progeny were scored by eye color and classified according to the inferred genotypes (see Fig. 2).

[a] The ratio of red eye : orange eye : white eye was tested for deviation from a 2:1:1 ratio using Chi-squared test. *** = $p < 1 \times 10^{-3}$; n.s. = $p > 0.05$

[b] Only half the male progeny will inherit the *Df(1)Hmr*$^{-}$ or *Hmr*^{1} hybrid rescue mutation in these crosses because the female parent is heterozygous.

[c] 11 males were tested by PCR; all carried the GAL4 transgene and none carried the UAS transgene.

[d] 9 males were tested by PCR; all carried the GAL4 transgene and 1 carried the UAS transgene. An additional 24 red-eyed males from an independent repetition of this cross were also tested by PCR; all carried the GAL4 transgene and none carried the UAS transgene.

[e] 8 males were tested by PCR; all carried the GAL4 transgene and none carried the UAS transgene.

[f] 7 males were tested by PCR; all carried the GAL4 transgene and none carried the UAS transgene.

[g] 9 males were tested by PCR; all carried the GAL4 transgene and none carried the UAS transgene.

[h] 8 males were tested by PCR; all carried the GAL4 transgene and none carried the UAS transgene.

[i] We infer that reduced viability of these males is caused by *Actin-GAL4* expressing GAL4 in the maternal germline, which is inherited by her progeny and activates transcription of the zygotically inherited *P{UAS-Dsim\Lhr}* transgene to a level sufficient to suppress the *Lhr*^{1} rescue mutation. Lethality caused by the insertion of the *UAS* transgene is unlikely, because it occurred with both independent insertions in these crosses (crosses 6 and 10), but not with the same insertions in crosses using *Tubulin-GAL4* (crosses 2 and 4).

RT-PCR experiments demonstrated that *UAS-Dsim*/*Lhr* was expressed in these crosses (Figure II.C.S3). We concluded that *UAS-Dsim*/*Lhr* expression specifically complements the Lhr^{1} mutation in hybrids, that *CG18468* is *Lhr*, and that *Lhr* is a major-effect hybrid lethality gene. For *Lhr* to fit the Dobzhansky-Muller model of functional divergence, *D. simulans Lhr*, but not *D. melanogaster Lhr*, must cause hybrid lethality (Figure II.C.1A). Crosses with three different *D. melanogaster* Lhr^{-} deletions produced essentially only F1 hybrid females, demonstrating that removal of *D. melanogaster Lhr* does not suppress F1 male lethality (Figure II.C.S4 and Table II.C.S2).

Genetic and molecular analyses have demonstrated that Hmr^{1} retains partial *Hmr* activity (Barbash, Roote, Ashburner 2000; Barbash et al. 2003). In contrast to the results shown in Table II.C.1, which used the null allele *Df(1)*Hmr^{-}, we found that rescue of hybrids by the hypomorphic mutation Hmr^{1} is suppressed by *D. simulans Lhr* expression (Table II.C.1 and Table II.C.S1). These data suggest that the lethal effect of *D. simulans Lhr* requires the presence of *D. melanogaster Hmr* function. The deleterious effects of a *D. melanogaster* Hmr^{+} duplication are suppressed by Lhr^{1} (Barbash, Roote, Ashburner 2000; Orr, Irving 2000), results that suggest, based on our characterization of the Lhr^{1} mutation, that *D. melanogaster Hmr* requires a functional *D. simulans Lhr* to cause lethality. These reciprocal genetic interactions are consistent with the model of *Hmr* and *Lhr* forming a Dobzhansky-Muller pair of interacting genes (Figure II.C.1A).

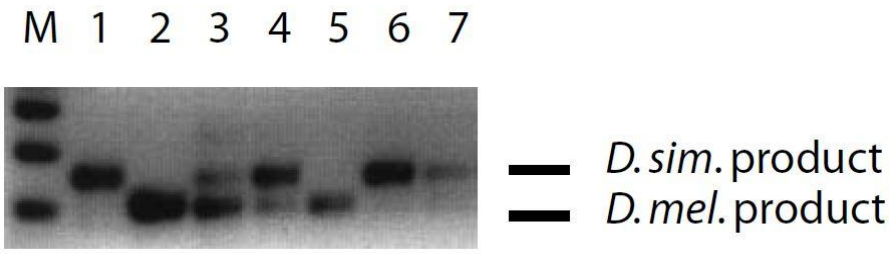

Figure II.C.S3 *UAS-Dsim\Lhr* is expressed in *Df(1)Hmr*– hybrid males that are fully viable

RT-PCR was performed on cDNA synthesized from RNA from red-eyed and white-eyed males described in Table II.C.1, crosses 7 and 11, using the primers 5'-CCAAGTCCTTTAACCAAAGCTACGA-3' and 5'-ACACTTGGTTTTCGGCACATCCGC- 3'. The PCR primers used span an insertion in *D. simulans Lhr* relative to *D. melanogaster Lhr* (see Figure II.C.1C), and thus amplify bands of 277 bp in *D. simulans* and 259 bp in *D. melanogaster*. Lane M, 100 bp ladder showing bands of 200, 300 and 400 bp. Lane 1, control PCR using genomic DNA from *D. simulans*. Lane 2, control PCR using genomic DNA from *D. melanogaster*. Lane 3, control PCR using an equal amount of DNA template from lanes 1 and 2. Lane 4, cDNA made from red-eyed flies in Table II.C.1, cross 7. Note that only half the flies will carry the *UAS-Dsim\Lhr* transgene. Lane 5, cDNA made from white-eyed flies in Table 1, cross 7. Lane 6, cDNA made from red-eyed flies in Table II.C.1, cross 11. Lane 7, cDNA made from white-eyed flies in Table II.C.1, cross 11. It is unclear why the *D. melanogaster* product is predominant in lane 5 and the *D. simulans* product predominant in lane 7. However, in both cases the red-eyed siblings have significantly more *D. simulans* product than the white-eyed siblings, which is consistent with expression of the *UAS- Dsim\Lhr* transgene.

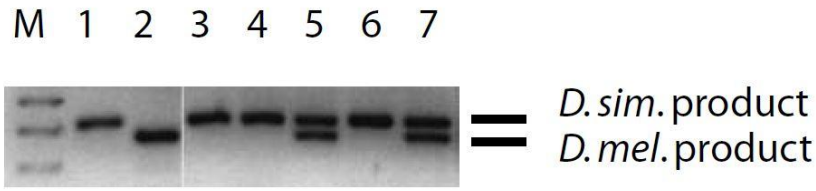

Figure II.C.S4 Three *D. melanogaster* deletions that remove *Lhr* function

DNAs from F1 hybrid females carrying a *D. melanogaster* deletion over a wild type *D. simulans* chromosome, and various control genotypes, were PCR amplified using the same primers as in Figure II.C.S3. These primers amplify from both species across the region containing the 16 amino acid-insertion *D. simulans* (Figure II.C.1C). Df/CyO *D. melanogaster* females were crossed to *D. simulans* males to generate F1 hybrid females. Lane M, 100 bp ladder showing bands of 200, 300 and 400 bp. Lane 1, control PCR using genomic DNA from *D. simulans*. Lane 2, control PCR using genomic DNA from *D. melanogaster*. Lane 3, DNA from *P{w+mC=lacW}l(2)k01209[k08901a] P{lacW}k08901b /IIsim* F1 hybrid females; Lane 4, DNA from *Df(2R)BSC44 /IIsim* F1 hybrid females; Lane 5, DNA from *CyO /IIsim* F1 hybrid females, from same cross as in lane 4; Lane 6, DNA from *Df(2R)BSC49 /IIsim* F1 hybrid females; Lane 7, DNA from *CyO /IIsim* F1 hybrid females from same cross as in lane 6.

Table II.C.S2 Testing *D. melanogaster Lhr*- defiencies for hybrid rescue.

		Female hybrids		Male hybrids	
Female parent	Male parent	Df/+	+/+	Df/+	+/+
Df(2R)BSC44/SM6a	*D. mauritiana w f*	68	65	0	0
Df(2R)BSC44/SM6a	*D. simulans C167.4*	111	110	0	1 [a]
Df(2R)BSC49/SM6a	*D. simulans w501*	96	83	0	0
Df(2R)BSC49/SM6a	*D. simulans C167.4*	12	10	1 [a]	0
$y^1\ w^{67c23}$; $P\{w^{+mC}=lacW\}l(2)k01209[k08901a]$ $P\{lacW\}k08901b/CyO$	*D. simulans w501*	59	44	0	0

Deficiency / + (Df/+) progeny are *Cy*+ and have straight wings; +/+ progeny carry the *SM6a* or *CyO* balancer chromosome and have curly wings.

[a] These F1 hybrid males may be patroclinous exceptions carrying the D. simulans Xchromosome but this could not be determined by visible markers in these crosses.

Functional divergence between species led us to examine the evolutionary forces driving the sequence divergence of *Lhr*. The high K_A/K_S value of 0.731 between *D. melanogaster* and *D. simulans* is consistent with either positive selection or relaxed selective constraint. We sequenced multiple alleles of *Lhr* from *D. melanogaster* and *D. simulans* and performed a McDonald-Kreitman test. The results of this test rejected the null hypothesis that these genes are evolving neutrally (Fisher's Exact Test, $P = 0.011$) and suggested that there is an excess of nonsynonymous fixations between the species (Table II.C.S3). Phylogenetic analyses further suggest that the K_A/K_S ratio has increased on branches leading to *D. melanogaster* and its sibling species (Figure II.C.S5).

The McDonald-Kreitman and K_A/K_S tests only consider alignable regions of the *Lhr* coding region. *Lhr* from *D. simulans* and its sister species *D. mauritiana* and *D. sechellia* each contain a 16–amino acid insertion, interrupting a potential leucine zipper domain, relative to *D. melanogaster* and outgroup species (Figure II.C.1C and Figure II.C.S2). Notably, we found that this insertion is precisely deleted in a second *D. simulans* stock named Lhr^2, which also produces viable F1 hybrid males (H.A. Orr personal communication). Although Lhr^2 contains additional amino acid substitutions relative to Lhr^+ alleles, its hybrid rescue phenotype suggests that the functional divergence of *D. simulans Lhr* may be caused by the 16–amino acid insertion.

Table II.C.S3 McDonald-Kreitman tests reject neutral evolution for *Lhr*

		Divergence		Polymorphism		
	Species or lineage	Nonsynon-ymous	Synon-ymous	Nonsynon-ymous	Synon-ymous	F.E.T.* *p* (2 tailed)
	D.mel. & *D.sim.*	50	20	12	16	0.011
Outgroup: *D.yak.* †	*D.mel.* lineage	27	11	1	4	0.043
	D.sim. lineage	19	6	11	12	0.073
Outgroup: *D.ere.* †	*D.mel.* lineage	22	11	1	4	0.136
	D.sim. lineage	23	6	11	12	0.022

* F.E.T. = Fisher's Exact Test.

† Some sites had three different nucleotides in *D. melanogaster*, *D. simulans* and the outgroup and thus could not be polarized to either lineage. Such ambiguous sites were excluded from the analysis. The different results obtained with the two different outgroups might be caused in part by differences in the ambiguous sites obtained with *D. yakuba* or *D. erecta*. These results suggest that the signal of positive selection reflects divergence along the lineages of both species.

Figure II.C.S5 Phylogenetic trees of *Lhr*

(A) A maximum-parsimony phylogenetic tree for *Lhr* in *melanogaster* subgroup species. The lengths of the branches are proportional to the nucleotide changes of the gene and the bootstrap values are indicated above the nodes. A Neighbor-Joining tree gave similar results except that the bootstrap value for the grouping of *D. simulans* and *D. sechellia* is 80. The Kimura 2-parameter model was used for the Neighbor-Joining tree. (B) A maximum-likelihood phylogenetic tree of *Lhr* gene built by the two-ratio model in PAML (CodonFreq=3 [estimating frequency for each codon], model=2, NSsites=0). The lineages leading to *D. melanogaster* and its siblings species were specified to be the foreground lineages and to have a different K_A/K_S value from the rest of the lineages. The number shown above each branch is its estimated K_A/K_S value. The tree length is defined as the number of nucleotide substitutions per codon. A two-ratio model, which assumes that *D. melanogaster* and its sibling species evolve with a different K_A/K_S ratio from the rest of the lineages, fits the data significantly better than the one-ratio model ($2*\Delta l=6.4169$, df=1, p=0.0113).

A.

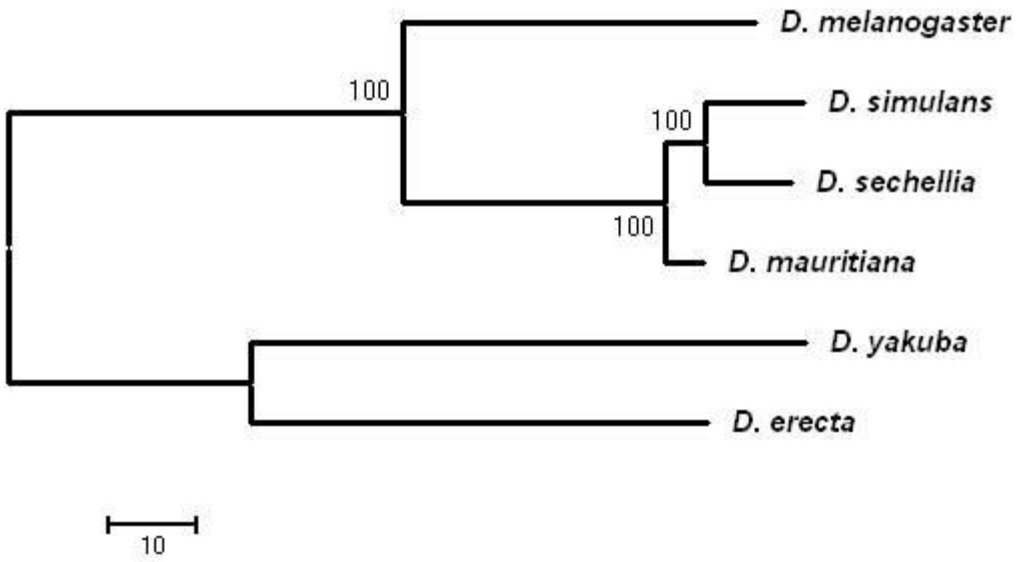
D. melanogaster
D. simulans
D. sechellia
D. mauritiana
D. yakuba
D. erecta
100
100
100
10

B

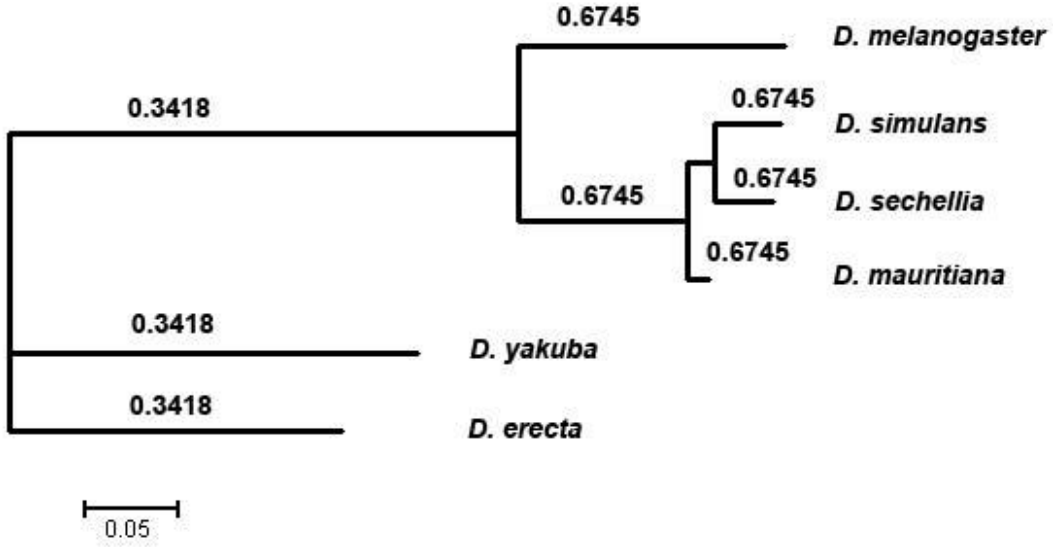
0.6745
D. melanogaster
0.3418
0.6745
D. simulans
0.6745
D. sechellia
0.6745
0.6745
D. mauritiana
0.3418
D. yakuba
0.3418
D. erecta
0.05

Heterochromatin Protein 1 (HP1) is a chromodomain-containing protein that localizes to heterochromatic regions of chromosomes and is required to maintain heterochromatic states (Eissenberg, Elgin 2000). LHR was previously identified (as CG18468) as interacting with HP1 in a yeast two-hybrid assay (Giot et al. 2003). We confirmed this interaction (Figure II.C.3A), and discovered that *D. simulans* LHR also interacts with *D. melanogaster* HP1 (Figure II.C.3B). Because *D. simulans* HP1 is nearly identical to *D. melanogaster* HP1 (Figure II.C.S6) we hypothesize that *D. simulans* LHR also binds to *D. simulans* HP1. This apparent conservation of HP1-binding function of LHR suggests that the intraspecific function of *Lhr* is conserved between *D. melanogaster* and *D. simulans*, in contrast to the interspecific function for hybrid lethality, which we have shown is specific only to *D. simulans Lhr*.

A *D. melanogaster* LHR–yellow fluorescent protein (YFP) fusion protein accumulated in a small number of foci (usually 1 to 2) in salivary gland nuclei (Figure II.C.S7), similar to HP1 (Powers, Eissenberg 1993). In polytene chromosomes, HP1 accumulates predominantly in the chromocenter and along the highly heterochromatic fourth chromosome as well as at telomeres and a number of bands along the euchromatic arms (Fanti et al. 2003). LHR-YFP has a similar pattern and predominantly colocalizes with HP1 (Figure II.C.3, C to E). We suggest that *Lhr* may be coevolving with rapidly evolving heterochromatic repetitive DNAs, consistent with the hypothesis that the molecular drive inherent in repetitive DNAs contributes to hybrid incompatibilities and speciation (Dover 1982; Henikoff, Ahmad, Malik 2001).

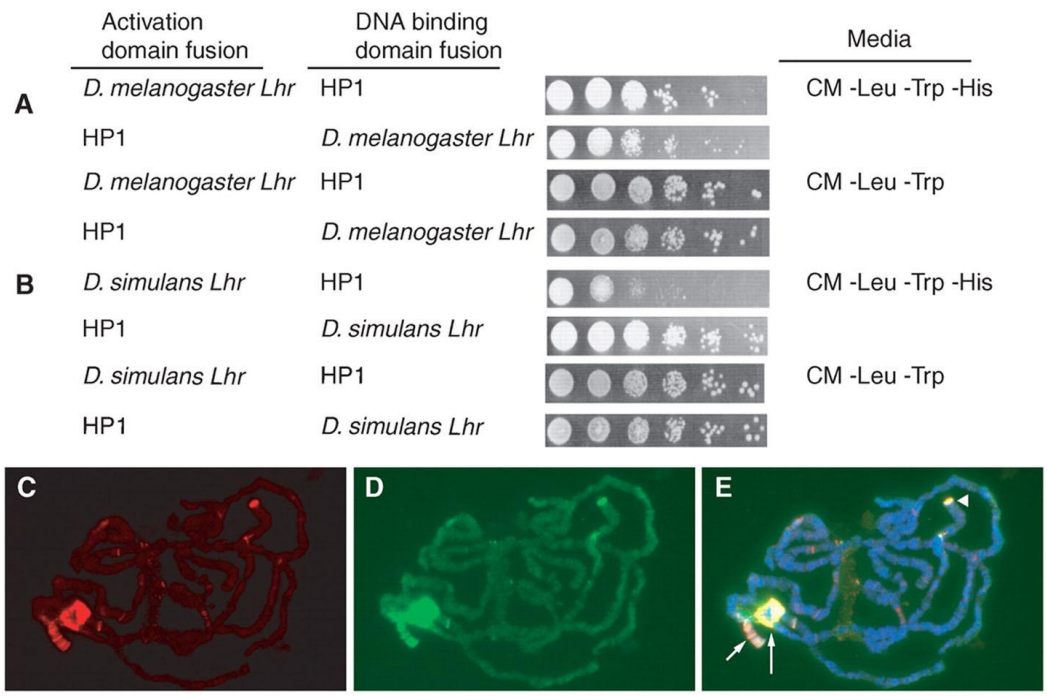

Figure II.C.3 LHR interacts and colocalizes with HP1

(A) *D. melanogaster* LHR interacts with *D. melanogaster* HP1. Yeast two-hybrid interactions were detected by activation of *HIS3* and growth on media lacking histidine; loading controls [complete media (CM) -Leu -Trp] contain histidine. (B) *D. simulans* LHR interacts with *D. melanogaster* HP1. (C to E) Colocalization of *D. melanogaster*YFP::LHR and HP1 on salivary gland polytene chromosomes. Chromosomes from *P*{*UAS-YFP::Lhr*}168-3/+;*P*{*GawB*}*C147*/+ third-instar larvae were incubated with primary antibodies to GFP and HP1, which were detected using rhodamine red-X–conjugated (red) and cyanine-conjugated (green) secondary antibodies, respectively. (C) Antibody to GFP to detect YFP::LHR. (D) Antibody to HP1. (E) Merge with 4',6'-diamidino-2-phenylindole signal (blue) to detect DNA. A predominant colocalization occurs at the chromocenter (long arrow), fourth chromosome (short arrow), and a telomere (arrowhead).

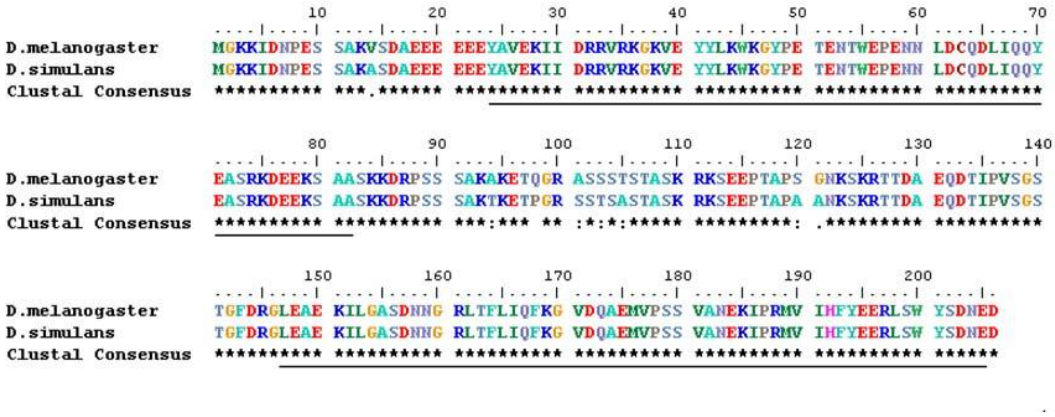

Figure II.C.S6 Alignment of HP1 orthologs from *D. melanogaster* and *D. simulans*

These proteins are 96.1% identical, the chromodomain (AA 24-82) and chromoshadow domains (AA 147-205), underlined, are identical.

A. B.

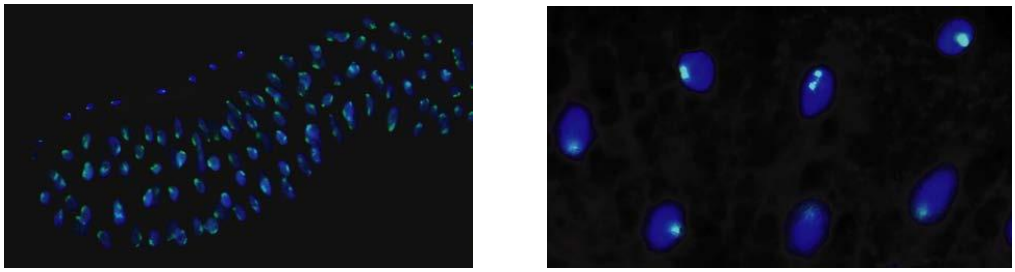

Figure II.C.S7 *D. melanogaster* LHR::YFP localization in salivary gland nuclei

Intact salivary glands from *P{UAS-Lhr::YFP}169-2/+; P{Act5C-GAL4}17bFO1/+* third instar larvae were fixed and stained with DAPI. Signals from YFP fluorescence and DAPI are shown in yellow and blue, respectively. (B) is a higher magnification view of a section of (A). Note the 1-2 foci of staining in most nuclei. Similar results were seen using an N-terminal fusion of YFP to LHR.

Hmr and *Lhr* cause F1 hybrid lethality because they are partially or fully dominant. The large number of HI genes estimated from other studies (Mallet 2006) may be mechanistically distinct because they are recessive and only cause HI when homozygous in F2 hybrids or in interspecific introgressions. However, our results also show that the interaction of *Hmr* and *Lhr* alone is insufficient to recapitulate hybrid lethality, because control crosses showed that expression of *D. simulans Lhr* does not cause lethality in a *D. melanogaster* pure-species background (Table II.C.1 and Table II.C.S1). Pontecorvo suggested that an interaction among the *D. melanogaster X* (which contains *Hmr*), *D. simulans* chromosome II (which contains *Lhr*), and *D. simulans* chromosome III causes hybrid lethality (Pontecorvo 1943). Hybrid lethality may therefore be enhanced by a multilocus interaction involving additional genes. Alternatively, *Hmr* and *Lhr* may be the only major-effect genes, but their lethal interaction requires a hybrid genetic background. We suggest that altered chromosome morphology and chromatin structure in hybrids due to the cumulative effects of species-specific differences in satellites, transposable elements, and other repetitive DNAs cause this hybrid genetic background effect.

III. INVESTIGATING THE EFECTS OF LHR DIVERGENCE ON ITS FUNCTIONS AND INTERACTIONS.

III.A INTRODUCTION

The Biological Species Concept is a widely accepted definition of species in which species are defined as groups of interbreeding populations that are reproductively isolated from other groups (Mayr 1963). Hybrids between closely related species are often inviable or sterile, and this inviability and sterility is collectively called hybrid incompatibility (HI). Crosses between *Drosophila melanogaster* and its sibling species *D. simulans* produce incompatible hybrids. In the cross of *D. melanogaster* females to *D. simulans* males, the F1 daughters are semi-viable but sterile, and the sons are inviable (Sturtevant 1920; Lachaise et al. 1986).

Two genes, *Hybrid male rescue (Hmr)* in *D. melanogaster,* and *Lethal hybrid rescue* (*Lhr*) in *D. simulans*, are major-effect contributors to hybrid incompatibility on the basis that loss-of-function mutations in each gene can independently suppress hybrid male lethality (Hutter, Ashburner 1987; Barbash et al. 2003; Brideau et al. 2006). *Lhr* encodes a small protein (319 AA) and appears to be *Drosophila* specific, as we are unable to identify homologs in vertebrates or invertebrates, including in other insect genera (Brideau et al. 2006). Furthermore, among *Drosophila* species, the coding sequence of *Lhr* is also highly divergent, with limited regions of identity as well as extensive indel variation. Between *D. melanogaster* and *D. simulans Lhr* has a high K_A/K_S value of 0.731, and population genetic analyses demonstrate that this high divergence is consistent with positive selection (Brideau et al. 2006).

LHR localizes to heterochromatic sites on salivary gland polytene chromosomes in a pattern similar to, but not completely overlapping with, Heterochromatin Protein 1 (HP1) (Brideau et al. 2006). HP1 is a well-studied chromosomal protein that is found in eukaryotes ranging from fission yeast to humans, and is encoded by the *Su(var)2-5* gene in *Drosophila* (Eissenberg et al. 1990; Singh, Georgatos 2002). HP1 localizes to pericentric and telomeric heterochromatin, and to approximately 200 euchromatic sites throughout the genome (Fanti et al. 2003; de Wit, Greil, van Steensel 2005). The localization of HP1 is consistent with its multiple functions in establishment and spreading of heterochromatin, telomere capping, and both silencing and activation of gene expression (Dorer, Henikoff 1997; Fanti et al. 1998; Lu et al. 2000; Hines et al. 2009).

Greil et al. (2007) identified four new heterochromatin proteins (HPs) based on their association with HP1, which they named HP3, HP4, HP5 and HP6. HP3 was independently identified as LHR (Brideau et al. 2006); HP4 was independently identified as the protein HP1-interacting protein (Hip) (Schwendemann et al. 2008); and HP6 was independently identified as the protein Umbrea (Joppich et al. 2009). Like mutations in HP1, mutations in HP4 and HP5 dominantly suppress position-effect variegation, while analysis of HP6 suggests that it has a role in telomere protection (Greil et al. 2007; Schwendemann et al. 2008; Joppich et al. 2009). HP3 (LHR), HP4 (Hip) and HP5 all have similar expression patterns as HP1, being enriched in ovaries and early embryos (Stolc et al. 2004). Based on their common localization to heterochromatin, their similar expression patterns, and their proposed physical interactions, HP1, LHR, HP4, and HP5 may form a multi-protein heterochromatic complex in vivo. I was interested in understanding the

interactions among these heterochromatic proteins because we have previously suggested that the association of LHR with heterochromatin contributes to hybrid incompatibilities and speciation (Brideau et al. 2006).

Of particular interest is whether and how the interactions and functions of LHR may be evolving. This interest stems from a fundamental prediction of the Dobzhansky-Muller model that HIs are asymmetric. Here this means that hybrid male lethality is caused specifically by the interaction of *D. melanogaster* HMR (mel-HMR) and *D. simulans* LHR (sim-LHR), and not by sim-HMR and mel-LHR. We confirmed this prediction of asymmetry for LHR by demonstrating that a loss-of-function mutation in sim-LHR suppresses hybrid male lethality, but loss-of-function deletions of mel-LHR do not (Brideau et al. 2006).

What is the nature of this functional divergence for an HI protein like LHR, especially in light of the evidence that LHR is rapidly evolving and has diverged under adaptive evolution? One possibility is that sim-LHR or mel-LHR has evolved a new function (neofunctionalization) distinct from their common ancestor. Another possibility is that sim-LHR or mel-LHR has lost ancestral functions. Finally, one could envision that divergence has led to complex or subtle changes in function.

We showed previously that sim-LHR retains the ability to interact with mel-HP1 in a yeast two-hybrid assay (Brideau et al. 2006), suggesting that LHR has not undergone a complete change in functional properties between *D. melanogaster* and *D. simulans*. Here I have extended this and other functional assays to LHR orthologs. First, I found that all LHR orthologs tested appear to have the same molecular interaction and localization properties. Second, and most surprising, I found that both *D. melanogaster* and *D.*

simulans Lhr can induce *D. melanogaster-D. simulans* hybrid lethality.

III.B MATERIALS AND METHODS

Cloning and DNA manipulations

The coding sequences for HP1, HP4, HP5, HP6 and seven *Lhr* orthologs were PCR amplified with primers listed below using Pfx DNA polymerase (Invitrogen) from the following sources: *D. melanogaster* Oregon R (for *Lhr*); *D. melanogaster* w^{1118} (for the HPs); *D. simulans* C167.4 (for *Lhr* and HP6), *D. yakuba* Y9 and *D. erecta* E1 and wild type strains of *D. ananassae*, *D. pseudoobscura* and *D. virilis* were from Aquadro or Clark labs. HP1, HP4, HP5, and Lhr orthologs were first amplified by RT-PCR (Invitrogen Superscript III) using 1µg of total RNA from embryos. All coding sequences were then cloned into pENTR-D-TOPO (Invitrogen) according to the manufacturer's instructions, and verified by sequencing.

Entry vectors containing the CDS of interest were then recombined with destination vectors in an LR Clonase-mediated reaction. The destination vectors used were: pHMW for cell culture transfections, pTWV and pTWV-attB for site-specific transgene integration, (pHMW and pTWV are described at http://www.ciwemb.edu/labs/murphy/Gateway%20vectors.html), pEXP-1 for the *in vitro* binding assay (Invitrogen), and pGADT7-AD and pGBKT7-DNA-BD for the yeast two-hybrid assays (K. Ravi Ram, A. Garfinkel, and M.F. Wolfner, Cornell University; personal communication). An *attB* site was added into pTWV by using primers F-5'-AAACCCAGGCCTATGCCCGCCGTGACCGTC-3' and R-5'-AAACCCAGGCCTGATGTAGGTCACGGTCTCG-3', to amplify the *attB* sequence from pTA-attB (personal communication from Michele Calos),

followed by digestion with *Afe*I, and ligation into the *Afe*I site in pTWV to create the plasmid pTWV-attB.

Site-directed mutagenesis of full length *Lhr* was done using the QuickChange site-directed mutagenesis kit (Stratagene) by following the manufacturer's protocol with the primers listed in the primers section. The PxDxL, PxVxS and both IxPxV motifs were changed to AxAxA and the LxVxV motif, was changed to LxAxA. The two amino acids in Region 1 (FL), and all four of the amino acids in Region 2 (RCRI) were converted to alanine.

Cell culture and DNA transfections

Drosophila Kc-167 cells were grown at 25°C in M3 medium (HyClone) until reaching a density of 10^6 cells/mL. Cells were then transfected with 1 μg DNA plus 10 μL Cellfectin (Invitrogen) in 1 mL of M3 media. Cells were grown for two additional days, and then either processed, or subjected to 2 hour heat shock and 4 hour recovery, and then processed. Nuclear extracts were prepared as follows: cells were pelleted, resuspended in 1 mL Buffer 1 (10 mM Tris-Cl pH 8.0, 300 mM sucrose, 3 mM $CaCl_2$, 2 mM $Mg(CH_3COO)_2$, 0.1% TritonX-100, 0.5 mM DTT) and homogenized 50 times in a dounce homogenizer (Bellco, pestle B). Cell extracts were centrifuged at 700xg for 5 minutes at 4°C, pellets washed with 1 mL Buffer 1, and centrifuged again at 700xg for 5 minutes at 4°C. Pellets were resuspended in 100 μL Buffer 2 (50 mM Tris-Cl pH 8.0, 25% glycerol, 5 mM $Mg(CH_3COO)_2$, 0.1 mM EDTA, 5 mM DTT) and either used for immunoprecipitation assays or mixed with SDS sample buffer.

Immunoprecipitation assays

Kc cell nuclear extracts were mixed with either mouse anti-MYC (2.5 μL, Roche) or mouse anti-HP1 (5 μL of monoclonal supernatant, DSHB) antibodies and 25 μL protein-G coupled magnetic beads (Invitrogen), brought to 500 μL in IP Buffer (1xPBS, 0.1% Triton X-100, 1 mM PMSF, 50X protease inhibitor cocktail [Roche], 1 unit DNase [Roche], 1 unit RNase [Roche]) and rotated for 4 hours at 4°C. Magnetic bead-antibody-protein complexes were then captured following the Invitrogen Dynabeads protocol, except for the final elution, where the beads were added directly to 4x SDS sample buffer and boiled for five minutes.

Western blots

Protein samples were run on 10% SDS polyacrylamide gels and transferred to PVDF (Millipore) membrane for 60 minutes at 100 V. Blots were blocked in 5% nonfat milk for 60 minutes, rinsed with TBS-T (1x TBS, 0.1% Tween-20) and incubated overnight at 4°C in primary antibody solution (1X TBS-T, 5% BSA, 0.02% NaN_3). Primary antibodies were used at 1:1000 for mouse anti-MYC (Roche), mouse anti-HP1 (DSHB), and rat anti-HA (Roche). Blots were washed 3 times for 10 minutes in TBS-T and incubated for 2 hours in secondary antibody solution (1X TBS-T, 2.5% nonfat milk). Horseradish peroxidase-conjugated anti-mouse, anti-rat, and anti-rabbit secondary antibodies (Jackson Labs) were used at 1:10,000. Blots were then washed 3 times for 10 minutes in TBS-T and developed using an ECL Western Blotting kit (Pierce).

In vitro binding assays

The coding sequences for HP1 and LHR-HA were cloned into the pEXP-1 vector (Invitrogen). Proteins were synthesized by mixing 1.0 μg of pEXP-1 DNA and 25 μL of the TnT quick-coupled transcription/translation kit according to the manufacturer's protocol and incubating the mixture at 30°C for 90 minutes (Promega). 15μL of each synthesized protein extract was then mixed with antibodies, beads, and IP buffer to 250 μL, as described above for the immunoprecipitation assay. Protein complexes were captured and immunoprecipitation was assayed by Western blot as above, except that rat anti-HA (Roche) was used for LHR pulldown.

Drosophila stocks and crosses

Flies were reared on standard yeast glucose media and raised at room temperature (~23°C) on a 12 hr light / 12 hr dark cycle. The *D. melanogaster* $In(1)w^{m4h}$; $Su(var)205^{5}/In(2L)Cy, In(2R)Cy, Cy^{1}$ and $y^{1}\ w^{67c23}$; $P\{w^{+mC}\ y^{+mDint2}=EPgy2\}HP4^{EY01733}$ and $y^{1}\ w^{67c23}$; $P\{w^{+mC}\ y^{+mDint2}=EPgy2HP5^{EY10901}$ stocks were obtained from the Bloomington Stock Center. w^{1118}; $HP6^{36-5}$ was a gift from Dr. Satoru Kobayashi and $In(1)w^{m4h}$; $Su(var)205^{04}/Cy\ Roi$ was obtained from Dr. Barbara Wakimoto (personal communication).

Purified *D. simulans, D. yakuba,* and *D. virilis Lhr-pTWV-attB* plasmid DNA was injected into the strain $y^{1}\ M\{vas\text{-}int.Dm\}ZH\text{-}2A\ w^{*}$; *M{3xP3-RFP.attP}ZH-86Fb* (Bischof et al. 2007) by Genetic Services (Cambridge, MA) using the ϕC31 site-specific integration method (Groth et al. 2004). The *D. melanogaster Lhr- pTWV* transgene did not contain the *attB* sequence and were transformed into w^{1118} using P-element mediated transformation. For the LHR localization assays in mutant HP backgrounds, the LHR-YFP stock used

for each LHR ortholog contained a recombinant chromosome consisting of *P{ w^{+mC} Scer\UAS-Lhr::Avic\Venus =UAS-Lhr::YFP}* and the salivary gland specific Gal4 driver *P{Scer\GAL4^{wB} $w^{+mW.hs}$=GawB}c729*. This recombinant *UAS-Gal4* chromosome was then crossed into the *HP* mutant backgrounds in order to assay LHR-YFP localization. For the LHR localizations assays in otherwise wild type background (both whole-mount and squashed polytene analyses) of each LHR-YFP transgene, F1 larvae heterozygous for the UAS-LHR-YFP transgene and salivary gland Gal4 driver c279 were analyzed.

Yeast two-hybrid assays

Yeast two-hybrid assays were performed as described in Brideau et al. 2006.

Immunofluoresence

For Kc cell staining, cells were transfected as above with Lhr-pHMW DNA, and were subjected to heat shock and recovery, followed by resuspension to a density of $1x10^4$ cells/mL. 100 µL of this suspension was incubated on poly-L-lysine treated coverslips for 1 hour. Excess cell suspension was aspirated away, and coverslips were washed with 1X PBS twice. Cells were fixed in 200 µL of 4% paraformaldehyde in PBS for 30 minutes at 37° C, and then rinsed with PBS. Cells were permeabilized by incubation in 0.2% Triton X-100 in PBS for 10 minutes at room temperature. 1% BSA in PBS was added as a blocking solution for 1 hour at room temperature. 200 µL of mouse anti-MYC antibody (Roche) diluted at 1:100 in PBS was added to the coverslips and cells were incubated at 4°C overnight. Cells were washed 4 times in PBS, and Alexa anti-mouse 488 secondary antibody (Invitrogen) was added at 1:300 in PBS for 1 hour at room

temperature. Coverslips were washed 3 times in PBS and mounted in Vectashield (Vector labs).

For whole-mount salivary gland preparations, tissues from third instar larvae were dissected in PTX (1X PBS, 0.3% Triton X-100). For detection of liveYFP, glands were fixed for 8 minutes in 3.5% paraformaldehyde in PTX and rinsed 3 times in PTX. During the third wash, DAPI was added to a concentration of 1 µg/ml and samples were incubated for 2 minutes at room temperature. Glands were then washed 3X in PTX for 5 minutes and mounted in Vectashield.

For polytene squashes, glands were dissected in 0.7% NaCl, fixed for 8 minutes with 1.85% paraformaldehyde in 45% acetic acid, and squashed. Chromosomes were incubated overnight at 4°C with the primary antibodies mouse anti-HP1 (DSHB) at 1:10 and rabbit anti-GFP (Invitrogen) at 1:100 in PBS + 0.05% Tween-20, followed by incubation for two hours at room temperature with Alexa anti-mouse 546 and Alexa anti-rabbit 488 secondary antibodies (Invitrogen) at 1:300 in PBS + 0.05% Tween-20. All samples were mounted in Vectashield.

Divergence Calculations

Orthologous coding sequences for each gene were obtained from Flybase (Grumbling, Strelets, Consortium 2006), aligned using ClustalW (Thompson, Higgins, Gibson 1994), and processed into .MEG format using MEGA (Kumar, Tamura, Nei 2004). Divergence data for nucleotide changes were calculated with DnaSP (Rozas et al. 2003).

Primers:

D. melanogaster Lhr

F- 5’-ATGAGTACCGACAGCGCCGAGGAA-3’

R- 5’-TCATGTTCTCAGCGTAGGCCG-3’

D. simulans Lhr

F- 5’-ATGAGTACCGACAGCGCCGAGGAA-3’

R- 5’-TCATGTTCTCAGCGTAGGCCG-3’

D. yakuba Lhr

F- 5’-ATGAGTACCGACAGCGCCGAGGAA-3’

R- 5’-TCATGTTCTTAGCGTAGGCCTTCTG-3’

D. erecta Lhr

F- 5’-ATGAGTACCGACAGCGCCGAGGAA-3’

R- 5’-TCATGTTCTCAGCGTAGGCCGCC-3’

D. ananassae Lhr

F- 5’-ATGAGCGAGGAAGTTGGGGCTCTT-3’

R- 5’-TCAATCTTTTTGTGAATGGCGACT-3’

D. pseudoobscura Lhr

F- 5’-ATGGATACCGAAGCGGGAATGGAC-3’

R- 5’-TTAACGTTTCTTTGGGCGCTTTGC-3’

D. virilis Lhr

F- 5’-ATGGATGGCTTGGAGGATGCATCC-3’

R- 5’-TCAGGAGCTTCTGTTGCGGGTCTT-3’

D. melanogaster Su(var)2-5

F- 5’-ATGGGCAAGAAAATCGACAACC-3’

R- 5’-TTAATCTTCATTATCAGAGTACC-3’

D. melanogaster HP4

F- 5’-ATGTCACCGAAGACTAAAAAAATG-3’

R- 5’-GATTGTCAGATTAGACTCC-3’

D. melanogaster HP5

F- 5’–ATGGATATTTTTGATATGG-3’

R- 5’-CGATTCTAACGCGGTCATTATTTC-3’

D. melanogaster HP6

F- 5’-ATGCCCAGCTCCACTTTGACG-3’

R- 5’-CTAGGCATTTCGTGATCGTTTCTTC-3’

D. melanogaster rhino

F- 5’-ATGTCTCGCAACCATCAGC-3’

R- 5’-TTACTTGGGCACAATGATCCTC-3’

IxPxV #1 to AxAxA

F-5’-GGTATCCCTTCCTTGCCATCGCGCAGGCGGAGCCCAAAATGGAC-3’

R-5’-GTCCATTTTGGGCTCCGCCTGCGCGATGGCAAGGAAGGGATACC-3’

LxVxV to LxAxA

F-5’-CCGGCATTTAGAAGCGGAGGCCCTCGCCCTCAT-3’

R-5’-ATGAGGGCGAGGGCCTCCGCTTCTAAATGCCGG-3’

IxPxV #2 to AxAxA

F-5’GCATTAGCCCACACAAAGCAAGAGCCAATGCCGCAAGTGCCAATAAA
AG-3’

R-5’CTTTTATTGGCACTTGCGGCATTGGCTCTTGCTTTGTGTGGGCTAATG
CC-3’

PxDxL to AxAxA

F-5’-GGTGAAAGAGCTCGCCGCAGCCAATGCCCTCAGTCCGGCC-3’

R-5’-GGCCGGACTGAGGGCATTGGCTGCGGCGAGCTCTTTCACC-3’

PxVxS to AxAxA

F-5'-CCACACAAAATAAGAGCCAATGCCGCAGCCGCCAATAAAAGAATC-3'

R-5'-GATTCTTTTATTGGCGGCTGCGGCATTGGCTCTTATTTTGTGTGG-3'

FL to AA

F-5'-GCGAATACGACGAAGCCGCCAAAGCGATACGGG-3'

R-5'- CCCGTATCGCTTTGGCGGCTTCGTCGTATTCGC-3'

RCRI to AAAA

F-5'-CGAAATACTACATTAAAGCCGCCGCCGCCCGGCTGAAGCGAGTG-3'

R-5'CACTCGCTTCAGCCGGGCGGCGGCGGCTTTAATGTAGTATTTCG-3'

III.C RESULTS

III.C.1 LHR interacts with HP1 and HP6

Based on previously reported results that LHR and HP1 interact in a yeast two-hybrid assay and co-localize at heterochromatic regions of salivary gland polytene chromosomes (Brideau et al. 2006), I wanted to determine whether these proteins interact directly. I therefore performed immunoprecipitation assays with extracts from two sources. First, I used nuclear extracts from *Drosophila* Kc cells that were transiently transfected with a LHR-MYC fusion construct. I found that endogenously expressed HP1 can immunoprecipitate with MYC-tagged LHR (Fig III.C.1A).

It is possible, however, that LHR and HP1 co-associate by each binding to another protein rather than directly binding to each other. Therefore, to test if LHR can bind directly to HP1, I performed an *in vitro* binding assay. I found that *in vitro* synthesized LHR-HA and HP1 also co-immunoprecipitate (Fig III.C.1B). In combination with the published yeast two-hybrid and

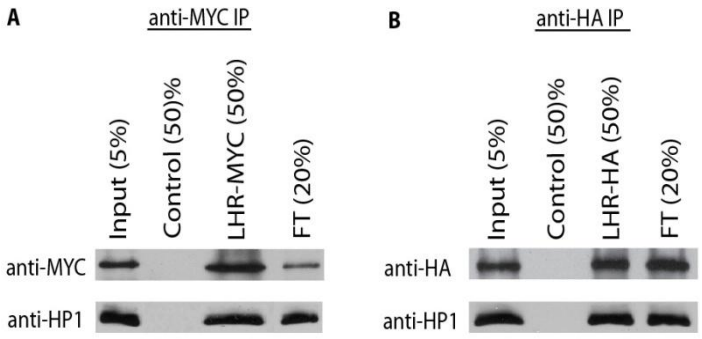

Figure III.C.1 HP1 immunoprecipitates with LHR

A) HP1 immunoprecipitates with LHR in extracts from *Drosophila* Kc embryonic tissue culture cells. Anti-MYC immunoprecipitated material from wild-type Kc cells (control) and LHR-MYC expressing cells were analyzed by Western blot using anti-MYC and anti-HP1 antibodies. The percent of each sample loaded is shown (%). Protein that did not immunoprecipitate is shown in the flow through lane (FT). B) LHR binds to HP1 in an *in vitro* binding assay. *In vitro* synthesized LHR-HA and HP1 proteins were mixed and the resulting complexes were immunoprecipitated with anti-HA antibody and analyzed by Western blot using anti-HA and anti-HP1 antibodies. Control lane is sample immunoprecipitated from an in vitro synthesis extract without DNA from either gene added.

immunofluorescence data, my *in vitro* results strongly suggest that LHR and HP1 co-localize in heterochromatin due to direct physical binding to each other. Because it has been suggested that LHR is part of a network of HP1-associated proteins (Greil et al. 2007) I used yeast two-hybrid to test if LHR interacts with HP4, HP5 and HP6. Of these three other HPs I examined, only HP6 interacts with LHR (Figure III.C.4 and data not shown), consistent with previously reported results (Giot et al. 2003).

III.C.2 LHR interacts with the chromo-shadow domain of HP1 and HP6 in the yeast two-hybrid system

Although *D. melanogaster* and *D. simulans* LHR are divergent in sequence, both orthologs can interact with HP1 (Brideau et al. 2006). This result suggests that the interaction between LHR and HP1 involves amino acids that are conserved between *D. melanogaster* and *D. simulans*. To test this hypothesis and to define the regions of LHR and HP1 responsible for mediating the interaction, I created a series of derivatives of each protein and tested these fragments in a yeast two-hybrid assay. Beginning with HP1, I found that the C-terminal chromo-shadow domain (CSD) is both necessary and sufficient to interact with full length LHR (Fig III.C.2A). This result is consistent with other findings showing that the CSD of HP1 mediates protein-protein interactions (Schwendemann et al. 2008; Delattre et al. 2000).

Since HP6 also interacts with LHR and has a chromo-shadow domain similar to HP1, it is possible that LHR simply interacts with any protein containing a CSD. This explanation may be unlikely, however, because I observed no interaction in a between LHR and the *D. melanogaster* HP1 paralog Rhino, which also contains a CSD (Fig III.C.S1).

Figure III.C.2 Identifying the interacting domains in HP1 and LHR

A) The chromo shadow domain of HP1 interacts with LHR. Full length *D. melanogaster* HP1 is shown with the chromo domain (CHD) and chromo-shadow domain (CSD) shaded. Fragments of HP1 that were tested for interaction with LHR in a yeast two-hybrid assay are shown below. The symbols on the right indicate non-interacting (-) and interacting (+) fragments. B) A 96 AA minimal interacting fragment (M), inferred from the LHR fragments tested, interacts with HP1. Full length LHR is shown with the BESS domain and predicted NLS (*) shaded. The amino acids shown for each of the five consensus pentamer motifs in LHR that were converted to alanine by site-directed mutagenesis and individually tested for interaction with HP1 are shown (top). None of the single motif mutants abolished interaction with HP1 in yeast two-hybrid assays. Fragments of LHR that were tested for interaction with HP1 in a yeast two-hybrid assay are shown below. The two hypothesized regions in fragment M essential for interacting with HP1 are labeled 1 and 2. C) Alignment of the putative NLS region (bottom) identified in mel-LHR from seven LHR orthologs. The two clusters of arginine and lysine residues consistent with an NLS are conserved for all LHR orthologs. D) The mutant LHR^{RCRI} protein has reduced binding to HP1 in an in vitro binding assay. Extract containing *in vitro* synthesized HP1 was mixed with extract containing either synthesized LHR-HA (wild type control) or LHR^{RCRI}-HA (mutant), and resulting complexes were immunoprecipitated with anti-HA antibody, followed by Western blot using anti-HA antibody. Control lane is sample immunoprecipitated from an in vitro synthesis extract without DNA from either gene added.

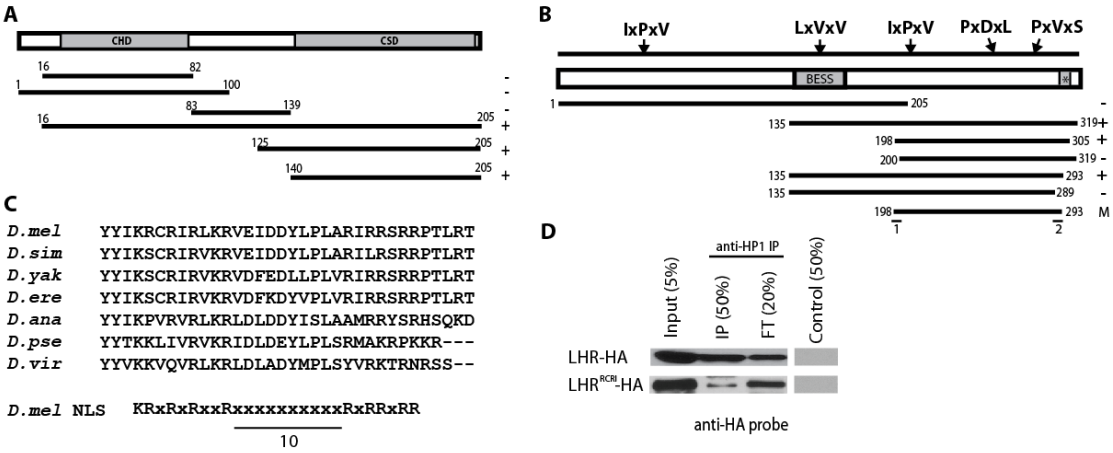
A
CHD
CSD
16
82
1
100
83
139
16
205
125
205
140
205
B
IxPxV
LxVxV
IxPxV
PxDxL
PxVxS
BESS
1
205
135
319
198
305
200
319
135
293
135
289
198
293
M
1
2
C
D. mel YYIKRCRIRLKRVEIDDYLPLARIRRSRRPTLRT
D. sim YYIKSCRIRVKRVEIDDYLPLARILRSRRPTLRT
D. yak YYIKSCRIRVKRVDFEDLLPLVRIRRSRRPTLRT
D. ere YYIKSCRIRVKRVDFKDYVPLVRIRRSRRPTLRT
D. ana YYIKPVRVRLKRLDLDDYISLAAMRRYSRHSQKD
D. pse YYTKKLIVRVKRIDLDEYLPLSRMAKRPKKR---
D. vir YYVKKVQVRLKRLDLADYMPLSYVRKTRNRSS--
D. mel NLS KRxRxRxxRxxxxxxxxxxRxRRxRR
10
D
anti-HP1 IP
Input (5%)
IP (50%)
FT (20%)
Control (50%)
LHR-HA
LHR^RCRIL-HA
anti-HA probe

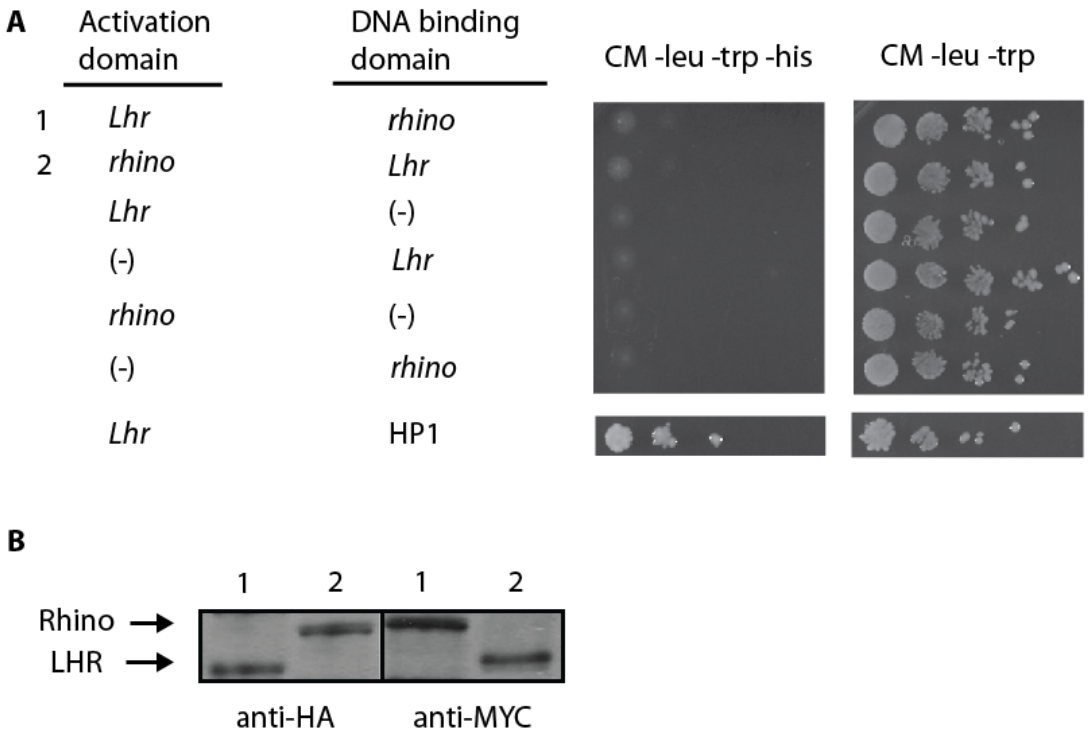

Figure III.C.S1 No interaction was detected between LHR and the HP1 paralog Rhino by yeast two hybrid analysis

Interactions were analyzed in yeast two-hybrid by activation of HIS3 and growth on complete media lacking histidine (-trp -leu –his); loading controls (-trp –leu) contain histidine. A) No growth is seen for both LHR-Rhino combinations; indicting that the two proteins do not interact. B) Genotypes 1 and 2 from (A) were tested by Western blot in order to demonstrate that both fusion proteins are expressed in yeast.

III.C.3 The carboxy terminus of LHR interacts with HP1 and HP6

Many proteins that interact with the chromo-shadow domain of HP1 contain either the consensus peptide pentamer PxVxL or variations of this motif (Smothers, Henikoff 2000; Huang, Myers, Xu 2006). I found no canonical HP1-binding motifs in *D. melanogaster* LHR, but did find five potential PxVxL variants (Fig III.C.2B). However, mutagenesis of each individual motif demonstrated that none of the 5 motifs are individually essential for the HP1 interaction. (Figure III.C.S2).

I therefore mapped the HP1 interaction domain in LHR by testing a series of LHR fragments for interaction in yeast two-hybrid assays. By analyzing the interacting and non-interacting two-hybrid fragments, I inferred that the smallest HP1-interacting fragment of LHR contains 96 amino acids and is located in the C-terminal half of the protein (labeled “M” in Fig III.C.2B). Further analysis revealed two regions (Fig III.C.2B, labeled 1, 2) within the 96 amino acid derivative (M) that appear critical for mediating the interaction with HP1. To test whether one or both of these regions are necessary for interacting with HP1, I mutagenized each region in full length LHR and tested for interaction. Region one is composed of two amino acids (FL), and converting both to alanine simultaneously did not affect the LHR-HP1 interaction (Figure III.C.S3A). Region 2 is composed of four amino acids (RCRI) that when simultaneously changed to alanine, severely compromise growth on –trp –leu –his plates in a yeast two-hybrid assay, suggesting a reduced interaction between LHR and HP1 (Figure III.C.S3B).

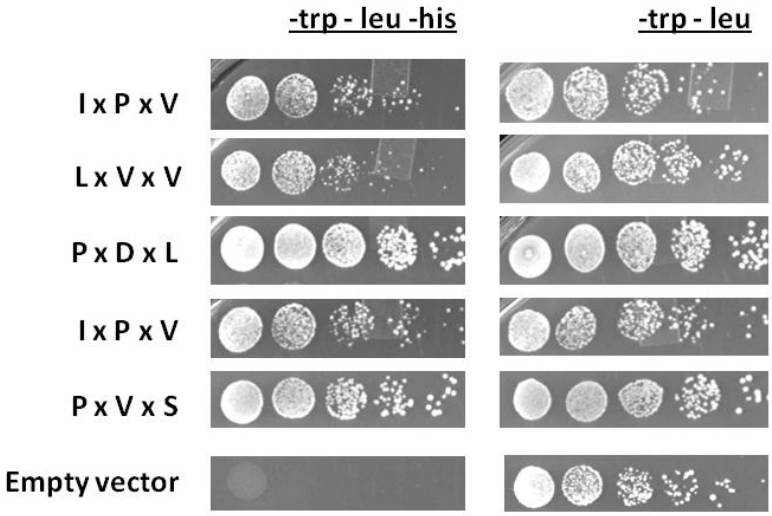

Figure III.C.S2 Testing if five PxVxL variants in LHR mediate the interaction with HP1 in yeast two-hybrid

Mutagenesis of the PxVxL variants in LHR failed to abolish interaction between LHR and HP1, indicating none are individually necessary to mediate this interaction. Growth in the (-trp –leu –his) column indicate an interaction, and growth in the (-trp –leu) column indicates both the activation domain and DNA binding domain plasmids are present.

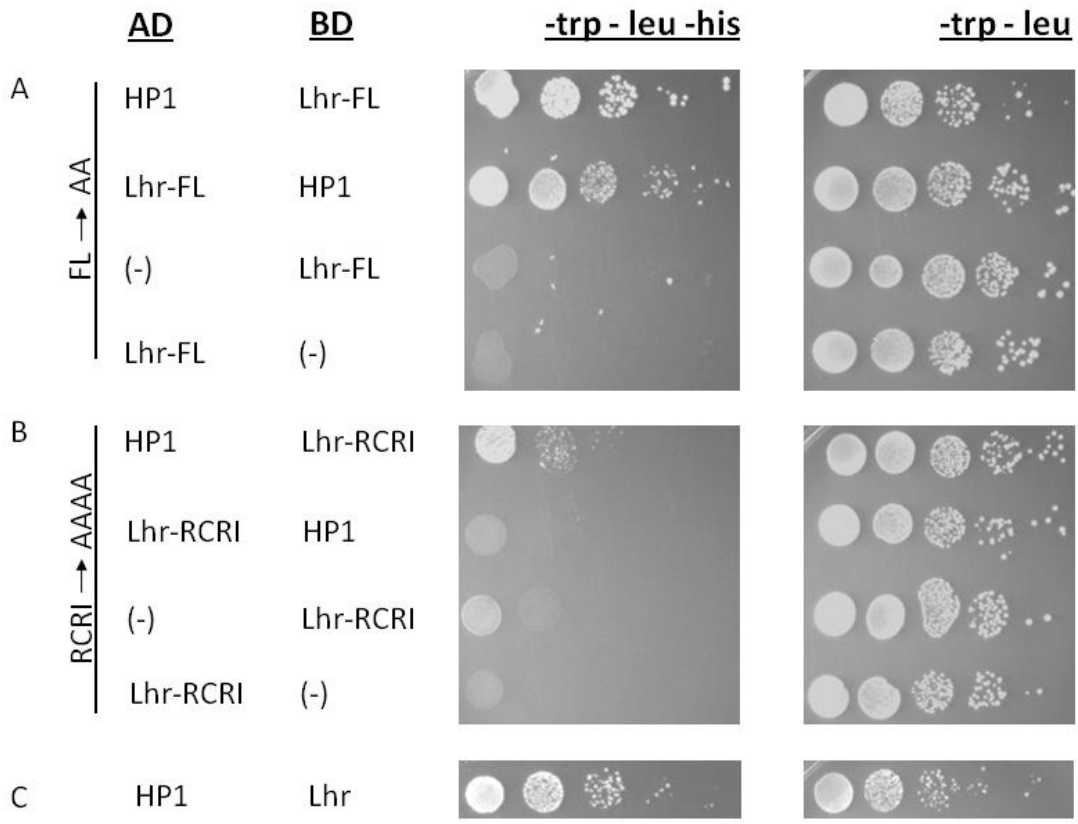

Figure III.C.S3 Testing if two regions within the 96 amino acid derivative in LHR mediate the interaction with HP1 in yeast two-hybrid

A) Converting the amino acids in region 1 (FL) to alanine failed to abolish interaction with HP1. B) Converting the amino acids in region 2 (RCRI) to alanine compromised yeast growth indicating a potentially reduced interaction. C) Positive control of wild type LHR with HP1 grows as expected. Growth in the (-trp –leu –his) column indicate an interaction, and growth in the (-trp –leu) column indicates both activation domain and DNA binding domain plasmids are present.

To confirm this loss of interaction, I tested whether the LHR^{RCRI} mutant protein could immunoprecipitate with HP1 in Kc cell extracts. I found that the LHR ^{RCRI} mutant protein did not immunoprecipitate with HP1 (Fig III.C.2D). However, I also found that LHR ^{RCRI}-MYC protein lost nuclear localization, which might be the cause of the lack of interaction with the nuclear localized HP1. (Fig III.C.S4). Consistent with the loss of nuclear localization, additional analysis of the amino acids of the region of LHR containing the RCRI motif revealed characteristics such as clusters of lysine and arginine residues that are indicative of a bipartite nuclear localization signal (NLS) (Fig III.C.2C) (Kalderon et al. 1984). I hypothesized that the RCRI residues in LHR have two roles: one for transporting LHR into the nucleus (Greil et al. 2007), and the other for mediating its interaction with HP1.

In order to test for loss of interaction without the complication of interfering with LHR nuclear localization, I used a cell-free *in vitro* binding assay. I found that compared to wild type LHR-HA, the *in vitro* synthesized LHR ^{RCRI} –HA mutant protein has reduced binding to HP1 (Fig III.C.2D). This reduction in binding combined with the apparent loss of nuclear localization (Figure III.C.S4), suggests that I have identified a region within LHR that is potentially important for mediating the binding to HP1 and for nuclear localization. Most of the LHR orthologs have a similar enrichment of lysine and arginine residues in this region that are indicative of an NLS (Fig. III.C.2C), which suggests that all LHR orthologs are imported into the nucleus. In contrast, the motif I identified in mel-LHR that is important for binding to HP1 is not identical even in sim-LHR and is entirely diverged in other species, which raises the question of whether the property of interacting with HP1 is conserved among LHR orthologs.

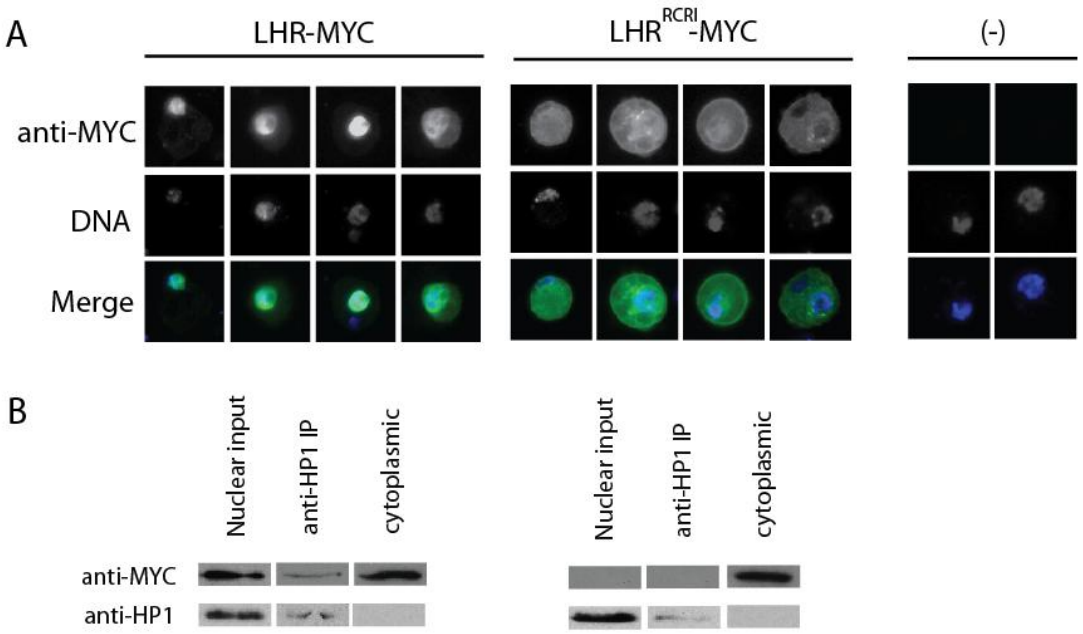

Figure III.C.S4 LHR^{RCRI}-MYC fails to localize to the nucleus.

A) *Drosophila* embryonic Kc cells transfected with LHR-MYC, LHR^{RCRI}-MYC, or empty vector (-). LHR fusion proteins were visualized with an anti-MYC antibody and DNA is stained with DAPI. LHR-MYC is predominantly nuclear, wheras LHR^{RCRI}-MYC is predominantly cytoplasmic. B) Western blots from nuclear and cytoplasmic extracts of cells transfected with LHR-MYC or LHR^{RCRI}-MYC are shown. LHR-MYC is nuclear and can immuoprecipitate with HP1 (left) and LHR^{RCRI}-MYC is cytoplasmic and unable to immunoprecipitate with HP1 (right). These results are consistent with the localization data in (A).

III.C.4 Heterochromatic localization of LHR depends on HP1 and HP5

We and others have shown that LHR interacts with two HPs that are potentially part of a larger network of heterochromatin proteins (Brideau et al. 2006, Greil et al. 2007) To test if one or more of these HPs are required to mediate the heterochromatic localization of LHR, I created a LHR-YFP fusion construct under control of the GAL4/UAS expression system, and generated transgenic flies that carry this *UAS-Lhr-Yfp* transgene. Experiments below demonstrate that these fusion proteins retain LHR hybrid lethality activity (Table II.C.2). I used a salivary-gland specific GAL4 driver in various HP mutant backgrounds and examined the localization of LHR by live YFP analysis or anti-GFP staining in fixed tissues. I found that LHR-YFP loses heterochromatic targeting and is redistributed throughout the nucleus in HP1 mutant larvae (Fig III.C.3B), consistent with a previous report that LHR requires HP1 for heterochromatic localization in embryonic tissue culture cells (Greil et al. 2007).

I discovered that HP5 is also required for LHR to localize to heterochromatin (Fig III.C.3E). The loss of bright foci and diffuse nuclear staining for LHR -YFP is similar in the HP5 and HP1 mutants. It is possible that the heterochromatic localization of LHR-YFP is lost in the HP1 and HP5 mutants because the protein is unstable. Western blots indicate, however, that the protein is present at a similar level in the mutant HP background as in the wild type background (Fig III.C.S5). In contrast to the HP1 and HP5 mutants, I did not observe any localization differences for LHR-YFP in HP4 or HP6 mutant animals (Fig III.C.3D,F).

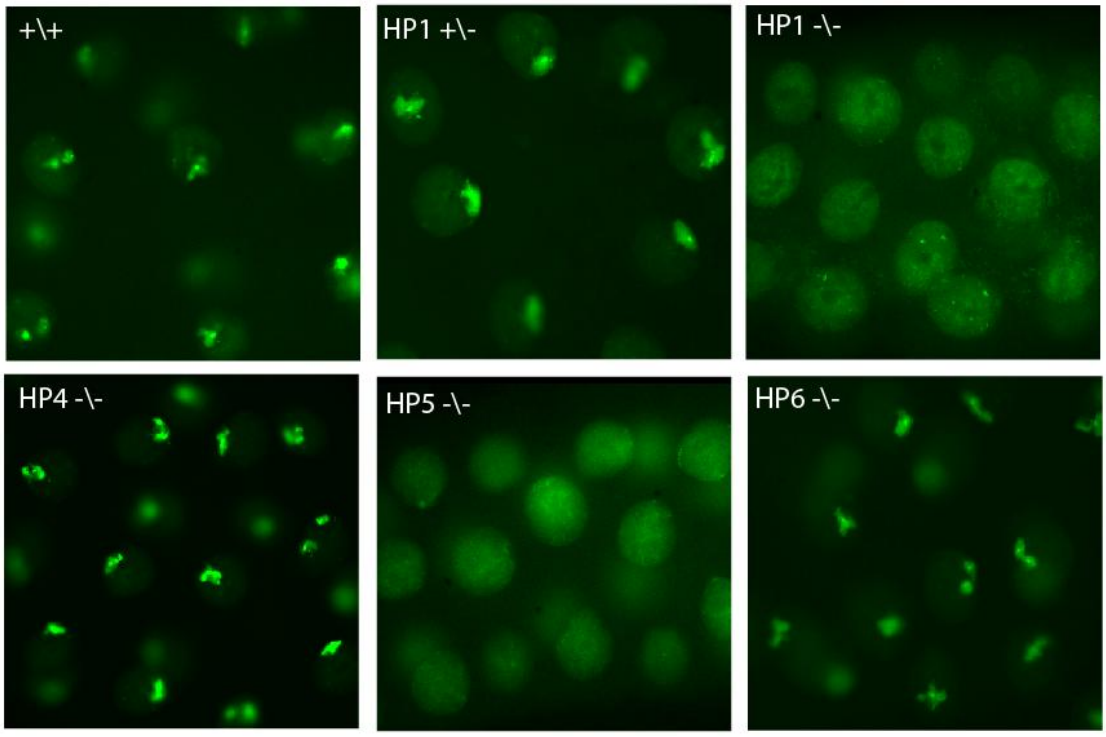

Figure III.C.3. LHR-YFP localization depends on HP1 and HP5.

Live YFP analysis of LHR-YFP in whole mount salivary glands from third instar larvae in wild-type and HP mutant backgrounds. The recombinant chromosome *P{w$^+$ UAS-mel-Lhr-Yfp}, P{w$^+$c729}* was crossed into mutant backgrounds for the four HPs I tested. The bright heterochromatic foci normally seen in wild type animals are absent in HP1 and HP5 mutants but not in *HP4* or *HP6* mutants.

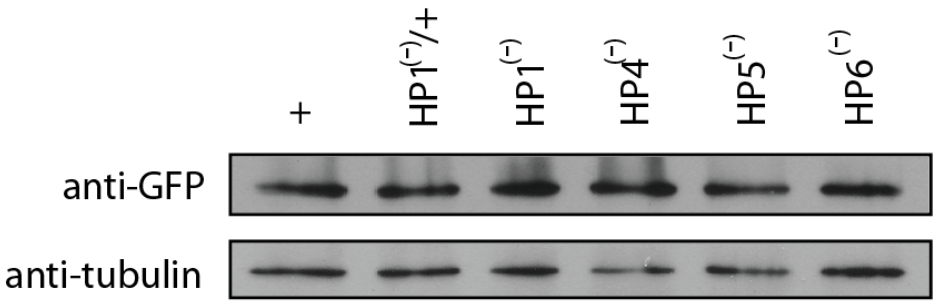

Figure III.C.S5 LHR-YFP is expressed and stable in HP mutants.

Extracts from third instar salivary glands were loaded on an SDS-PAGE gel and analyzed by Western blot using anti-GFP and anti-tubulin antibodies. Relative to the tubulin loading controls, LHR-YFP is present at similar levels in wild type animals and in all the HP mutants analyzed.

III.C. 5 LHR orthologs interact with HP1 and HP6

I previously found that both *D. melanogaster* and *D. simulans* LHR can interact with HP1 from *D. melanogaster*. Considering the high divergence among LHR orthologs, I tested if this property of HP1 interaction is conserved among more distant orthologs. I cloned the coding sequences from five additional LHR orthologs and found that all of them interact with *D. melanogaster* HP1 in a yeast two-hybrid assay (Figure III.C.4.A). I then tested whether these LHR orthologs can also interact with *D. melanogaster* and *D. simulans* HP6, because HP6 has a much higher rate of divergence between *D. melanogaster* and *D. simulans* than HP1 (Table III.C.1). I found that all seven LHR orthologs tested interact with both mel-HP6 and sim-HP6 (Figure III.C.4B, C). These data demonstrate that LHR interactions with heterochromatin proteins discovered in *D. melanogaster* are likely to be conserved among *Drosophila* despite highly variable rates of evolution of these proteins.

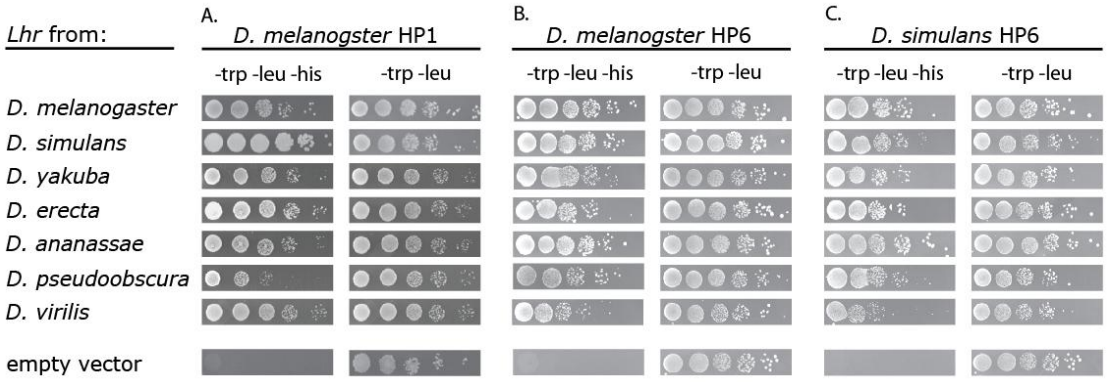

Figure III.C.4 Seven LHR orthologs interact with HP1 and HP6.

A) LHR from seven Drosophila species interacts with *D. melanogaster* HP1 in a yeast two-hybrid assay. Interactions were detected by activation of HIS3 and growth on media lacking histidine; loading controls [-trp –leu] contain histidine. The same seven LHR orthologs also interact with (B) *D. melanogaster* HP6 and (C) *D. simulans* HP6.

Table III.C.1 Divergence of heterochromatin proteins between *D. melanogaster* and *D. simulans*

Gene	K_a	K_s	K_a/K_s
Su(var)2-5 (HP1)	0.017	0.017	0.135
Lhr (HP3)*	0.078	0.106	0.731
HP4 (Hip)	0.017	0.121	0.127
HP5	0.079	0.100	0.790
HP6 (Umbrea)	0.132	0.133	0.988

*- values are from Brideau et al. 2006

III.C. 6 Four LHR orthologs localize to heterochromatin when expressed in *D. melanogaster*

The above experiments demonstrate that LHR from all species tested can interact with *D. melanogaster* HP1. I have also found, however, that both HP1 and HP5 are required in *D. melanogaster* for LHR to localize to heterochromatin. Since the mechanism by which HP5 controls LHR localization is unknown, and HP5 is also rapidly evolving (Table III.C.1), it was unclear if other *Drosophila* LHR orthologs would localize to heterochromatin *in vivo*. I tested this using LHR orthologs from 3 species having a range of divergence from *D. melanogaster*, *D. simulans*, *D. yakuba,* and *D. virilis*. I transformed UAS-driven LHR-YFP fusion constructs from these species into *D. melanogaster* using the ϕC31 site-specific integration system (Groth et al. 2004). Using this system, transgenes can be inserted into the same position in the genome, allowing a direct comparison between *Lhr* orthologs without complications from variable position effects on transgene expression.

I was unable to obtain a transformant of *D. melanogaster* LHR-YFP into the same *attP* site, so instead I used three independent transgene insertion lines. Live YFP analysis in whole mount salivary glands showed similar bright foci for all three orthologs when compared to *D. melanogaster* LHR-YFP (Fig III.C.5). Anti-GFP staining in polytene squashes demonstrated that the foci observed in the whole mount tissues for all four *Lhr* orthologs overlap with the pericentric heterochromatin at the chromocenter. I also co-stained for HP1 and found that all four *Lhr* orthologs co-localize with *D. melanogaster* HP1 when expressed in *D. melanogaster* (Fig III.C.6). These results demonstrate that the property of heterochromatin localization is likely conserved among *Lhr* orthologs.

Figure III.C.5. Four LHR orthologs localize to similar foci when expressed in *D. melanogaster*.

Live YFP analysis in whole mount salivary glands from third instar larvae expressing LHR-YFP from *D. melanogaster*, *D. simulans*, *D. yakuba,* and *D. virilis*. For each *Lhr* ortholog tested, *D. melanogaster* females carrying the LHR-YFP transgene were crossed to males carrying a salivary-gland specific GAL4 driver, and YFP analysis was performed on the F1 heterozygous larvae. DNA was stained using DAPI.

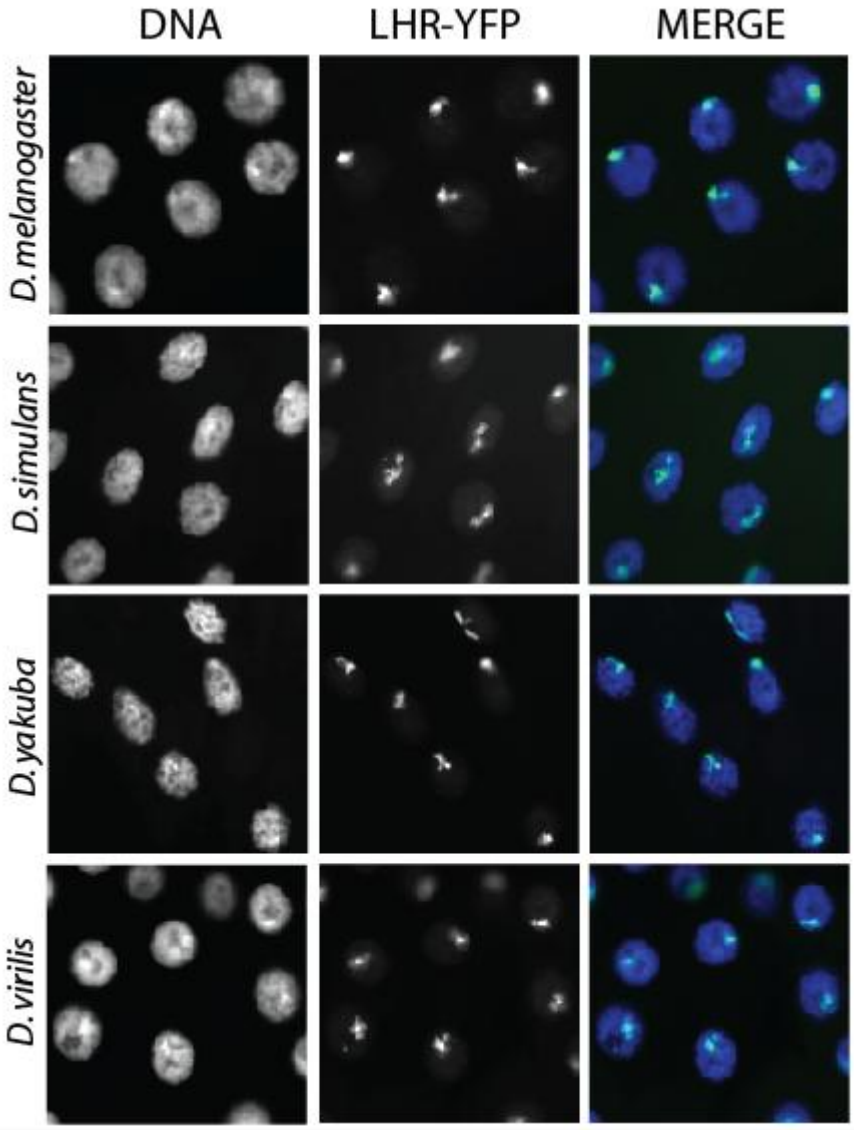
DNA
LHR-YFP
MERGE
D. melanogaster
D. simulans
D. yakuba
D. virilis

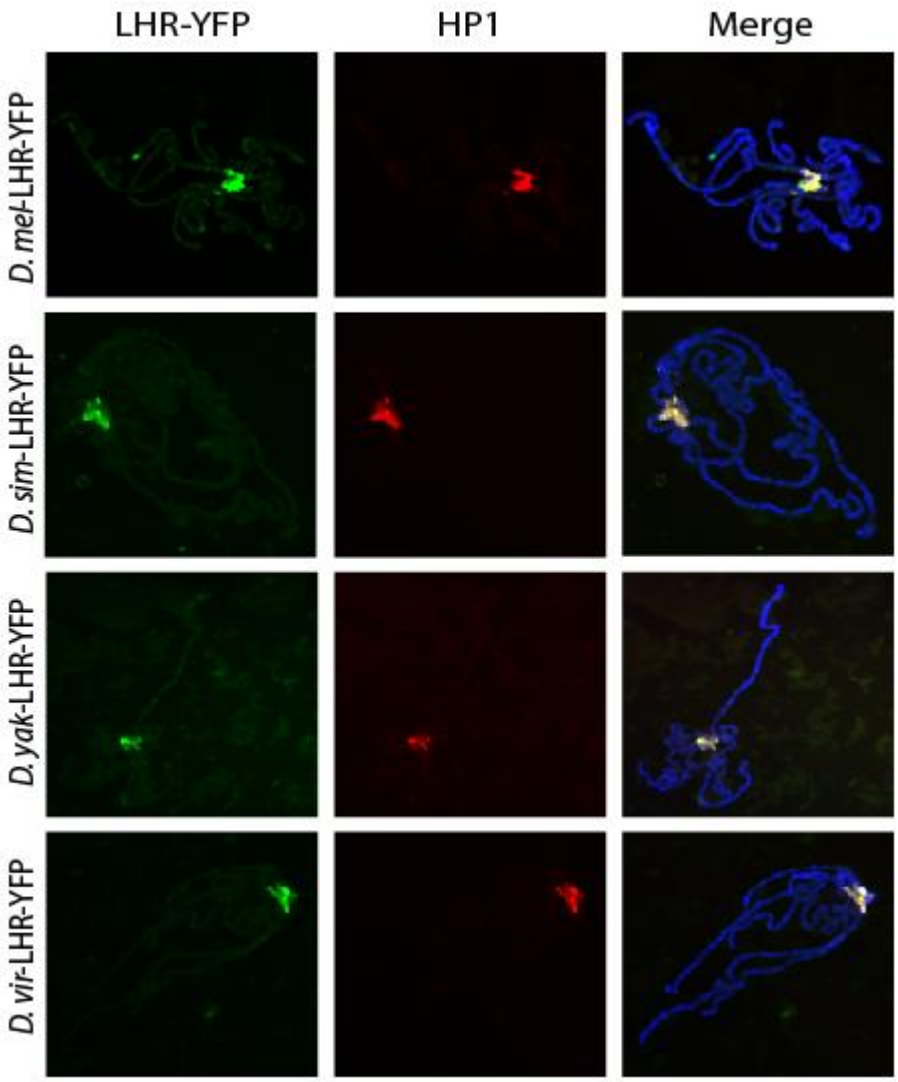

Figure III.C.6. Four LHR orthologs co-localize with HP1 at the chromocenter.

Salivary gland polytene squashes co-stained with anti-GFP (green), anti-HP1 (red) and DAPI (blue in merge). The same crosses were used as in Figure III.C.5.

III.C.7 *D. melanogaster Lhr* has hybrid lethal activity

The above results suggest that LHR has not evolved different interaction or localization properties between *D. melanogaster* and *D. simulans*, or among outgroup species. These findings raise the question of whether the hybrid lethality activity of sim-LHR is unique. I tested this using the genetic assay previously developed to identify the *sim-Lhr* gene. I crossed *D. melanogaster* females heterozygous for a *D. melanogaster UAS* driven *Lhr-Yfp* transgene and the *Actin5C Gal4* driver to *D. simulans Lhr*^{1} males, and scored the hybrid male progeny (Fig III.C.S6). In these crosses, I am testing whether the ubiquitous *Lhr* expression from the *Actin-Gal4* driver can suppress the hybrid male rescue from the *D. simulans Lhr*^{1} line. This cross was performed with two independent *D. melanogaster Lhr-Yfp* insertion lines, and control crosses demonstrated that expressing either *mel-Lhr-Yfp* transgene was not lethal to *D. melanogaster* (Table III.C.2).

In crosses to the *D. simulans Lhr*^{1} strain to generate hybrids, I found that *mel-Lhr-Yfp* suppressed rescue of hybrid males by *Lhr*^{1} like untagged *sim-Lhr* transgenes did previously (Brideau et al. 2006), as judged by the presence of approximately half of the *Gal4*-containing sons (red-eyed class) compared to the control cross. I confirmed by PCR that the rescued red-eyed males only carried the *Gal4* transgene (n=10 for each cross), thus concluding that the reduction in red-eyed males is caused by lethality of sons inheriting both the *Gal4* and *UAS-Lhr-Yfp* transgenes. These results demonstrate that the hybrid lethality function of *Lhr* is not unique to *D. simulans Lhr*. I also performed similar experiments with *Lhr-Yfp* transgenes from *D. simulans*, *D. yakuba* and *D. virilis* and those results are described in the Appendix C.

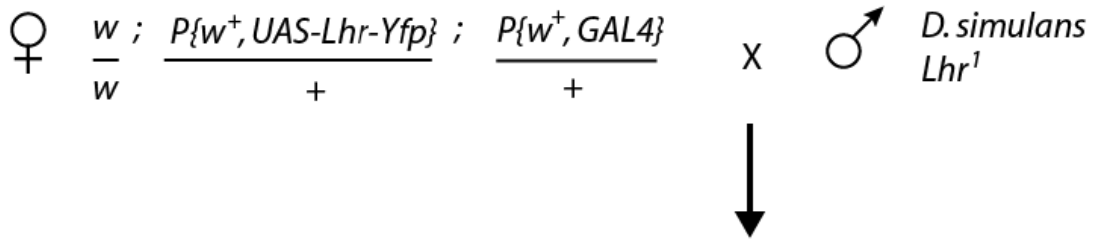

Expected genotypic ratio if Lhr ortholog expression is:

Eye color:	Possible Genotypes	Viable		Lethal	
Red	UAS/+ ; GAL4/+	1 } 2		0 } 1	
	+/+ ; GAL4/+	1		1	
Orange	UAS/+ ; +/+	1	1	1	1
White	+/+ ; +/+	1	1	1	1

Figure III.C.S6. Complementation crosses to test for suppression of hybrid male rescue.

D. melanogaster female parents heterozygous for *GAL4* and *UAS-Lhr-Yfp* transgenes were crossed to *D. simulans* males. Both the transgenes are marked with w^+, and the *GAL4*-containing transformant has a darker eye color and is epistatic to the lighter *UAS*-containing transformants. Therefore, the red-eye class of progeny could potentially be composed of two different genotypes.

Table III.C.2 Hybrid males from crosses testing if *D. melanogaster Lhr* has hybrid lethal activity

	F1 Progeny Class		Number of progeny	
D. melanogaster mother	Phenotype	Genotype	*D. mel* control cross	*D. sim Lhr*[1] cross
mel-Lhr-1[a]	Red-eyed male	UAS/+ ; GAL4/+ +/+ ; GAL4/+	278	134
	Orange-eyed male	UAS/+ ; GAL4/+	148	107
	White-eyed male	+/+ ; GAL4/+	143	141
		Total[e]	569 [n.s.]	382 [***]
mel-Lhr-2[b]	Red-eyed male	UAS/+ ; GAL4/+ +/+ ; GAL4/+	221	334
	Orange-eyed male	UAS/+ ; GAL4/+	93	8
	White-eyed male	+/+ ; GAL4/+	102	314
		Total[e]	416 [n.s.]	781 [***]

[a,b] – Two different insertions of the *D. melanogaster Lhr-Yfp* transgene on the second chromosome, full genotype: *w/w; P{w*$^{+mC}$ *UASLhr::Venus=UAS-mel-Lhr::YFP}/+; P{Act5CGAL4}17bFO1/+*

[c] - The ratio of red eye : orange eye : white eye was tested for deviation from a 2:1:1 ratio using Chi-squared test. *** = $p < 1 \times 10^{-3}$; n.s. = $p > 0.05$

III.D DISCUSSION

III.D.1 LHR is part of a complex of heterochromatin proteins

A number of heterochromatin proteins have been characterized and named (HP3-6) based on their association with HP1 (Greil et al. 2007). Interestingly, these HP1 interacting proteins have two distinct patterns of molecular evolution (Table III.C.1). Both HP1 and HP4 are well conserved between *D. melanogaster* and *D. simulans* with low K_A/K_S values that are typical of genes evolving under stabilizing selection, while LHR (HP3), HP5, and HP6 have high K_A/K_S values that suggest adaptive evolution or relaxed constraint. I was therefore interested to explore further the relationship between LHR and HP4-6. Giot et al. (2003) reported that LHR interacts with HP1 and HP6 in a large-scale yeast two-hybrid screen. I previously confirmed this result for HP1, and have done so here for HP6. I have further shown here that HP1 immunoprecipitates with LHR in cell-culture extracts, and that LHR binds to HP1 in an *in vitro* assay. These data indicate that the interaction between LHR and HP1 is likely to be direct.

Greil et al. (2007) demonstrated that LHR (HP3), HP4, and HP5 are all dependent on HP1 for proper localization to heterochromatin in Kc cells. Here I developed an *in vivo* localization assay using YFP-tagged LHR transgenes expressed in salivary glands, in order to take advantage of the resolution available in their large polytenized nuclei. I have confirmed with this assay that HP1 is essential for proper heterochromatic localization of LHR. I then tested mutants in other HPs and found that HP5, but not HP4 or HP6, is required for heterochromatic localization of LHR.

Joppich et al. (2009) have reported that similar to LHR, HP4 (Hip) binds to HP1 and HP6 (Umbrea) *in vitro*, and that these proteins colocalize at

pericentric heterochromatin and form a complex *in vivo.* These authors further proposed that the association between HP6 and HP1 is mediated by heterodimerization of the chromo-shadow domain in each protein, similar to the known homodimerization of the CSD in HP1. Structural investigation by Cowieson and colleagues (2000) suggests that CSD dimerization results in formation of a protein-protein interaction pit that is predicted to bind one peptide per CSD dimer. LHR, HP4, and HP5 all interact with both HP1 and HP6, but do not interact with each other. These interaction results combined with the limitation of CSD dimers to only bind one peptide, suggest that LHR, HP4 and HP5 are unlikely to simultaneously bind to HP1 or HP6 CSD dimers or to HP1/HP6 heterodimers. Instead, these data suggest that LHR, HP4, and HP5 interact with HP1 in distinct complexes.

Because I did not detect an interaction between LHR and HP5, the localization dependency of LHR on HP5 further suggests that HP5 indirectly enables LHR to localize to heterochromatin. Furthermore, because HP5 also depends on HP1 for heterochromatic localization, I suggest either that an HP1-HP5 complex establishes a chromatin domain that becomes accessible to LHR, or that HP5 interacts with other proteins responsible for recruiting LHR.

The genomic mapping results reported by Greil et al. (2007) suggest that LHR localizes to several sites in the genome independently of HP1 and HP5. How is LHR recruited to these sites? Two possibilities are that LHR is a DNA binding protein and directly recognizes repetitive elements or specific sequences, or that additional proteins are responsible for this recruitment. I also found that despite being able to interact with HP6, LHR does not depend on HP6 for heterochromatic localization in salivary glands. This result

suggests that either LHR interacts with HP6 in a tissue or developmental context other than third instar salivary glands, or that it may never interact with HP6 *in vivo*. Based on the discordant expression patterns of LHR and HP6, I suggest that these two proteins are unlikely to interact *in vivo*.

III.D.2 Investigating the HP1 interacting motif in LHR

I discovered that LHR interacts with the chromo-shadow domains of HP1 and HP6. Unlike many other CSD-interacting proteins, I did not find a PxVxL-like motif in LHR responsible for mediating the interaction. However, I did identify four amino acids (RCRI), that when mutated partially disrupt the binding of LHR to HP1. The RCRI motif and adjacent residues in LHR are similar to the non-PxVxL HP1-interacting domains found in HP2, HP4 and SU(VAR)3-7, which also have an enrichment of positively charged amino acids It is also important to note that the RCRI motif is not entirely responsible for interacting with the CSD, as the minimal interacting fragment is 96 amino acids, and mutagenesis of the RCRI motif in full length LHR does not completely abolish binding to HP1. This is also similar to HP2, which contains two small necessary regions within a 99 amino acid region that are sufficient for interaction with HP1 (Stephens et al. 2005).

In addition to mediating the interaction with HP1 and HP6, I found that the RCRI motif may also be part of the nuclear localization signal of LHR. I abolished nuclear localization of LHR in Kc cells by mutating these four amino acids, and this region of LHR has properties common to an NLS, such as a large number of lysine and arginine residues and two clusters of basic residues separated by a 10 amino acid spacer (Fig III.C.S2). I also found that the NLS characteristics that I discovered for mel-LHR are conserved for other

LHR orthologs, consistent with the results that the four LHR orthologs I tested localize to heterochromatin when expressed in *D. melanogaster*. In contrast, the RCRI HP1-interacting motif is not conserved among LHR orthologs, yet all orthologs I tested interact with mel-HP1. These results suggest that the RCRI motif may not directly bind HP1, but instead, the alanine mutations I introduced disrupt the secondary structure of this region or stability of the protein and therefore interfere with HP1 binding. This result may also suggest that the neighboring lysine and arginine residues that are conserved in LHR orthologs are more directly involved in HP1 binding.

III.D.3 Conserved interactions, localization and functional properties of *Lhr* orthologs

The high rate of evolution of *Lhr* raised my interest in examining whether *Lhr* functional properties are conserved among *Drosophila* orthologs. More specifically, the previous discoveries that *Lhr* diverged between *D. melanogaster* and *D. simulans* under adaptive evolution, and that only *sim-Lhr* but not *mel-Lhr* causes hybrid lethality, strongly suggested that *Lhr* has undergone significant functional changes between these two species. I found, however, that two heterochromatin-related properties of the LHR protein are conserved across species. First, LHR from seven *Drosophila* species interacts in yeast two-hybrid with two *D. melanogaster* heterochromatin proteins, HP1 and HP6, as well as with *D. simulans* HP6. Second, I found that the four LHR orthologs we tested co-localize with HP1 at heterochromatic regions when expressed in *D. melanogaster*.

I infer from these results that LHR localization to heterochromatin via binding to HP1 is both an ancestral and conserved property among

Drosophila. From my data, I cannot exclude an alternative possibility that some LHR orthologs do not localize to heterochromatin in their native species despite doing so when expressed in *D. melanogaster*. This alternative, however, seems unlikely. First, I have shown that LHR heterochromatic localization likely depends on direct binding to HP1, and HP1 is highly conserved among *Drosophila*. Second, such a scenario would require an LHR ortholog to have evolved so as to have lost or changed protein interactions that likely occur in the ancestral state, while retaining the ability to interact with the same proteins from the *D. melanogaster* lineage.

These data clearly suggest that LHR has not undergone a complete change of function between *D. melanogaster* and *D. simulans*, or among other species. I therefore tested *Lhr* from *D. melanogaster* for its ability to induce hybrid male lethality. Because an asymmetry in the effects of *D. melanogaster* and *D. simulans Lhr* mutants on hybrid rescue was observed previously, I predicted that the addition of a *D. melanogaster Lhr* transgene would not complement the *D. simulans* Lhr^1 mutation, and thus not be lethal. Contrary to my prediction, I found that *Lhr* from *D. melanogaster* suppressed Lhr^1 rescue and killed hybrid males.

How do I reconcile this discovery with our previous report? I suggest that the functional changes between *D. melanogaster* and *D. simulans Lhr* orthologs are likely to be quantitative, and be easily masked by gene dosage effects. The transgenic complementation experiments reported here expressed *D. melanogaster Lhr* in hybrids in addition to that expressed from the endogenous *mel-Lhr* gene. In contrast, in our previous deletion experiments hybrids expressed only a single endogenous copy of *mel-Lhr*. In addition, the Gal4-UAS system used here may express *Lhr* to a level higher

than in wild type animals.

Interestingly, I detected a difference in the proportion of orange-eyed hybrid males carrying the mel-Lhr transgene compared to previous experiments with sim-Lhr transgene (Table III.C.2). This class of progeny only inherits the *UAS-Lhr-Yfp* transgene, and thus should be equally as viable as the white-eyed siblings that inherit no transgenes (Figure III.C.S4). However, previously we noticed a reduction in viability of the orange-eyed class carrying the *D. simulans UAS-Lhr* transgene, likely due to maternal inheritance of the GAL4 protein (Brideau et al. 2006). In contrast, for two independent *mel-Lhr-Yfp* transgenic lines tested, I see a much larger proportion of orange-eyed hybrid males. The number of orange-eyed males is variable among the two *mel-Lhr-Yfp* lines used, possibly because of position effects, as these lines are independent random insertions of the same transgene. However, I still detect a significant difference in the orange-eyed class relative to the white siblings (F.E.T. $p < 0.001$) for both *mel-Lhr-Yfp* lines when compared to our previous result with *sim-Lhr*. I conclude that *Lhr* from both *D. melanogaster* and *D. simulans* are able to induce hybrid lethality, but that *sim-Lhr* is more potent than *mel-Lhr.*

III.D.4 Rapidly evolving heterochromatin proteins and hybrid incompatibilities

The heterochromatic localization and conserved interaction with rapidly evolving HPs may help explain the conservation of LHR localization in the face of its rapid evolution. Many satellite DNAs and transposable elements have diverged in sequence and abundance between *D. melanogaster* and *D. simulans* ((Lohe, Roberts 1988; Vieira et al. 1999). In addition, several

heterochromatin-associated proteins have evolved extensively between *D. melanogaster* and *D. simulans* (Table III.C.1; Delattre et al. 2000; Stephens et al. 2005), and it has been suggested that association with rapidly evolving heterochromatic sequences is the cause of the divergence of these proteins.

This co-evolution between heterochromatic sequences and their interacting proteins implies that the proteins may mislocalize when expressed in a different species. One example is the centromeric protein Cid. The distantly related *D. bipectinata* Cid fails to localize to the centromere when expressed in *D. melanogaster* Kc cells (Vermaak, Hayden, Henikoff 2002). Recent work by Bayes and Malik (2009) suggests that satellite DNA divergence affects heterochromatin binding by the OdsH protein, leading to hybrid sterility. These authors found that the OdsH protein from *D. simulans* and *D. mauritiana* have different localization patterns when expressed in a *D. simulans*. The authors found that unlike OdsHsim, OdsHmau localizes to the *D. simulans* Y chromosome, and propose that this difference in localization leads to decondensation of the *D. simulans* Y, resulting in incorrectly packaged heterochromatin and potentially hybrid sterility.

Therefore, it is possible that similar to Cid and OdsH, the direct association of LHR with rapidly evolving DNAs contributes to its divergence. However, unlike Cid and OdsH, I did not detect localization differences among the four LHR orthologs that we tested in *D. melanogaster*. These results suggest that LHR is unaffected by the divergence in satellite and transposable element sequences in these species, and may not be a DNA binding protein. As an alternative, it is possible that other HPs are directly co-evolving with heterochromatic DNA sequences, and that LHR co-evolves with these proteins. This co-evolution with heterochromatin proteins may explain how the

localization and interaction properties of LHR are conserved, but the primary sequence is not.

IV. ADDITIONAL ANALYSIS OF LHR INTERACTORS.

IV.A.1 INTRODUCTION

In 1943, based on a series of pseudo-backcross experiments, Pontecorvo suggested that the number of loci involved in *D. melanogaster-D. simulans* hybrid lethality was at least nine. We have shown in Chapter II that two of these genes interact genetically to form a Dobzhansky-Muller pair of hybrid incompatibility loci. In addition to interacting with *Hmr* in hybrids, LHR is proposed to be part of a network of heterochromatin-associated proteins in pure species *D. melanogaster* (Greil et al. 2007). I have demonstrated that LHR is in this network of HPs based on its interactions and localization, (Chapter III). Here in Chapter IV, in order to understand how LHR and its interactors are involved in hybrid male lethality, I report additional analysis of proteins associated with LHR.

My first approach was to test if HP1 and HP4-6 genetically interact with *Lhr* in hybrids to modulate *Lhr*-dependent hybrid male rescue. In order to test for genetic interactions, I took advantage of two *D. simulans* rescue alleles, Lhr^1 and Lhr^2. Each of these alleles is frequently used in hybrid crosses in the lab, and our general consensus is that Lhr^1 rescues hybrid males to a high level, while Lhr^2 rescues to a low level. Therefore, I looked for suppression of rescue in crosses to Lhr^1 males, and for enhancement of rescue in crosses to Lhr^2. For each cross, *D. melanogaster* females heterozygous for a mutant HP chromosome and a balancer chromosome were crossed to *D. simulans* Lhr^1 or Lhr^2 males, and the F1 progeny were scored.

The second approach I took to understand *Lhr* and its interactors was to investigate the interaction between LHR and HMR. Previously, it has been

demonstrated that *Lhr* and *Hmr* interact genetically (Barbash, Roote, Ashburner 2000; Orr, Irving 2000). Additionally, we showed that *Hmr* is required for the hybrid lethal activity of *Lhr* (Brideau et al. 2006). While the Dobzhansky-Muller model outlines two interacting loci, it does not explicitly explain the nature of the lethal or sterile interaction. I therefore sought to test if the genetic interaction between *Lhr* and *Hmr* that leads to hybrid male lethality was due to a physical association of their encoded proteins. Therefore, I tested if *Hmr* and *Lhr* interact using a yeast two-hybrid assay.

It is unclear if the HP interactions and heterochromatic localization are important for the hybrid lethal activity of LHR. In Chapter III, I reported that LHR-YFP localization to heterochromatin in *D. melanogaster* is dependent on HP1 and HP5. One of the major goals of the HP1-LHR domain mapping experiments in Chapter III was to create an LHR mutant that was no longer able to interact with HP1. After creating a non HP1-interacting LHR mutant, my plan was to introduce this construct to hybrids through the complementation assay outlined in Chapters II and III. By using this assay with the non HP1-interacting LHR mutant, I would be able to test if binding to HP1 and localizing to heterochromatin were essential for the hybrid lethal activity of LHR. Unfortunately, I was not able to identify amino acids that when mutated abolish 100% of the binding to HP1. In addition, the complication of the HP1-interacting motif in LHR also likely being part of its NLS made my goal of testing a non HP1-interacting LHR mutant in the Lhr^1 complementation assay unfeasible. Here, as my third approach into understanding the role of LHR interacting proteins in hybrid lethality, I use the *HP5* mutant to test if the heterochromatic localization of LHR is required for its lethal activity.

IV.B MATERIALS AND METHODS

Fly strains and crosses

Flies were reared on standard yeast glucose media and raised at room temperature (~23°C) on a 12 hr light / 12 hr dark cycle. The *D. melanogaster* *Su(var)2-5*^{05} and *HP4-6* mutant lines used were obtained from the Bloomington Stock Center, except for *HP6*$^{36-5}$ which was a gift from Satoru Kobayashi (Mukai et al. 2007). The additional *HP1* mutant stocks were obtained from Barbara Wakimoto. The LHR-YFP line used contained a recombinant chromosome consisting of the *UAS-Lhr-Yfp* transgene *P{ w*$^{+mC}$ *Scer\UAS-Lhr::Avic\Venus =UAS-Lhr::YFP}* and the salivary gland specific *Gal4* driver c729 *P{Scer\GAL4*^{wB} *w*$^{+mW.hs}$*=GawB}c729.* This recombinant UAS/GAL4 chromosome was then crossed into the HP5 mutant background in order to assay LHR-YFP localization in hybrid males lacking HP5. The *D. simulans* line used was *w*^{501}*/Y* and the *D. mauritiana* stocks W139 and Iso 105 were used, and are described in (Barbash 2007). All hybrid crosses were initiated with 20 zero-to-one day-old *D. melanogaster* virgin females and 30 four-to-five day-old *D. simulans* or *D. mauritiana* males. Crosses were changed every 3-4 days for a total of four collections. For the *D. simulans* crosses, second instar larvae were picked and sorted based on YFP signal in the salivary glands and color of the mouth hooks. Hybrid male larvae were confirmed by PCR genotyping with primers to the *D. melanogaster kl-5* gene on the Y chromosome. For the *D. mauritiana* crosses, progeny were counted for at least 15 days after removing the parents, until no more progeny eclosed.

Yeast two-hybrid assays

Yeast two-hybrid assays were performed as in Chapters II and III. Full length *Hmr* and *Hmr* derivatives were cloned into the pENTR-D-TOPO vector and verified by restriction digest and sequencing. Resulting entry clones were then recombined into vectors pGADT7-AD and pGBKT7 DNA-BD as in Chapters II and III.

LHR-YFP localization assays

LHR-YFP signal was detected by live YFP analysis as in Chapter III, with the exception that the larvae examined in hybrid crosses were in the second instar stage.

Statistical analysis

Fishers Exact Test (FET) was performed online at http://faculty.vassar.edu/lowry/VassarStats.html for data in Tables IV.C.1 and IV.C.2. A two-tailed test was used because the expectation of how the *HP* mutants may affect the level of Lhr^1 and Lhr^2 rescue was uncertain. However, it is likely that Lhr^1 would have more power for detecting suppression of rescue and Lhr^2 for detecting enhancement.

IV.C RESULTS AND DISCUSSION

IV.C.1 Modulating hybrid male rescue with *HP* mutant lines

In Chapter III it was confirmed that LHR is part of a suite of heterochromatin proteins based on their similar localization properties and interactions. In this section, I wanted to analyze HP1 and HP4-6 in relation to LHR, and to test if mutations in these HPs affect *Lhr*-dependent hybrid

incompatibility. For these crosses, I used *D. simulans Lhr* rescue alleles in combination with mutant *HP* lines. By first rescuing the hybrid males with *Lhr* mutants, I was able to detect if the number of surviving hybrid males changes in the presence of various mutant *HP* chromosomes.

We have found that the Lhr^1 line normally rescues to a high level. Therefore, I would be more likely to detect a decrease in the number of hybrid male progeny inheriting the mutant *HP* chromosome, or dominant suppression of Lhr^1 rescue. We have also found that the Lhr^2 mutation rescues males to a low level, therefore it is most likely that I would see an increase in the number of hybrid male progeny inheriting the mutant *HP* chromosome, or dominant enhancement of Lhr^2 rescue. I crossed several *HP* mutant lines to Lhr^1 or Lhr^2 and the results are shown in Table IV.C.1 and Table IV.C.2.

Mutations in *HP1* do not appear to significantly suppress Lhr^1 rescue, as judged by examining two different alleles (Table IV.C.1, footnotes b and c). However, there is a high amount of variability for the number of hybrid progeny among the three *HP1* lines used and between replicates of the same allele. The *D. melanogaster* mothers in the HP4 and HP5 mutant crosses to Lhr^1 were different than the other HP lines used because they were homozygous for the mutant chromosome. Although the mutant progeny from these crosses have no balancer siblings to compare to, I compared the total number of F1 males to the number of F1 females. Assuming that all F1 progeny inherit the mutant chromosome, and that Lhr^1 rescue is high, I would expect a similar number of male and female progeny if there was no dominant suppression of rescue. This expectation of a similar number of F1 males and females is what I observed with the *HP5* mutant cross (footnote f).

Table IV.C.1 Testing *HP* mutants for a dominant effect on *Lhr*^{1} rescue

			F1 hybrid females		F1 hybrid males		Relative viability		
D. mel **female**	***D. sim*** **male**	**Temp °C**	**Mut/+**	**Bal/+**	**Mut/+**	**Bal/+**	**M/F Bal/+**	**M/F Mut/+**	**F.E.T.**[a]
HP1-1[b]	*Lhr*^{1}	23	201	221	78	72	0.33	0.39	0.392
HP1-1[b]	*Lhr*^{1}	23	121	115	33	47	0.41	0.27	0.154
HP1-2[c]	*Lhr*^{1}	23	44	15	30	15	1.00	0.68	0.392
HP1-2[c]	*Lhr*^{1}	23	104	139	129	76	0.55	1.24	<0.001
HP1-4[d]	*Lhr*^{1}	23	45	29	37	56	1.93	0.82	0.008
HP4[e]	*Lhr*^{1}	23	1132		743			0.66	<0.001*
HP5[f]	*Lhr*^{1}	23	544		633			1.16	
HP6-1[g]	*Lhr*^{1}	23	335	352	228	228	0.65	0.68	0.717

[a] - Inhomogeneity in the numbers of the 4 classes of progeny was tested by Fisher's Exact Test.
Full genotypes of *D. melanogaster* females are as follows: [b] - In(1)w^{m4h}; Su(var)205^{5}/In(2L)Cy, In(2R)Cy, Cy^{1},
[c] - Su(var)2-5^{01} / Bc Gla, [d] - Su(var)2-5^{02} / Bc Gla, [e] - y^{1} w^{67c23}; P{w^{+mC} y$^{+mDint2}$=EPgy2}CG8044^{EY01733} ,
[f] - y^{1} w^{67c23} P{w^{+mC} y$^{+mDint2}$=EPgy2}HP5^{EY10901}, [g] - w^{1118}; net^{1} P{w^{+mGT}=GT1}CG15636^{BG01429}/Bc Gla,
* - statistically significant difference from an expected 50/50 ratio tested by X^2 analysis.

In the *HP4* mutant cross, I observed a lower number of hybrid males compared to hybrid females (footnote e). Although the number of progeny I recovered was statistically different than an expected 1:1 ratio (*), I still recovered a large number of hybrid males, indicating that HP4 does not strongly suppress rescue by Lhr^1. Furthermore, recovering less than an equal proportion of hybrid males to females is not uncommon in hybrid crosses, and the *HP4* results are similar to some of the *HP1* and *HP6* crosses except for the much greater total number of flies.

Two alternative possibilities for the mutant HPs that do not dominantly suppress rescue by Lhr^1 are that they have no effect on *Lhr* rescue, or that they enhance *Lhr* rescue. I found that each mutant HP tested enhanced rescue in at least one cross to Lhr^2 (Table IV.C.2, compare Mut/+ to Bal/+ hybrid males). One potential concern is that the number of reference males (Bal/+) is very low in more than half of these crosses. However, these results are consistent with Lhr^2 being a low level rescue mutation, and helpful for interpreting results from this assay. It is also possible that the balancer chromosomes I used suppress Lhr^2, however, this seems unlikely as I used five different balancers on three different chromosomes.

I conclude that all four mutant HPs tested at least partially enhance Lhr^2 rescue, with the caveat that not all crosses with each mutant HP allele enhanced rescue. These results are interesting in light of the localization dependency and interaction data in Chapter III. Because LHR depends on both HP1 and HP5 for localization, and mutations in each of these HPs enhance Lhr^2 rescue, it may suggest that these interactions and the heterochromatic localization are important for the hybrid lethal activity of LHR. I will explore this possibility further in section IV.C.3 below.

Table IV.C.2 Testing *HP* mutants for a dominant effect on *Lhr²* rescue

			F1 hybrid females		F1 hybrid males		Relative viability		
D. mel **female**	***D. sim*** **male**	**Temp °C**	**Mut/+**	**Bal/+**	**Mut/+**	**Bal/+**	**M/F Bal/+**	**M/F Mut/+**	**F.E.T.[a]**
Df(Lhr)[b]	*Lhr²*	18	351	348	179	50	0.14	0.51	<0.001
		25	232	227	60	6	0.03	0.26	<0.001
HP1[c]	*Lhr²*	18	46	55	27	0	0.00	0.59	<0.001
	Lhr²	25	41	33	1	0	0.00	0.02	1
HP1[d]	*Lhr²*	18	21	35	36	1	0.03	1.71	<0.001
	Lhr²	25	173	240	29	6	0.03	0.17	<0.001
	Lhr²								
HP1[e]	*Lhr²*	18	50	49	41	6	0.12	0.82	<0.001
	Lhr²	25	186	173	123	63	0.36	0.66	0.001
	Lhr²								
HP4[f]	*Lhr²*	18	39	21	3	0	0.00	0.08	0.545
	Lhr²	18	57	63	49	7	0.11	0.86	<0.001
	Lhr²	25	209	184	69	7	0.04	0.33	<0.001
	Lhr²	25	53	37	19	4	0.11	0.36	0.051
HP5[g]	*Lhr²*	23	772	667	71	1	0	0.09	<0.001
HP6[h]	*Lhr²*	18	278	299	59	34	0.11	0.21	0.007
	Lhr²	25	290	244	135	99	0.41	0.47	0.387

[a] - Inhomogeneity in the numbers of the 4 classes of progeny was tested by Fisher's Exact Test. Full genotypes of *D. melanogaster* females are as follows: [b] - *Df(2R)BSC44/SM6a*, [c] - *In(1)w^{m4h}; Su(var)205^{5}/In(2L)Cy,In(2R)Cy,Cy^{1}*, [d] - *w^{m4h}; Su(var)2-5^{04}/CyRoi*, [e] - *Su(var)2-5^{02}/BcGla*, [f] - *y^{1} w^{67c23}; P{w^{+mC} y$^{+mDint2}$=EPgy2}CG8044^{EY01733}/TM3, Sb^{1} Ser^{1}*, [g] - *y^{1} w^{67c23}; P{w^{+mC} y$^{+mDint2}$=EPgy2}HP5^{EY10901}/FM7i, Act-Gfp*, [h] - *w^{1118}, HP6$^{36-5}$ /BcGla*

Similarly, because the HP6 mutant enhances rescue at 18° C, it indicates that the interaction I previously detected between LHR and HP6 may be required for hybrid male lethality. This theory is in contrast to what I suggested earlier, that there is likely no relevant *in vivo* interaction (Chapter III). One possible explanation for this discrepancy is that LHR and HP6 indeed interact as suggested by the yeast two-hybrid and genetic cross data, and that these proteins are present together in more tissues than originally estimated. Surprisingly, although I did not detect an interaction between HP4 and LHR in yeast or in the localization assay, the *HP4* mutant may enhance *Lhr* rescue. One potential explanation could be that the effect of HP4 is indirect, and possibly mediated through its interactions with HP1 and HP6. In fact, many of the mutant *HPs* could affect localization of LHR indirectly by altering heterochromatin structure. The results from this section are discussed further in Chapter V.

IV.C.2 Exploring the LHR-HMR interaction

One of the defining characteristics of a D-M pair is that the proteins have diverged in the two hybridizing parental species such that when re-introduced in the hybrids, the interaction is incompatible. The Barbash lab has previously shown that both *Lhr* and *Hmr* are divergent between *D. melanogaster* and *D. simulans*, and that specifically *mel-Hmr* and *sim-Lhr* are responsible for the lethal interaction (Brideau et al. 2006). For these reasons, I was interested to test if *Hmr* and *Lhr* interact in yeast two-hybrid assays in interspecific combinations in addition to pure species combinations.

I found that *Lhr* and *Hmr* from *D. melanogaster* and *D. simulans* appear to interact in all interspecific combinations (Figure IV.C.1). Reciprocal

experiments switching which protein was fused to the activation domain and DNA binding domain show variability in the assay (Figure IV.C.1B), and the *D. simulans* pure species combinations have a lower amount of growth compared to all other combinations tested. Because mel-HMR and sim-LHR interact in this assay, these results may suggest that the hybrid lethal interaction predicted by the D-M model is due to these two major HI proteins physically interacting. These results further suggest that the interaction between mel-HMR and sim-LHR is not a gained interaction specific to the hybrids, because the intraspecific combinations also interact (Figure IV.C.1B).

Work in our lab has shown that *Hmr* is evolving under recurrent positive selection, and that the MADF domains present in different HMR orthologs potentially have divergent binding specificities (Maheshwari, Wang, Barbash 2008). To determine if the LHR interaction is mediated by a conserved region of HMR, I extended my yeast two-hybrid analysis by testing if HMR fragments interact with LHR. *Hmr* encodes a large protein with regions resembling MADF and BESS domains, as well as stretches of simple sequence repeats (Maheshwari, Wang, Barbash 2008).

In order to map the region in HMR that mediates the interaction with LHR, I created a series of derivatives shown in Figure IV.C.2. I found that none of the five HMR derivatives I tested recapitulated the interaction that I detected for full length HMR. These results suggest the possibility that the derivatives I used disrupted the secondary structure of the LHR-interacting domain in HMR. It is also possible that full length HMR is needed to bind to LHR, or that multiple regions within HMR are necessary. One additional possibility is that these HMR derivatives are unstable in yeast; however this potential problem remains untested.

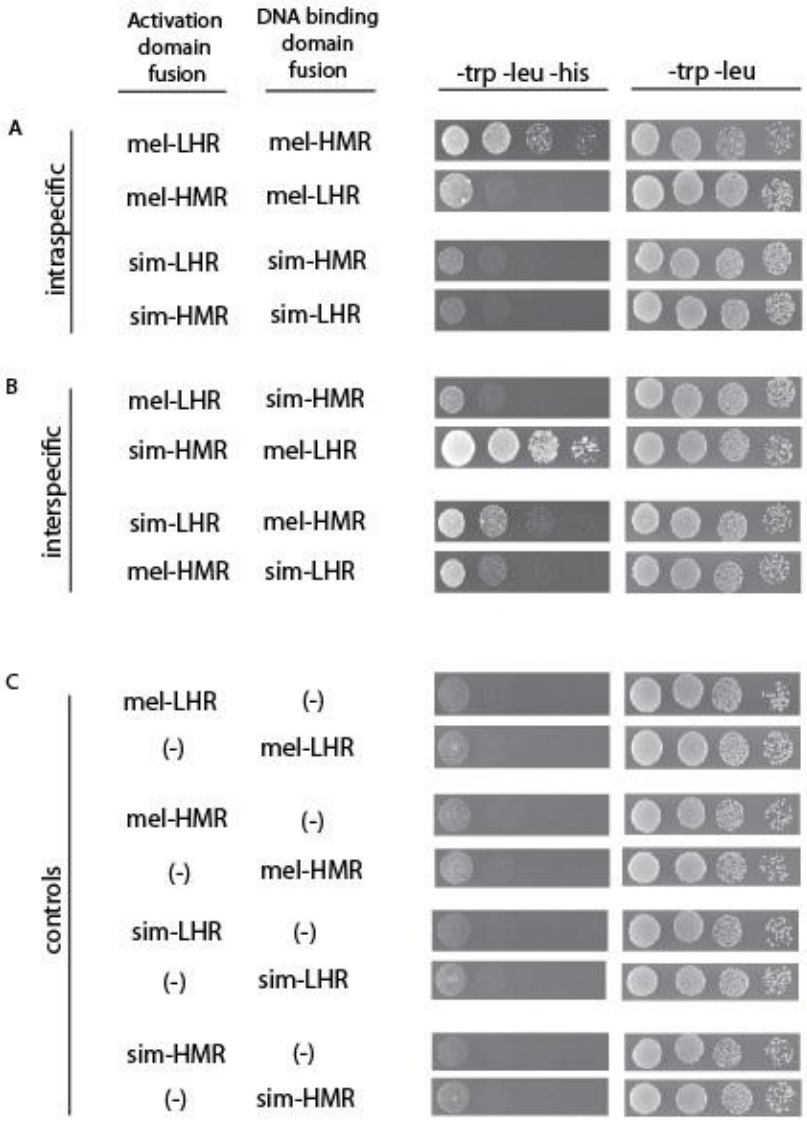

Figure IV.C.1 Testing if LHR and HMR interact

HMR and LHR interact in (A) intraspecific and (B) interspecific combinations in a yeast two-hybrid assay. No interaction was detected in the negative controls in (C). Interactions were detected by activation of HIS3 and growth on complete media lacking histidine (-trp -leu –his); loading controls (-trp –leu) contain histidine.

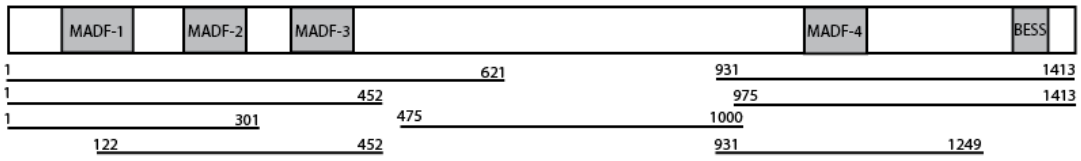

Figure IV.C.2 HMR derivatives tested for interaction with LHR

None of the HMR fragments I tested interact with LHR. Full length *D. melanogaster* HMR is shown with the MADF domains and the putative BESS domain shaded. Fragments of HMR that were tested for interaction with LHR in a yeast two-hybrid assay are shown below the cartoon of the protein.

IV.C.3 ADDITIONAL ANALYSIS WITH HP5 MUTANTS

It was intriguing that the *HP5* mutant affected LHR's localization even though I do not detect a direct interaction between the proteins (Chapter III). It is possible that LHR and HP5 do indeed interact, but that I was unable to detect it in my yeast two-hybrid experiments. It is also possible that HP5 affects LHR localization through an intermediate protein, or by specifying a specific chromatin state. HP5 depends on HP1 for localizing to heterochromatin, and *HP5* is a dominant suppressor of position-effect variegation (Greil et al. 2007). This result suggests that HP5, in concert with HP1, is involved in the structure or maintenance of heterochromatin. I therefore was interested to test if the loss of heterochromatic localization of LHR in *HP5* mutants affected the ability of LHR to cause hybrid male lethality.

In order to test this experimentally and to make any clear conclusions, I needed to establish a number of criteria. Due to the developmental defects in hybrid males (Bolkan et al. 2007), I could only examine second instar larvae. Therefore, I first needed to make sure that expression from the *UAS-Lhr-Yfp* transgene was reliably detectable in second instar larvae. I found that LHR-YFP signal was detectable in the salivary glands of these larvae (Figure IV.C.3). Second, I wanted to examine LHR localization in hybrids. I found that sim-LHR-YFP is not mislocalized in the salivary glands of a normal hybrid cross (Figure IV.C.3). In Chapter III, I reported that four LHR orthologs are able to cause hybrid male lethality. I was therefore interested to test if each of these orthologs is also mislocalized in a *D. melanogaster HP5* mutant background. I found that like mel-LHR, sim-LHR, yak-LHR, and vir-LHR also all lose heterochromatic localization due to the *HP5* mutation (Figure IV.C.4).

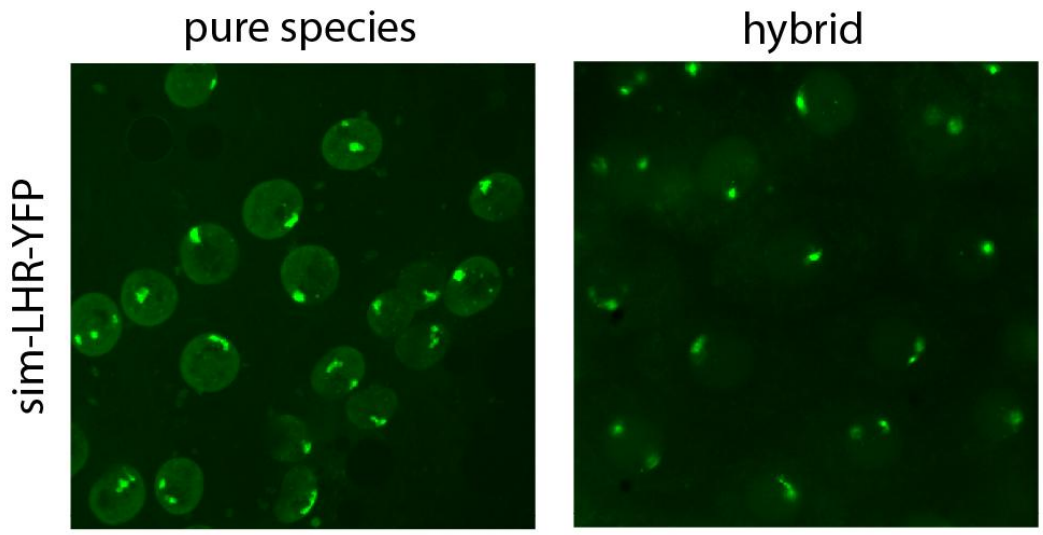

Figure IV.C.3 Analyzing LHR-YFP localization in hybrid males

LHR-YFP localizes in second-instar larvae to bright foci in F1 hybrid males in a pattern similar to pure species controls. *D. melanogaster* mothers carrying the *sim-Lhr-Yfp* transgene were crossed to either *D. melanogaster* w^{1118} (pure species) or *D. simulans* w^{501} (hybrid). Localization was detected by live YFP analysis and males were identified by PCR.

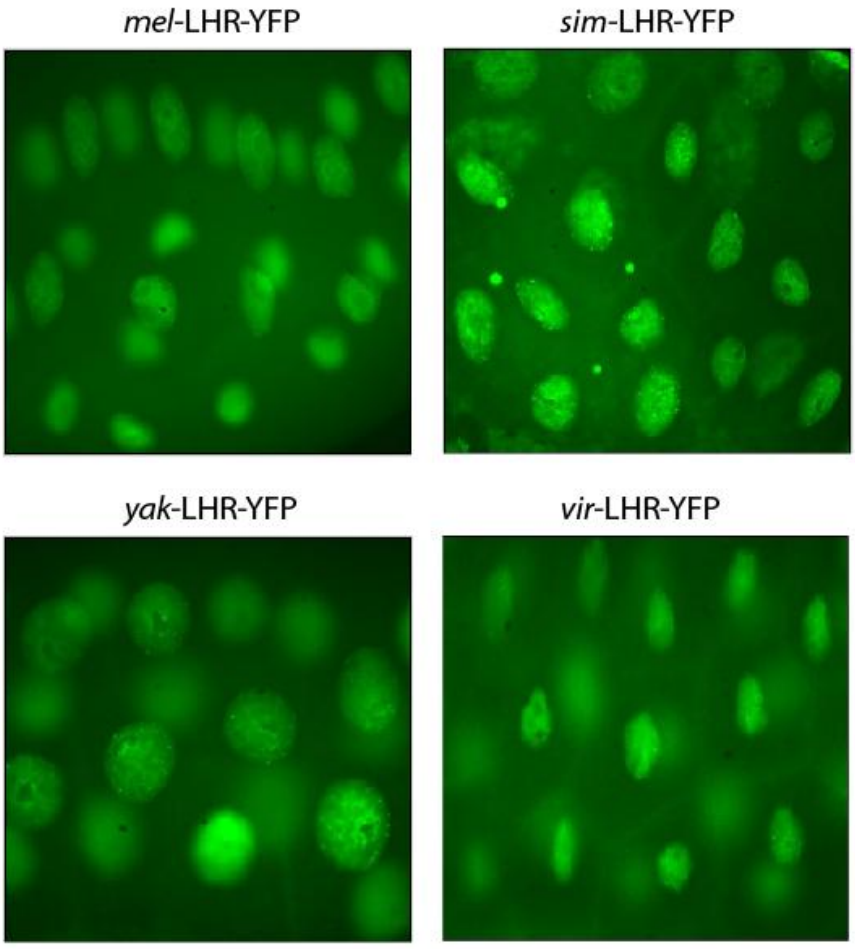

Figure IV.C.4 LHR ortholog mislocalization in an *HP5* mutant line

Four LHR-YFP orthologs lose heterochromatic localization when expressed in a *D. melanogaster HP5* mutant background. For each LHR ortholog tested, *HP5* mutant females were crossed to males carrying the LHR reporter chromosome and the F1 progeny were examined. LHR-YFP localization was similar in both male and female F1 larvae.

Collectively, these results suggest that loss of HP5 would cause both mel-LHR and sibling-LHR to lose heterochromatic localization in hybrids between *D. melanogaster* and its sibling species. Based on this reasoning, I tested if crosses between *D. melanogaster HP5* mutant females and either *D. simulans* or *D. mauritiana* males produce viable hybrid sons. I used *D. mauritiana* in addition to *D. simulans,* because crosses between *D. melanogaster* and *D. mauritiana* are generally more successful than crosses with *D. simulans*. Additionally, the *D. mauritiana* background is more sensitive to detect genetic interactions as the presence of pharate male progeny indicates a low level of rescue past the normally lethal late third instar stage (Barbash, Roote, Ashburner 2000).

The first experiment used *D. melanogaster* females heterozygous for the *HP5* chromosome and a balancer chromosome for the purpose of comparison similar to the hybrid crosses outlined above (Table IV.C.1,2). I found that no hybrid males survived (Table IV.C.3), indicating no difference in hybrid males that inherit a wild-type or mutant copy of HP5. Hybrid females were recovered, and the number of hybrid females inheriting the *HP5* mutant chromosome was not statistically different than the number inheriting the wild-type HP5 balancer chromosome. These results suggest that the *HP5* mutation has no effect on hybrid female viability. However, the males that inherit the *HP5* mutant chromosome will have no zygotic wild-type HP5.

Table IV.C.3 Testing for suppression of hybrid male lethality with HP5 mutants

male parent [a]	F1 female progeny		F1 male progeny	
	HP5 $^{-}$/+	**FM7i**	**HP5 –/Y**	**Bar**
10-18[b]	458 n.s.	398	0	0
W139[b]	219 n.s.	176	0	0
***w*$^{501\ c}$**	284 n.s.	233	1*	0

[a] – *D. melanogaster* virgin females of the genotype*: y*^{1} *w*^{67c23} *P{w*$^{+mC}$ *y*$^{+mDint2}$*=EPgy2}HP5*^{EY10901}*/FM7i, Act-Gfp* were crossed to *D. mauritiana* ([b]) or to *D. simulans* (c) males and the F1 progeny were scored.

*- exceptional male inheriting both the X and Y chromosome from the *D. simulans* father

n.s. – The observed number of F1 females inheriting the *HP5* mutant chromosome was not significantly different than the expected value by Chi-square analysis $p > 0.05$.

One caveat to the HP5 hybrid crosses above is that I used heterozygous *D. melanogaster* mothers, and because HP5 is expressed highly during early embryogenesis (Gauhar 2008), HP5 may have been maternally deposited into the hybrid embryos. To address this issue, I repeated the hybrid crosses above but with homozygous *HP5* mutant females. I found that homozygous *D. melanogaster HP5* mutant females crossed to *D. mauritiana* males fail to produce viable hybrid males or even pharate males (~300 F1 females, ~20 dissected pupae).

Together, the hybrid crosses with heterozygous and homozygous *HP5* mothers suggest that a mutation in HP5 is not enough to rescue hybrid male lethality, and further suggest that the heterochromatic localization of LHR is not required for its hybrid lethal activity. The reasoning behind this latter point is that based on data above (Figure IV.C.4), the HP5 mutation likely causes both *D. melanogaster* and the sibling species LHR orthologs to lose heterochromatic localization in the hybrids from these crosses, yet these males still die, suggesting that LHR does not need to localize to heterochromatin in order to cause hybrid male lethality. In order to strengthen this hypothesis, we still need to test whether the HP5 mutation mislocalizes LHR-YFP in the hybrid larvae.

How do I reconcile this result with those reported earlier in Chapter III and Chapter IV suggesting a role for many HPs in LHR function? Immunofluoresence analysis indicates that LHR-YFP predominantly localizes to heterochromatic regions of polytene chromosomes. However, LHR and several other HPs also associate with euchromatin (Fanti et al. 2003; Greil et al. 2007). It is therefore possible that the interactions between LHR and these HPs that contribute to hybrid male lethality occur at euchromatic sites.

Alternatively, although the majority of the heterochromatic signal disappears in *HP5* mutants, it is possible that LHR still associates with a fraction of heterochromatin and cannot be detected within the resolution of my assay.

V. DISCUSSION AND FUTURE DIRECTIONS

Post-zygotic hybrid incompatibility (HI) refers to barriers against the reproductive success of hybrid zygotes such as hybrid sterility and inviability. When I began work on this thesis, only four HI genes had been discovered and initially characterized, three of which were found in *Drosophila*.
Part of the manuscript in Chapter II is work performed in the lab describing the identification and cloning of a fifth HI gene, *Lethal hybrid rescue (Lhr).* The rest of my work on *Lhr* is subsequent to this discovery, and provides a good starting point toward understanding the properties and functions of LHR and, ultimately, how it causes hybrid male lethality. In this chapter I present the broad conclusions of my work and provide future perspectives on the study of *Lhr*.

V.A Identifying key protein partners of LHR

It has been proposed that the lethality of *D. melanogaster-D.simulans* hybrid males is due to an incompatibility of two or more genes from the parental species (Sturtevant 1920; Pontecorvo 1943; Hutter et al. 1990; Brideau et al. 2006). Chapter II contains experiments demonstrating that *Hmr* and *Lhr* interact genetically to cause the lethality of hybrid males. In Chapter IV, I showed that the lethal interaction of *Hmr* and *Lhr* may be mediated by a physical interaction of the two encoded proteins. In Chapter II it was shown that *mel-Hmr* and *sim-Lhr* specifically interact to cause lethality based on the Dobzhansky-Muller model for HI evolution. Therefore, I tested whether *Hmr* and *Lhr* interact in yeast two-hybrid in both pure species and interspecific combinations, and found this to be true. These results suggest that the physical interaction between LHR and HMR is not unique to the hybrid

background, but that somehow their interaction in hybrids is deleterious.

This conclusion is still consistent with the D-M model of HI. For example, consider that *Hmr* and *Lhr* are “a” and “b” in the two-locus D-M model in Chapter I (Figure I.A.1). In this model, *Hmr* and *Lhr* would interact in the ancestral species. Then as the two populations split, *Hmr* acquires new functions and interactions in population 1 (*D. melanogaster*), but still interacts with *Lhr*. Likewise, *Lhr* evolves and acquires new functions and interactions in population 2 (*D. simulans*), but still interacts with *Hmr*. Then in the hybrid, it is the combination of the newly acquired functions and interactions of *Hmr* and *Lhr* that becomes deleterious. My data match this model, but we must also consider the caveat that *sim-Lhr* is not deleterious in *D. melanogaster* where *mel-Hmr* is also present. How can I explain this?

I suggest that during the evolution of *Lhr* in *D. simulans* new interactions were developed, and that the absence of these *D. simulans* interactors in *D. melanogaster* explains why *Lhr* alone is insufficient to cause HI when present in pure species *D. melanogaster*. Although I now suggest that the physical association of LHR and HMR in the hybrids is deleterious, the mechanism of the interaction that causes lethality remains unknown. One possibility is that both LHR and HMR associate with DNA or chromatin. This possibility is consistent with the hypothesis that altered chromosome morphology and chromatin structure due to species specific differences in repetitive elements, cause the hybrid background effect (Brideau et al. 2006).

One important aspect in understanding how the interaction between LHR and HMR kills hybrid males is determining in the cellular and possibly subcellular localization of the lethal interaction. Data in Chapters II and III show that LHR associates with heterochromatic sequences. Consistent with

these data, preliminary experiments in the lab suggest that LHR and HMR co-purify with HP1 (H. Kwak, D. Barbash, unpublished). I believe that it will be necessary to establish that LHR and HMR are present at the same locations in the cell through techniques such as immunoflourescence and chromatin-immunoprecipitaton. In Chapter III, I showed that LHR depends on one of its interacting partners, HP1, for heterochromatic localization. Additionally, because *Hmr* has a major-effect on hybrid male lethality, and HMR and LHR interact, I think a useful extension of the LHR-YFP localization assay I have developed is to examine LHR localization in *Hmr* mutant larvae.

As I mentioned earlier, the interaction between LHR and HMR is not sufficient to cause hybrid male lethality. I therefore wished to examine other LHR-interacting proteins to determine their potential role in the functions of LHR. In 2003, as part of a large-scale yeast two-hybrid screen, LHR (as CG18468) was reported to interact with four proteins (Giot et al. 2003). One of these proteins was Heterochromatin Protein 1 (HP1), which is probably the best studied non-histone chromosomal protein. When I started this work, much was known about HP1, but almost nothing was known about LHR. I therefore hoped to explore this interaction in order to learn more about LHR.

After I began this work with HP1 and LHR, three other heterochromatin proteins were identified and named HP4, HP5 and HP6 based on their association with HP1 (Greil et al. 2007). LHR was also included in this analysis and named HP3, and together these proteins were proposed to form a network of interacting proteins. I wanted to determine the relationship between these HPs and LHR, and first started with analysis in pure species *D. melanogaster*. I have shown that of the four HPs I tested, LHR interacts with HP1 and HP6 in yeast two-hybrid, expanding the number of confirmed LHR-

interacting proteins to three. Additionally, these interactions are conserved for at least seven Drosophila *Lhr* orthologs (discussed in V.D below). I have further shown that LHR binds directly to HP1, and this binding is required for localization of LHR. Consistent with this binding, we have shown that LHR colocalizes with HP1 at the pericentric chromocenter, fourth chromosome, and telomeres, which are all heterochromatic regions of polytene chromosomes.

I also discovered that LHR depends on HP5 for heterochromatic localization despite not detecting an interaction between the two proteins. I believe that HP5 is a good candidate for additional study for a number of reasons. First, because HP5 is one of only two proteins we have identified that mislocalizes LHR, we can hopefully use this result to address if the heterochromatic localization of LHR is critical to its functions. This approach is discussed further in section V.B below. Second, like LHR, HP5 is also highly divergent between *D. melanogaster* and *D. simulans*. One major challenge will be to connect the rapid evolution of these proteins to their function. And third, very little is known about HP5 aside from localizing to heterochromatin, interacting with HP1, and modifying position effect variegation.

We could study additional properties of HP5 to potentially learn more about LHR, such as identifying additional interacting proteins, examining the localization and expression throughout development, understanding how the HP5 protein localizes to chromatin, and ultimately determining the function of HP5. Although I did not detect an interaction between LHR and HP5 in a yeast two-hybrid assay, a mutation in *HP5* enhances Lhr^2 rescue, indicating a genetic interaction. Therefore, it may be worth testing if these two proteins interact in another experimental system, such as co-immunoprecipitation from embryo or cell culture extracts.

Additional experiments are also needed in order to confirm that the effect I detected on LHR localization in the *HP5* mutant stock is specifically caused by lack of HP5. The *HP5* mutant is a P-element insertion into the 5' UTR. We could excise this P-element in order to create precise and imprecise excision lines. Proper localization of LHR in a precise excision line would demonstrate that the P insertion causes the effect, and strengthen the argument that the mislocalization is due to the *HP5* mutation or nearby genes. Another key issue here is whether the HP5 mutant I have been using is null. As a complement to the precise excision, an imprecise excision that deletes enough surrounding sequence to disrupt HP5 would create an additional *HP5* mutant stock that we could then use for further analysis.

Earlier I presented the hypotheses of newly evolved interactors in the parental species and the defective chromatin structure in hybrids as two models to explain why LHR is only lethal in the hybrid background. Because the interactions with HP1 and HP6 are conserved, it is unlikely that these HPs are the newly acquired LHR-interactors outlined above. If this model of HI is true, this suggests that additional proteins are required to cause HI. In Chapter IV, I found that mutations in each of these HPs enhance *Lhr*-dependent hybrid male rescue. Together, the effects of mutations in these HPs on *Lhr*-dependent rescue and on heterochromatin structure strengthen the alternative argument that aberrant chromatin structure contributes to hybrid lethality.

V.B The heterochromatic localization of LHR and its role in hybrid male lethality

After discovering that LHR interacts and co-localizes with HP1, I was immediately interested in testing if this association with HP1 and localization to heterochromatin are critical to the hybrid lethal function of LHR. As described above, in order to test this hypothesis I attempted to create a mutant form of LHR unable to interact with HP1. Although I managed to identify a novel HP1-interacting domain in LHR, the region I identified is not completely responsible for mediating the interaction and is also part of a NLS, and for these reasons this project was suspended.

Alternatively, the experiments with an *HP5* mutant explained in Chapter IV.C were one way to test if the heterochromatic localization but not the interaction with HP1 is required for the lethal activity of LHR. The results from these experiments suggest that the predominant heterochromatic localization is not required for the hybrid lethal function of LHR. Based on the results in Chapter IV.C, I assumed that the *HP5* mutation would mislocalize LHR in hybrids. To confirm this assumption, one still needs to examine the LHR-YFP localization in F1 hybrid progeny from crosses using *D. melanogaster* females that are homozygous mutants for *HP5* and express the LHR-YFP transgene.

HP5 has also been proposed to have a role in modulating heterochromatin structure based on a PEV assay (Greil et al. 2007). It is possible that *HP5* affects LHR localization by globally disrupting heterochromatin. This explanation seems unlikely as HP1 retains strong chromocenter localization in *HP5* mutants (my unpublished results). This result also means that LHR mislocalization is not a secondary effect to HP1

mislocalization. When considered in combination with no detectable interaction between LHR and HP5 in yeast two-hybrid, these results suggest that HP5 indirectly recruits LHR, or creates a chromatin environment that LHR recognizes for localization (Figure V.B.1).

Preliminary experiments suggest that HP5 dominantly affects the heterochromatic localization of LHR. Surprisingly, I found that LHR-YFP is mislocalized in heterozygous *HP5* females. This mislocalization may not be a maternal effect, as LHR-YFP is mislocalized in heterozygous daughters produced from both homozygous and heterozygous *HP5* mutant mothers. Furthermore, the LHR in WT sons (non *HP5* mutant) produced from heterozygous mothers localizes to heterochromatic foci (my unpublished results). This result suggests that the genotype of the mother may not matter in determining LHR localization, however I did not test whether LHR is mislocalized in heterozygous *HP5* daughters from wild type mothers. As mentioned above, all of these experiments addressing the dominance and maternal effect of HP5 on LHR localization are preliminary and need to be repeated. This line of experiments may serve as a good starting point for investigation into the relationship between LHR and HP5.

Figure V.B.1 Two alternative models for how HP5 affects LHR localization

A) HP5 and HP1 create a chromatin environment that is recognized by LHR. In this example, HP1 recognizes the methylated lysine 9 on histone H3 (H3K9me2) and recruits additional HP1 molecules, as well as HP5. LHR can then identify the chromatin state created by HP5 and HP1, and bind to HP1 dimers. B) HP5 modifies the chromatin state or a chromatin-associated protein which is then recognized by LHR. In this model, HP1 binds to dimethylated H3K9, and HP5 then binds to HP1 dimers. HP5 then modifies HP1 (or possibly other proteins) which become specific targets for LHR, and LHR is then recruited to chromatin.

A

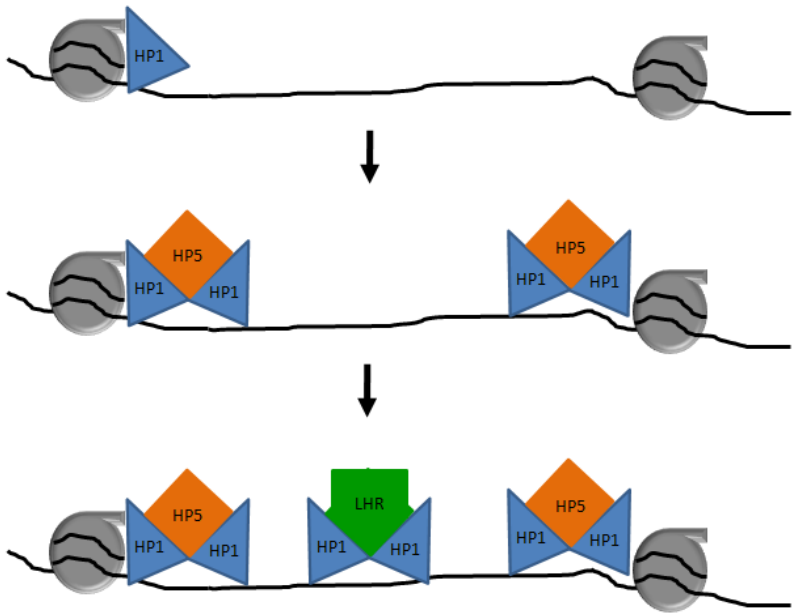
HP1
HP5
HP1
HP1
HP5
HP1
HP1
HP5
HP1
HP1
LHR
HP1
HP1
HP5
HP1
HP1

B

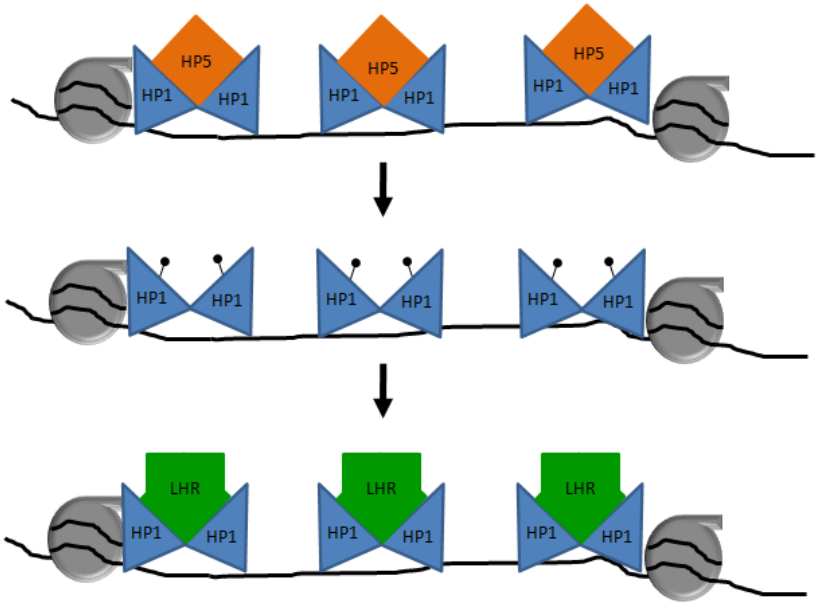
HP5
HP1
HP1
HP5
HP1
HP1
HP5
HP1
HP1
HP1
HP1
HP1
HP1
HP1
HP1
LHR
HP1
HP1
LHR
HP1
HP1
LHR
HP1
HP1

V.C Determining the function of LHR

As mentioned earlier, the only known function of LHR is that it is lethal to hybrid males. One of the main goals in the lab is to discover the function of LHR in pure species. Additionally, determining the function of LHR in pure species *D. melanogaster* and *D. simulans* may lead to a better understanding of how LHR kills *D. melanogaster-D. simulans* hybrid males. For example, one could compare the phenotypes of *Lhr* mutations among the two parental species and their hybrids. Along this line of reasoning, I have described my initial attempts at determining the function of LHR in *D. melanogaster* flies carrying an *Lhr* knockout allele in Chapter VI. I used this mutation is a variety of tests related to the heterochromatic association of LHR.

Unfortunately, each of these experiments either produced negative results, or the results were inconclusive. Unlike mutations in other genes that encode heterochromatin proteins such as *Su(var)3-7* and *Su(var)2-5*, mutations in *Lhr* do not appear to affect the establishment or maintenance of heterochromatin. Although our PEV experiment was inconclusive, it is possible that LHR affects a subset of heterochromatic regions, and that the Sb^{v} reporter is not located in one of those regions. Many different PEV reporters are now available in a variety of genomic locations, and testing if the Lhr^{KO} allele modifies a small number of these would be a good way to address this issue.

The knockout of *Lhr* also does not affect the X chromosome structure in pure species in a manner similar to *Su(var)3-7* and *Su(var)2-5*. Although I saw no gross effect in pure species, this does not rule out a role for *Lhr* in regulating the chromatin state of the X chromosome in hybrids. Other groups have described aberrant condensation of the X chromosome (Hutter, Roote,

Ashburner 1990; Chatterjee et al. 2007) and mislocalization of the male-specific lethal (MSL) complex (Pal Bhadra, Bhadra, Birchler 2006) in male hybrids. It has also been shown that the *D. simulans* Lhr^{1} mutation restores the morphology of the X chromosome, and sequestration of the MSL complex to the X chromosome in male hybrids (Pal Bhadra, Bhadra, Birchler 2006).

Many of the HI genes identified are associated with DNA. I have shown that by binding to HP1, LHR associates with heterochromatin. LHR is also known to associate with hundreds of protein-coding genes (Greil et al. 2007). Another interesting area to explore is the specific sequences where LHR localizes. One could then compare the difference in sequence or localization among *D. melanogaster* and *D. simulans* and their hybrids. Additionally, quite a few of the HI loci have a pure species function related to fertility. Therefore, it seems reasonable to examine expression of *Lhr* in the ovaries and testes and to search for fertility defects in Lhr^{KO} flies.

V.D Exploring the relationship between sequence divergence and function

One of the major challenges in studying a rapidly evolving protein is connecting the sequence divergence to the biological basis of the sequence evolution. Chapter II contains data demonstrating that *Lhr* is rapidly evolving under positive selection. I have also reported here that HP5 and HP6 are also highly divergent between *D. melanogaster* and *D. simulans*. This means that LHR, along with HP5, HP6 and SU(VAR)3-7 compose a group of rapidly evolving, heterochromatin-associated, HP1-interacting proteins. To test the significance of the sequence divergence of LHR on its functions and interactions I analyzed *Lhr* orthologs using several approaches.

First, I found that LHR from seven *Drosophila* species interacts with both HP1 and HP6. I also identified a domain in *D. melanogaster* LHR that is part of a nuclear localization signal and, when mutated, affects binding to HP1. Comparing this NLS/HP1-interacting domain identified in *D. melanogaster* to the seven orthologs that interact with HP1 and HP6 reveals that the clustering of charged amino acids indicative of an NLS, but not the exact sequence of this region are conserved. These studies highlight the power of using an evolutionary approach to guide analysis of functional proteins domains. Consistent with these results, four LHR orthologs co-localize with HP1 at heterochromatic regions when expressed in *D. melanogaster*.

One of the major predictions of the D-M model is that HIs are asymmetric. In Chapter II, we confirmed this asymmetry for *Lhr*, by demonstrating that loss-of-function mutations in *sim-Lhr* rescue hybrid males, but deletions of *mel-Lhr* do not. Furthermore we suggested that *sim-Lhr* interacts with *mel-Hmr* to form a D-M pair of interacting loci. In Chapters III and VI, I show that in addition to having the same molecular interaction and localization properties, four *Lhr* orthologs can induce hybrid lethality. These results demonstrate that despite the sequence divergence among *Lhr* orthologs, *Lhr* is not asymmetric in its HI activity as reported previously, and suggest that *sim-Lhr* and *mel-Hmr* are not a unique D-M interacting pair.

V.E One potential model for the hybrid lethal activity of LHR

The lethality of hybrids between *D. melanogaster* and *D. simulans* is specific to males that carry the *D. melanogaster* X chromosome. It has been proposed that *Hybrid male rescue (Hmr)* and possibly other factors on the *mel*-X interact with *Lhr* and additional factors on the *D. simulans* autosomes to

cause this lethality (Pontecorvo 1943; Barbash et al. 2000; Brideau et al. 2006). I have shown here that HMR and LHR likely interact in both intraspecific and interspecific combinations. I have also shown that *mel-Lhr* and *sim-Lhr* can both induce hybrid male lethality. These results suggest that both *D. melanogaster* and *D. simulans* LHR interact with mel-HMR to cause hybrid lethality.

Additionally, LHR interacts with HP1 and HP6, and mutations in HP1 and HP4-6 enhance *Lhr*-dependent rescue. Furthermore, the heterochromatic localization of LHR may not be required for hybrid male lethality. Together, these results suggest that LHR interacts with HMR and the HPs at euchromatic sites in the genome, and collectively these proteins somehow influence the chromatin structure in hybrids such that it is deleterious (Figure V.E.1). This model suggests that despite the emphasis of the association of LHR with heterochromatin, the non-heterochromatic loci may be most important for the hybrid lethal function. Testing of this model will require detailed high resolution mapping of LHR binding sites in the genome, and careful examination of the developmental defects in dying hybrids, especially those related to chromatin structure.

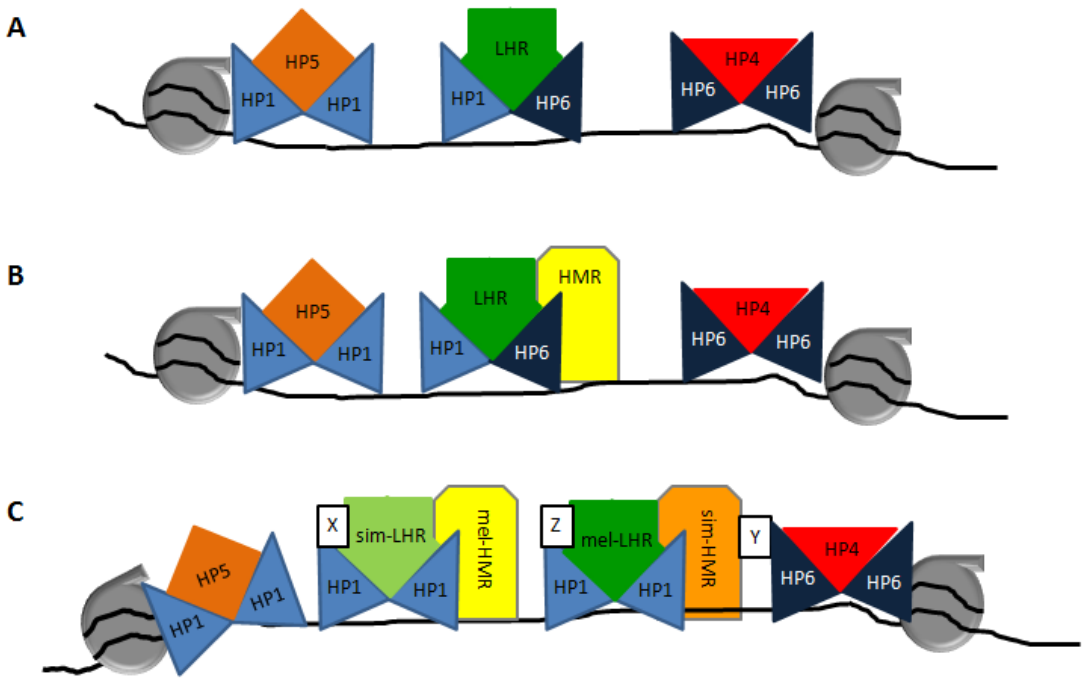

Figure V.E.1 Three models for LHR protein interactions

A) Heterochromatin proteins LHR, HP4 and HP5 interact with HP1 dimers, HP1-HP6 heterodimers, or HP6 dimers, predominantly at heterochromatin but also at euchromatic sites. B) HMR may interact with LHR in pure species at distinct chromatin sites. In this example, LHR, HP4 and HP5 localize normally. The LHR in the figure refers to any of the four LHR orthologs that were expressed in *D. melanogaster* as described in Chapter III and VI. C) Interaction of LHR, HMR and several HPs in the hybrid background. In this scenario, LHR and HMR interact in interspecific combinations with additional unknown interacting proteins (X, Y, and Z). The spacing and interactions of all the proteins and the chromatin structure are slightly disturbed, potentially leading to incompatibilities.

APPENDICES

The first three chapters of this appendix are investigations of *Lhr* that I completed, but for technical reasons or because they are negative results, have not been published. These chapters should however, serve as a record of some additional approaches to study *Lhr*. The fourth chapter of the appendix is a published manuscript from work I completed during my rotation in Prof. K. Whitlock's lab as a first-year student.

Appendix A: Quantifying the strength of interactions between seven LHR *orthologs and D. melanogaster HP1*

A.1 Introduction

We have demonstrated that *Lhr* is rapidly evolving in a manner consistent with positive selection (Brideau et al. 2006). In the same study, we also discovered an asymmetry in the effects of mutations in *D. melanogaster* and *D. simulans Lhr* on hybrid males. Specifically, we found that removal of *Lhr* from *D. simulans* fathers but not *D. melanogaster* mothers suppresses F1 hybrid male lethality. I have also shown that despite this divergence in sequence, the *D. melanogaster* LHR properties of interacting and co-localizing with HP1 are conserved for *D. simulans* and other LHR orthologs (Brideau et al. 2006). I was therefore interested to test if the sequence divergence of LHR had an effect on its binding affinity to HP1. Additionally, one hypothesis based on the association of LHR and HP1 is that the hybrid lethal activity of LHR is dependent on HP1. These results could therefore have interesting implications for understanding the hybrid lethal activity of *Lhr*. For example, if *D. simulans* LHR showed a 10-fold higher affinity for HP1 than

D. melanogaster LHR, this could potentially explain the asymmetry we noticed between *D.melanogaster Lhr* and *D.simulans Lhr*. I tested if seven LHR orthologs have different affinities for HP1 by using a semi-quantitative yeast two-hybrid assay. It has previously been shown that the strength of interaction between two proteins predicted by this assay generally correlates with that determined *in vitro*, allowing detection of high-, intermediate-, and low-affinity interactions (Estojak, Brent, Golemis 1995). For the assay, I selected the substrate chlorophenol red-β-D-galactopyranoside (CRPG) because it is more stable and sensitive than the commonly used substrates X-Gal and ONPG (Wittrup, Bailey 1988; Craig 1998).

A.2 Materials and methods

Plasmids and yeast strain

The Clontech vector pGADT7-AD was modified to contain the Gateway cloning cassette (Invitrogen), and was a gift from K. Ravi Ram, A. Garfinkel, and M. F. Wolfner (Cornell University; personal communication). The DNA binding domain plasmid pBTM116 was also modified to contain the Gateway cassette, and was a gift from I. Liachko and B.K. Tye, (Cornell University; personal communication). Seven *Lhr* orthologs were each recombined into the pBTM vector and *D. melanogaster HP1* was recombined into pGAD. Each of the CDSs used were subcloned from pENTR/D-TOPO vectors into the appropriate two-hybrid destination vector via LR recombination according to the manufacturer's instructions (Invitrogen). All resulting pGAD and pBTM fusion constructs were verified by restriction digestion. pGAD-HP1 and pBTM-LHR constructs were transformed into the two-hybrid strain EGY40 carrying the pSH18-34 reporter plasmid (Fields, Song 1989) using a LiAc/PEG

procedure (Zymo Research).

Liquid culture assay

Independent colonies of yeast containing the pGAD-HP1 and pBTM-*Lhr* plasmids were picked and cultures were grown overnight in SD medium (CM – leu –trp –ura). 1.0 mL of each culture was transferred into 4.0 mL of fresh SD media, and cultures were incubated at 30° with shaking until the cells were in mid-log phase. The OD_{600} was recorded and 1.5 mL of cells were pelleted for 30 seconds at 13,000 rpm. The supernatant was removed, and cells were washed with 1.0 mL of Buffer 1 (100mM HEPES, 150mM NaCl, 5mM L-Aspartate, 1% BSA, 0.05% Tween 20, pH 7.25). Cell were pelleted by centrifugation, and resuspended in 300 µL of Buffer 1. 100µL of the cell suspension was transferred to a new microfuge tube, and flash frozen in liquid nitrogen for 1 minute. Frozen tubes were then placed in a 37°C water bath for 1 minute until thawed, and this freeze/thaw cycle was repeated three times. 0.7 mL of Buffer 2 (2.23mM CPRG in Buffer 1, filter sterilized) was added to each tube of cells, samples were thoroughly mixed, and the starting time was recorded. When the color of each sample turned from bright yellow to yellow-grey/red, the color development reaction was stopped by adding 0.5 mL of 3.0 mM $ZnCl_2$, and the stop time was recorded. Cell debris was pelleted by centrifugation, and the supernatant was transferred to new tubes. The OD_{578} of each sample was taken, and β–galactosidase units were calculated as follows: β–galactosidase units = $1000 \times OD_{578} / (t \times V \times OD_{600})$ where t = elapsed time of incubation (min), V = 0.1 x concentration factor (the concentration factor above is 1.5 mL/0.3 mL = 5). For each *Lhr* ortholog, 10 independent colonies were tested.

A.3 Results and Discussion

The β–galactosidase activity for yeast containing pGAD-HP1 and pBTM-*Lhr* for seven *Lhr* orthologs are presented in Table A.1. The mean and standard deviation were calculated for independent replicates of each ortholog, and are summarized in Table A.2. For some samples, the OD_{578} was outside the linear range of the assay (0.25-1.8) and these results were excluded in calculating the summary table. Four of the *Lhr* orthologs tested (*D. melanogaster, D. simulans, D. ananassae and D. virilis*) had a similar value for average β –galactosidase activity (22-39 units). Yeast containing the *D. erecta* construct had an intermediate level (79 units), and yeast with the *D. yakuba* and *D. pseudobscura* pBTM-*Lhr* had a level of β –galactosidase activity an order of magnitude higher than all the other orthologs (467-485 units). Although technical replicates were consistent (data not shown), a high level of variability was found for the biological replicates for each *Lhr* ortholog tested. This point is best illustrated by the standard deviation ranging from 20% of the average number of units at its lowest (*D. virilis*), to 58% at its highest value (*D. melanogaster*).

Collectively, these data lead to two conclusions. The first is that despite the high amount of variability, I detected activity for each of the *Lhr* orthologs tested, which confirms that all seven *Lhr* orthologs assayed interact with *D. melanogaster* HP1 using a second yeast reporter system. The second is that the liquid culture β–galactosidase assay using CPRG as a substrate is not consistent enough to reliably be used as a measure of binding affinity between two proteins.

Table A.1 Beta-galactosidase units for LHR orthologs

Data collected for each *Lhr* ortholog-HP1 combination tested. All paramaters collected are listed, as well as the calculated number of β–galactosidase units.

***Lhr* ortholog**	**Sample**	**OD_{600}**	**OD_{578}**	**t (min)**	**V**	**Units**
D. melanogaster	1	0.83	1.77	18	0.50	236.28
	2	0.47	0.20	100	0.50	8.66
	3	0.44	0.34	100	0.50	15.60
	4	0.49	0.51	100	0.50	20.65
	5	0.37	0.07	100	0.50	3.91
	6	0.43	0.41	100	0.50	18.93
	7	0.42	0.86	100	0.50	41.00
	8	0.49	0.72	100	0.50	29.49
	9	0.44	1.31	100	0.50	60.14
	10	0.51	0.82	100	0.50	32.37
D. simulans	1	0.94	0.57	45	0.50	27.03
	2	1.10	0.48	45	0.50	19.48
	3	0.83	0.90	45	0.50	47.75
	4	1.03	0.45	45	0.50	19.43
	5	0.84	0.33	45	0.50	17.17
	6	0.92	0.36	45	0.50	17.48
	7	0.97	0.51	45	0.50	23.55
	8	0.93	0.41	45	0.50	19.47
	9	0.78	0.31	45	0.50	17.75
	10	0.87	0.00	45	0.50	0.00

Table A.1 (Continued)

Lhr ortholog	Sample	OD_{600}	OD_{578}	t (min)	V	Units
D. yakuba	1	0.85	2.78	6	0.50	1096.25
	2	0.88	1.03	6	0.50	392.76
	3	0.79	1.28	6	0.50	541.88
	4	0.92	0.80	6	0.50	290.71
	5	0.71	0.19	6	0.50	87.67
	6	1.02	0.11	6	0.50	35.95
	7	0.83	1.33	6	0.50	531.57
	8	0.95	1.55	6	0.50	544.43
	9	0.84	1.26	6	0.50	502.78
	10	0.99	0.00	6	0.50	0.00
D. erecta	1	0.70	0.61	26	0.50	66.86
	2	0.78	0.46	26	0.50	45.46
	3	0.91	1.64	26	0.50	138.77
	4	0.80	0.36	26	0.50	35.12
	5	0.74	1.17	26	0.50	121.60
	6	0.78	1.32	26	0.50	129.91
	7	0.63	0.71	26	0.50	86.19
	8	0.72	0.81	26	0.50	86.07
	9	0.80	0.47	26	0.50	44.92
	10	0.60	0.31	26	0.50	40.07

Table A.1 (Continued)

Lhr ortholog	Sample	OD_{600}	OD_{578}	t (min)	V	Units
D. ananassae	1	0.82	0.38	26	0.50	36.15
	2	0.54	0.12	26	0.50	16.26
	3	0.73	0.48	26	0.50	50.86
	4	0.62	0.20	26	0.50	24.65
	5	0.75	0.32	26	0.50	32.69
	6	0.67	0.03	26	0.50	3.80
	7	0.66	0.07	26	0.50	7.65
	8	0.56	0.05	26	0.50	6.84
	9	0.94	1.32	26	0.50	108.37
	10	0.82	2.41	26	0.50	227.10
D. pseudobscura	1	0.45	0.53	8	0.50	293.62
	2	0.75	1.90	8	0.50	636.03
	3	0.57	1.01	8	0.50	439.46
	4	0.46	1.38	8	0.50	759.34
	5	0.66	1.50	8	0.50	571.54
	6	0.74	1.03	8	0.50	347.24
	7	0.61	0.98	8	0.50	400.57
	8	0.68	2.53	8	0.50	937.41
	9	0.60	1.85	8	0.50	767.00
	10	0.70	1.64	8	0.50	584.76

Table A.1 (Continued)

Lhr ortholog	Sample	OD_{600}	OD_{578}	t (min)	V	Units
D. virilis	1	0.88	0.05	30	0.50	3.95
	2	0.87	0.38	30	0.50	29.21
	3	0.79	0.27	30	0.50	22.84
	4	0.73	0.25	30	0.50	22.59
	5	0.69	0.11	30	0.50	10.56
	6	0.89	1.69	30	0.50	125.94
	7	0.80	0.34	30	0.50	27.88
	8	0.78	0.42	30	0.50	36.05
	9	0.91	1.92	30	0.50	141.50
	10	0.74	1.89	30	0.50	171.52

Table A.2 Summary of β–galactosidase activity in yeast for seven *Lhr* orthologs The average number of β-galactosidase units and standard deviation were calculated excluding samples outside the linear range of the assay. The range of both the standard deviation and β-galactosidase units is quite large among each *Lhr* ortholog tested.

***Lhr* ortholog**	**Avg β-gal units**	**Std Dev**
D. melanogaster	28.4	16.4
D. simulans	22.9	7.2
D. yakuba	467.4	103.6
D. erecta	79.5	39.4
D. ananassae	39.9	9.6
D. pseudobscura	485.2	162
D. virilis	27.7	5.5

Appendix B: Phenotypic analysis of an Lhr knockout line

B.1 Introduction

One of the major goals in the study of *Lhr* is discovering its function in pure species. Unfortunately, the only mutant stocks available are either in *D. simulans*, or are deficiencies uncovering many genes in *D. melanogaster*. Therefore, in order to specifically investigate *Lhr* within *D. melanogaster* and take advantage of the many genetic and molecular tools available, our lab created a null mutant (Barbash, Ji, Prasad, unpublished). To accomplish this, we used the ends-out method of homologous recombination to generate an *Lhr* knockout line (Gong, Golic 2003). In this method, a DNA construct is homologously recombined into the target genomic location, disrupting the gene of interest.

Our targeting construct inserted a mini-*white* gene into *Lhr*, deleting ~12 amino acids and creating a mutant with reduced transcriptional activity (Ji, Barbash unpublished). Initial genetic characterization demonstrated that the *Lhr*-^{KO} mutation we generated was homozygous viable, indicating that *Lhr* is not an essential gene. We also failed to detect any gross developmental defects or mutant phenotypes in the *Lhr*-^{KO} flies. Therefore, as part of an ongoing investigation of the function of *Lhr* in pure species, I analyzed the *Lhr*-^{KO} line using three assays. These assays were selected based on the heterochromatin-association of LHR, and test both markers and structure of heterochromatin, as well as chromosome morphology.

For the first assay, I tested if the localization of different heterochromatin markers was disrupted in the *Lhr*-^{KO} larvae. For example, in *Su(var)3-9* mutants H3K9 di-methylation and HP1 localization are severely reduced at the chromocenter (Schotta et al. 2002). The proteins Su(var)3-9,

and HP1, as well as the histone mark H3K9me2 are hallmark signals of heterochromatin establishment and structure. Therefore, to test whether *Lhr* plays a role in hetereochromatin establishment, I stained for HP1 and H3K9me2 at the chromocenter in *Lhr*-^{KO} larvae.

For the second assay, I chose to examine the morphology of the polytene chromosomes in *Lhr*-^{KO} larvae. This experiment was designed based on the observation that the male X chromosome is bloated in mutants of heterochromatin proteins *Su(var)3-7* and HP1 (Spierer et al. 2005). LHR has many similarities to SU(VAR)3-7, and binds directly to HP1, so for these reasons, I was interested to explore if *Lhr* mutants have a similar effect on the male X chromosome.

The third approach I used to investigate the function of *Lhr* was a position effect variegation (PEV) assay. Early descriptions of PEV were explained as being caused by chromosomal rearrangements that result in the affected gene being transposed from its normal euchromatic position to close proximity to heterochromatin, and silenced to a varying degree (Girton, Johansen 2008). For example, the w^{m4} mutation in the *white* gene displayed a mottled phenotype, with each eye having some mutant and some normal facets (Muller 1930). Many PEV modifiers have been discovered on the basis that they suppress or enhance the mottled phenotype seen in the eye (Schotta et al. 2003). It is estimated that up to 150 loci produce a PEV modifying phenotype when mutant (Weiler, Wakimoto 1995; Schulze, Wallrath 2007). If heterochromatin is involved in causing PEV, and mutants in modifier proteins alter this variegation phenotype, it suggests that these modifiers are involved in the establishment or maintenance of heterochromatin.

Based on this model, whether a gene has a function in heterochromatin structure can be predicted by observing the phenotype of the mutant in a PEV assay. Many of the modifiers studied to date are either structural components of heterochromatin or modify chromosomal proteins, such as the two strong PEV suppressor proteins, HP1 and JIL-1 (Girton, Johansen 2008). We were therefore interested if *Lhr* has a role in heterochromatin structure by testing our Lhr^{KO} allele in a PEV assay.

B.2 Materials and methods

Antibody staining of whole-mount salivary glands

Polytene squashes and anti-HP1 staining was performed as described in Chapter II. The primary anti-H3K9me2 antibody (Upstate #07-441) was used at 1:100 with Alexa Fluor (555) goat anti-rabbit secondary antibody at 1:300.

Polytene squashes and Orcein staining

Males and females were sexed by the larval gonad. Salivary glands from male wandering third instar larvae were dissected in Ringer's Solution (150 mM NaCl, 4mM KCl, 3mM $CaCl_2$), and fixed in 45% acetic acid for 3-5 minutes. The glands were then squashed on a glass slide and dehydrated in 100% ethanol for 20 minutes. The slides were air dried and a drop of lacto-aceto-orcein (1% orcein in 1:1 mixture of 85% lactic acid, 60% acetic acid) was applied, followed by the addition of a cover slip.

PEV assay

Most of this work was performed by Nick Abel, an undergraduate researcher whom I supervised in the lab of Dr. Daniel Barbash. 8 mutant or

wild-type females were crossed to 8 Sb^V [*T(2;3)*Sb^V*, In(3R)Mo,* Sb^1*,* sr^1*/TM3, Ser]* males. The mutant stocks used were *HP1 [*w^{m4h}*;* $Su(var)2\text{-}5^{04}$*/ Cy Gfp], Df(Lhr) [Df(2R)BSC44/SM6a], Dp(Lhr) [w;P{CARY.attP2,ϕ[*w^+*, mel-Lhr-HA]}]* and Lhr^{KO}. Canton S (CS) was used as a wild-type control line. We scored 30 dorsal bristles from 30 males and 30 females at 25°C. Bristles were scored as long (wild-type) or short (*Stubble*), in both the heterozygous mutant F1 progeny and their balancer siblings. The variegated phenotype is a mixture of wild-type and stubble bristles. Mutants that enhance variegation will produce mostly wild-type bristles, and those that suppress variegation will produce mostly stubble bristles.

B.3 Results and Discussion

Localization of heterochromatin markers

As a proxy for heterochromatin structure in the Lhr^{KO} line, I chose to look at the classic structural heterochromatin protein HP1, and the histone modification it recognizes, di-methylated H3K9. I found that in whole-mount salivary gland preparations, the chromocenter staining pattern appears the same for both HP1 and H3K9me2 in Lhr^{KO} and wild-type larvae (Figure B.1). Based on these results, I conclude that HP1 is not dependent on *Lhr* for its localization to pericentric heterochromatin. Because SU(VAR)3-9 is responsible for methylating H3K9, these results further suggest that SU(VAR)3-9 is also unaffected by the loss of *Lhr*. Together, these results likely eliminate the possibility that *Lhr* is necessary for heterochromatin establishment.

However, these results do not completely rule out the hypothesis that *Lhr* is important for heterochromatin maintenance. This point is illustrated

using the heterochromatin gene *Su(var)3-7* as an example. Mutations in *Su(var)3-7* do not affect the localization of HP1 or H3K9 methylation, indicating that heterochromatin is correctly established. Yet *Su(var)3-7* is a strong suppressor of PEV, and a structural component of heterochromatin (Spierer et al. 2005). Therefore, it may be possible, that *Lhr* is analogous to *Su(var)3-7,* and has a role in heterochromatin maintenance even though it does not affect HP1 localization or H3K9me2 levels. I will test this hypothesis later in this section of the Appendix.

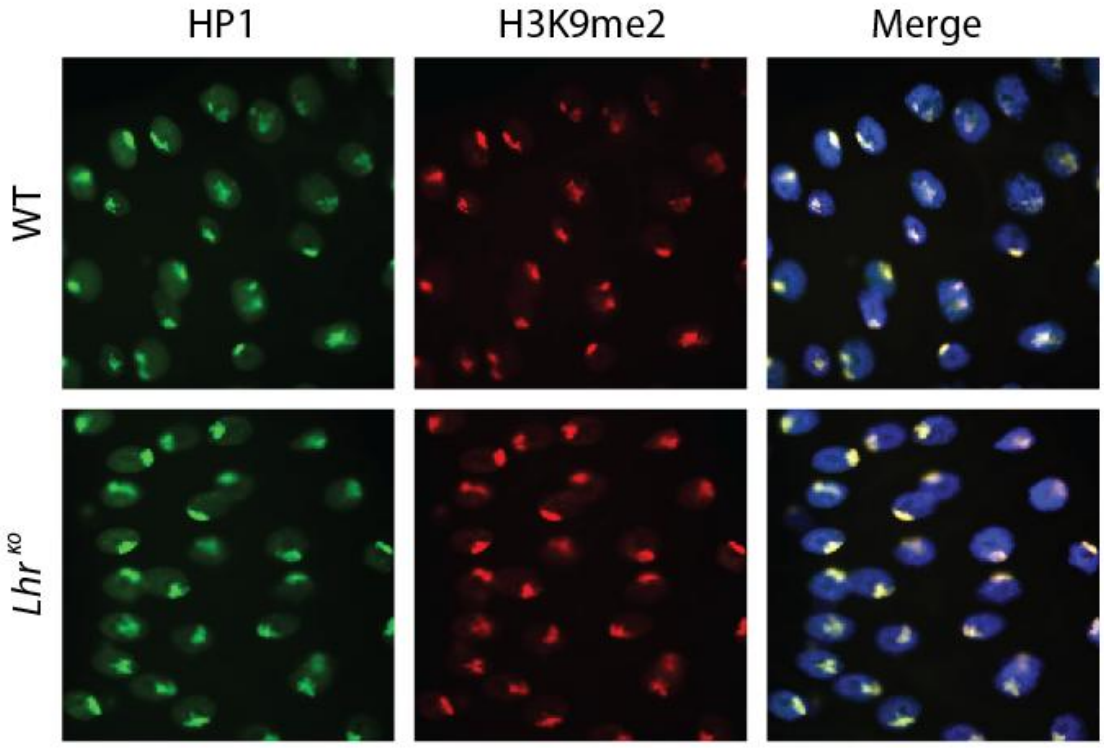

Figure B.1 *Lhr* does not affect the localization of HP1 or H3K9me2 to heterochromatic foci in salivary glands.

Larvae were co-stained with anti-HP1 and anti-H3K9me2 antibodies and DNA was detected with DAPI. The localization of HP1 and H3K9me2 is similar in both male and female Lhr^{KO} larvae and wild-type (w^{1118}) larvae, males are shown.

Chromosome morphology

Polytene chromosomes from male larvae lacking heterochromatin proteins HP1 and SU(VAR)3-7 display a shortened and bloated X chromosome (Spierer et al. 2005). LHR has many similar properties to SU(VAR)3-7, including directly interacting with HP1. To test whether *Lhr* deficient male larvae also have an aberrant X chromosome, I stained polytene chromosomes with the DNA stain orcein and examined chromosome morphology. I found that unlike *Su(var)3-7* and *HP1* mutant males, the Lhr^{KO} males appear to have a wild-type X chromosome (Figure B.2). This result suggests that the X chromosome is males is not sensitive to the dosage of *Lhr* like it is to the dosage of *Su(var)3-7* and *Su(var)2-5* (HP1).

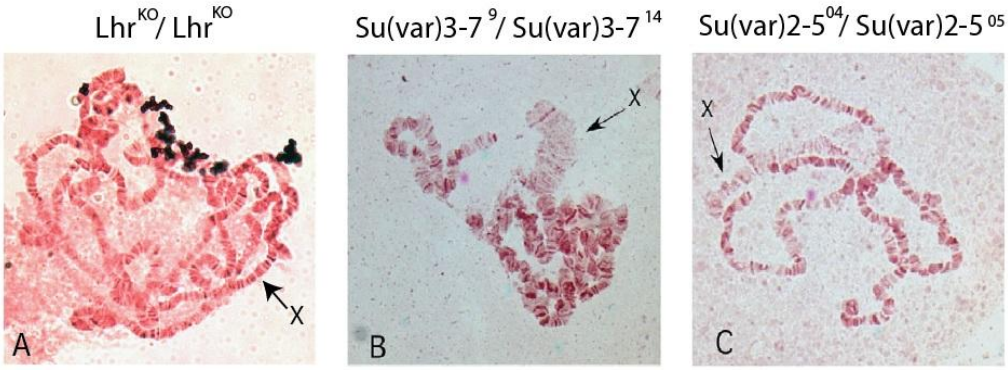

Figure B.2 Examining chromosome morphology in *Lhr^{KO}* male larvae

The X chromosome is not bloated in the *Lhr^{KO}* larvae (A) as it is in the *Su(var)3-7* (B) and *Su(var)2-5* (C) mutant larvae. Salivary glands from *Lhr^{KO}* males were dissected, squashed, and stained with Orcein. Panels (B) and (C) are from (Spierer et al. 2005).

PEV Assay

The major goal of this assay was to use *Lhr* mutants as a measure of the effect that wild-type *Lhr* has on heterochromatin. We were unable to make use of the commonly used eye reporter w^{m4} for our PEV assay due to the presence of a *white* gene in the Lhr^{KO} allele. Instead, we used the antimorphic *Stubble* allele Sb^{v}, because the effect on variegation can be quantified by counting the number of mutant bristles (Belyaeva et al. 2003). As controls for the assay we included *HP1*, which is a dominant suppressor of variegation, and Canton S, which should have no effect on the variegation. For the *Lhr* analysis, we used the Lhr^{KO} chromosome, a deficiency chromosome that deletes *Lhr,* and a chromosome carrying an additional copy of *Lhr*+ driven by its endogenous promoter.

Based on the Canton-S results, we determined the baseline of bristle variegation to be 22.3 *Stubble* bristles (Table B.1, Figure B.3). This number of bristles was used for comparison with all other alleles tested as a substitute for their balancer siblings. Although the most appropriate analysis is to test the mutant allele relative to the balancer siblings, we only collected data for the balancer chromosome in the *HP1* cross where both *HP1* and *Cy* were scored. As expected, the *HP1* mutant chromosome was a strong suppressor of variegation, and had a statistically significant increase in the number of *Stubble* bristles compared to Canton-S wild type chromosomes (Table B.1). Unexpectedly, we found that the *Cy* balancer carrying siblings in the *HP1* mutant cross had a statistically significant increase in the number of mutant bristles compared to wild-type. This result may be explained by the fact that the balancer chromosome has many genetic aberrations, and may have accumulated a mutation that affects PEV.

The results with our *Lhr*^{KO} chromosome are consistent with the results with *HP1*, the number of *Stubble* bristles significantly increases when compared to Canton S (Table B.1). This result suggests that similar to HP1, *Lhr* is also a dominant suppressor of variegation. However, results from the Df(*Lhr*) chromosome we used do not have the same pattern, and appear to have significantly less *Stubble* bristles than the wild-type control (Table VI.B.1). The additional genes absent in the deficiency may explain this difference as ~15 genes are deleted on this chromosome, including *Bap55* which is a component of the chromatin remodeling brahma complex. The absence of this known chromatin protein may be affecting the PEV suppression activity of Df(*Lhr)*. Unlike published work with Su(var) proteins like HP1, we did not detect a significant difference between our Dp(*Lhr*) line and the wild type control. This result was not completely unexpected, as only about 10% of the haplo-*Su(var)* genes studied to date also have triplo-enhancer effects (Girton, Johansen, 2008).

At face value, the data from the PEV assay indicate that we were not able to produce consistent results with different genetic backgrounds and the *Sb*^{v} allele to be able to make any definitive conclusions about *Lhr*. Further analysis is needed to differentiate the contributions from the genetic background on both the mutant and balancer chromosomes, as well as the effects of genes neighboring *Lhr*. Additionally, it is also possible, that *Lhr* has no effect on the third-chromosome *Sb*^{v} reporter, but it might affect PEV reporters located in heterochromatin on other chromosomes.

A.

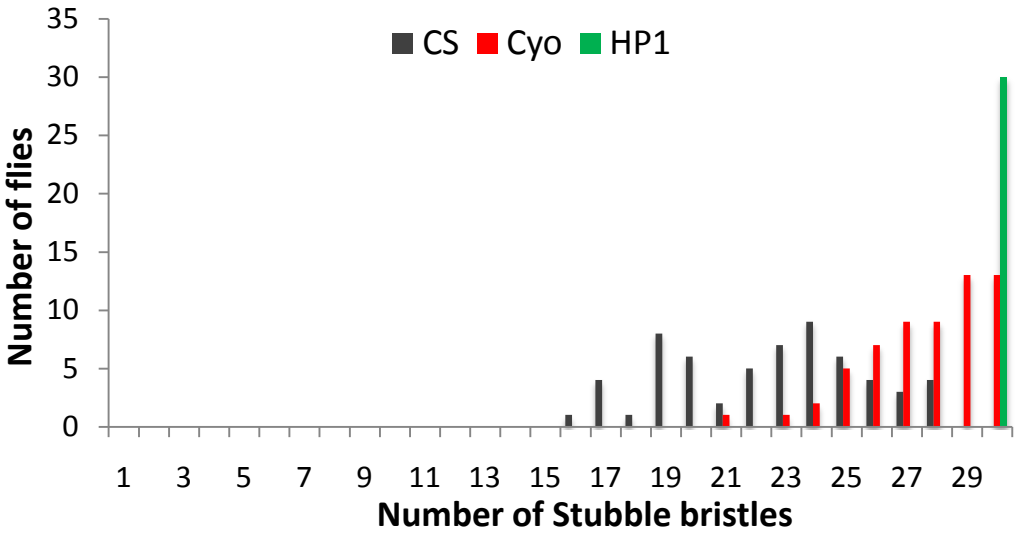

B.

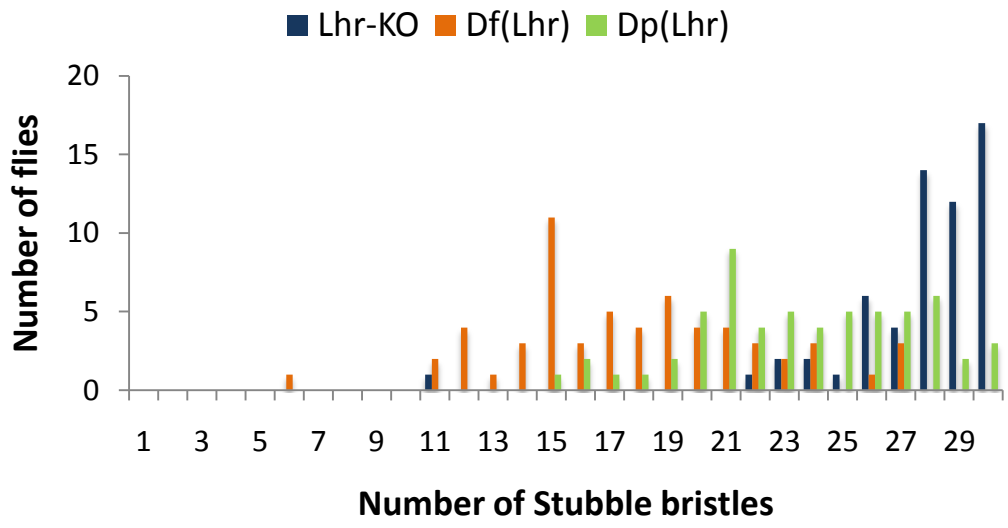

Figure B.3 Distribution of *Stubble* bristles in experimental and control progeny. The number of flies with a corresponding number of mutant *Stubble* bristles is shown for A) control and B) *Lhr* experimental crosses. For example, for the HP1 mutant chromosome (Green in A), 30 flies had 30 *Stubble* bristles.

Table B.1 Average number of *Stubble* bristles in recovered progeny. The average number of *Stubble* bristles and the standard deviation were calculated for each of the six lines tested in the PEV assay. We also calculated if the average number of bristles in each line was statistically different from the Canton S reference. All lines tested except for Dp(*Lhr*) are statistically different[a] from Canton S.

	Genotype	Avg	SD	p-value[a]
Control	CS[b]	22.5	3.23	
	HP1[c]	30.0	0.00	<0.0001
	Cy[d]	27.7	2.04	<0.0001
Experimental	*Lhr*^{KO} [e]	27.8	2.97	<0.0001
	Df(*Lhr*)[f]	17.8	4.40	<0.0001
	Dp(*Lhr*)[g]	23.6	3.77	0.0828

[a] – The mean of each mutant tested was compared to Canton S by a two-tailed unpaired t-test, 95% confidence interval, 29 degrees of freedom.

The genotypes of the lines used in this assay are:

[b] – Canton S

[c,d] - *w*^{m4h}*; Su(var)2-5*^{04}*/ Cy Gfp,* scored both non-*Cy* [c] and *Cy* [d]

[e] – *Lhr*^{KO}

[f] - *Df(2R)BSC44/SM6a*, scored non-*SM6a*

[g] *-w; P{CARY.attP2,ϕ[w*$^{+}$*, mel-Lhr-HA]*

Appendix C: Testing the hybrid lethal activity of Lhr orthologs

C.1 Introduction

In Chapter III I showed that *D. melanogaster Lhr* can induce hybrid lethality similar to what we found for *D. simulans Lhr* (Chapter II), and that four *Lhr* orthologs have similar localization and interaction properties. Here in the Appendix, I will present data on whether two additional *Lhr* orthologs can complement suppression of rescue by Lhr^1. These data were meant to be included into Chapter III, but technical issues in the design of the crosses precluded precise interpretation.

The Lhr^1 complementation crosses in Chapters II and III were designed to have the *UAS-Lhr* and *Gal4* transgenes on separate chromosomes in the *D. melanogaster* mothers, allowing for independent assortment of the transgenes into the F1 progeny. Then, the progeny were classified into one of three categories, and their genotypes were inferred based on eye color (see Figure II.C.2). The Lhr^1 complementation crosses outlined here in this chapter of the Appendix are similar to those earlier crosses, except that the both the *UAS-Lhr-Yfp* and *Gal4* transgenes are on chromosome III in the mother (Figure C.1). Similar to the experiments above, the progeny from these crosses were scored and classified based on eye color.

However, because the mothers in these crosses were heterozygous for each transgene on chromosome III, and the exact chromosomal location of the *Actin-Gal4* transgene was unknown, I was unable to predict the pattern of transgene segregation in the F1 progeny. I was also uncertain whether the UAS parental stocks were homozygous for the *UAS-Lhr-Yfp* transgenes. This uncertainty in the parental stocks made me equally unsure that the mothers used in the crosses actually contained both transgenes as expected. As a

result of these complications, I was unable to draw conclusions based on the data I collected, and the results below are presented with some interpretation on the hybrid lethal activity of these additional *Lhr* orthologs.

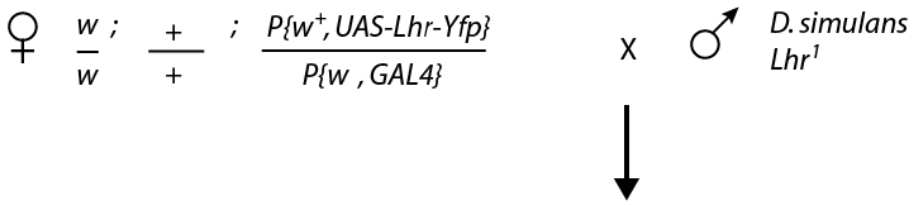

Expected genotypic ratio if Lhr ortholog expression is:

Eye color:	Possible Genotypes	Viable		Lethal	
Red	UAS/+ ; GAL4/+	1	2	0	1
	+/+ ; GAL4/+	1		1	
Orange	UAS/+ ; +/+	1	1	1	1
White	+/+ ; +/+	1	1	1	1

Figure C.1 Complementation crosses to test for suppression of hybrid male rescue

D. melanogaster female parents heterozygous for *GAL4* and *UAS-Lhr-Yfp* transgenes on chromosome III were crossed to *D. simulans* males. Both the transgenes are marked with w^+, and the *GAL4*-containing transformant has a darker eye color and is epistatic to the *UAS*-containing transformants which has a lighter eye color. Therefore, the red-eye class of progeny could potentially be composed of two different genotypes. The expected 2:1:1 ratio if the expression of the *Lhr* transgene is viable assumes that the *Gal4* and *UAS* transgenes are at least 50 cM apart and assort independently. However, because we do not know the distance between the *UAS-Lhr-Yfp* and *Gal4* transgenes, this predicted ratio of F1 progeny may not be correct.

C.2 Materials and Methods

The transgenic fly lines used are the same as described in Chapter III. The *D. melanogaster* mothers heterozygous for two transgenes were selected as non-TM6 progeny from crosses between homozygous *UAS-Lhr-Yfp* females and *Actin-Gal4/TM6* males.

C.3 Results and Discussion

Using the genetic assay developed in Chapter II and III, I tested whether four *Lhr* orthologs can suppress Lhr^{1} hybrid male rescue. I have already established that *D. simulans* (Chapter II) and *D. melanogaster* (Chapter III) *Lhr* have hybrid lethal activity in this assay; therefore these two orthologs serve as controls. Here in the Appendix, I am extending this Lhr^{1} complementation analysis to *D. yakuba* (*yak-Lhr*) and *D. virilis* (*vir-Lhr*) *Lhr* orthologs.

The results obtained for both *D. melanogaster* and *D. simulans Lhr* are similar to the results in previous chapters. I found that crossing females carrying either *mel-Lhr* or *sim-Lhr* to *D. melanogaster* males produced F1 progeny not significantly different than the predicted 2:1:1 ratio (Table C.1). I also found that crosses with both *yak-Lhr* and *vir-Lhr* produce F1 progeny in this same 2:1:1 ratio. These results indicate that despite not knowing the exact location of the transgenes, progeny were produced at similar frequencies as predicted earlier. These results also demonstrate that within *D. melanogaster* the expression of all four *Lhr* orthologs is not lethal, and further suggest that testing for deviation from the 2:1:1 ratio in the hybrid crosses may be sufficient to determine if the *Lhr* orthologs tested have hybrid lethal activity.

Table C.1 Hybrid males from crosses testing if four *Lhr* orthologs have hybrid lethal activity

D. melanogaster mother	F1 Progeny Class		Number of progeny	
Lhr ortholog	Phenotype	Genotype	*D. mel* control cross	*D. sim Lhr*[1] cross
mel-Lhr[a]	Red-eyed male	UAS/+ ; GAL4/+	282	540
		+/+ ; GAL4/+		
	Orange-eyed male	UAS/+ ; GAL4/+	162	80
	White-eyed male	+/+ ; GAL4/+	175	534
		Total[e]	619 [n.s.]	1154 [***]
sim-Lhr[b]	Red-eyed male	UAS/+ ; GAL4/+	139	257
		+/+ ; GAL4/+		
	Orange-eyed male	UAS/+ ; GAL4/+	72	8
	White-eyed male	+/+ ; GAL4/+	77	265
		Total[e]	288 [n.s.]	530 [***]

Table C.1 (continued)

yak-Lhr[c]	Red-eyed male	UAS/+ ; GAL4/+ +/+ ; GAL4/+	83	161
	Orange-eyed male	UAS/+ ; GAL4/+	37	10
	White-eyed male	+/+ ; GAL4/+	45	156
		Total[e]	165 [n.s.]	327 [***]
vir-Lhr[d]	Red-eyed male	UAS/+ ; GAL4/+ +/+ ; GAL4/+	158	406
	Orange-eyed male	UAS/+ ; GAL4/+	76	104
	White-eyed male	+/+ ; GAL4/+	86	378
		Total[e]	320 [n.s.]	888 [***]

[a,b,c,d] *–D. melanogaster* females of the genotype: *w/w; P{ w*$^{+mC}$ *Scer\UAS-Lhr::Avic\Venus =UAS-Lhr::YFP} / P{Act5CGAL4}17bFO1,* where the *Lhr* gene is from the corresponding species listed in the table.

[e] - The ratio of red eye: orange eye : white eye was tested for deviation from a 2:1:1 ratio using Chi-squared test. *** = $p < 1 \times 10^{-3}$; n.s. = $p > 0.05$

In crosses to the *D. simulans Lhr*^{1} strain to generate hybrids, I found that both *mel-Lhr-Yfp* and *sim-Lhr-Yfp* have hybrid lethal activity, as evidenced by the number of F1 hybrid males being significantly different than the expected 2:1:1 ratio (Figure C.1, Table C.1). Similar results were also obtained with *Lhr-Yfp* transgenes from *D. yakuba* and *D. virilis* (Table C.1), and in all cases, both the red eyed and orange-eyed class of males have fewer progeny than predicted, causing the deviation from the expected 2:1:1 ratio. I confirmed by PCR that the rescued red-eyed males only carried the *Gal4* transgene (n= 5 for each cross), thus concluding that the reduction in red-eyed males is caused by lethality of sons inheriting both the *Gal4* and *UAS-Lhr-Yfp* transgenes. These results demonstrate that the YFP tag does not alter the hybrid lethal function of LHR, and also that the ability to induce lethality in hybrids between *D. melanogaster* and *D. simulans* is conserved for the four *Lhr* orthologs tested.

I should also note that testing for deviation from the 2:1:1 ratio is probably most appropriate for testing if expression of the *UAS-Lhr-Yfp* transgenes cause lethality within *D. melanogaster*. Perhaps a better test for hybrid lethality is a 3x2 contingency table comparing the 3 classes of progeny obtained in the pure species and hybrid crosses for each of the *Lhr* orthologs. Performing this 3x2 analysis for each of the four *Lhr* transgenes resulted in significant tests for each transgene ($p < 1 \times 10^{-3}$, 2 degrees of freedom), again indicating that all four *Lhr* orthologs I tested have hybrid lethal activity.

In Chapter III, I reported that *Lhr* from both *D. melanogaster* and *D. simulans* are able to induce hybrid lethality, but that *sim-Lhr* is more potent than *mel-Lhr* based on the number of orange-eyed males recovered. Here I also note that among the *Lhr-Yfp* transgenes inserted into the same genomic

position, *D. simulans* and *D. yakuba* have a similar proportion of viable orange-eyed males. In contrast, for *D. virilis Lhr-Yfp*, the relative number of orange-eyed males to white-eyed males is similar to what I found for the *D. melanogaster* transgenes. I suggest that the evolution of *Lhr* in *D. simulans* and *D. yakuba* has caused these two orthologs to have more potent hybrid lethal activity.

As mentioned in Chapter III, the *D. simulans*, *D. yakuba*, and *D. virilis Lhr-Yfp* transgenes were inserted into the third chromosome of *D. melanogaster* at position 86Fb using the ϕC31 integration system (Groth et al. 2004). Although the position of the *Actin-Gal4* driver and *D. melanogaster Lhr-Yfp* transgenes are currently unknown, I believe the results in this chapter of the Appendix can be interpreted to demonstrate that four *Lhr* orthologs can induce *D. melanogaster-D. simulans* hybrid lethality.

Appendix D: Development of GnRH cells: Setting the stage for puberty[2]

This paper was published in Molecular and Cellular Endocrinology in 2006. My contribution to this work was imaging of GnRH receptor expression shown in Figure D.5 as part of my rotation project in the lab of Dr. Kate Whitlock.

D.1 Abstract

Cells containing gonadotropin-releasing hormone (GnRH) are essential not only for reproduction but also for neuromodulatory functions in the adult animal. A variety of studies have hinted at multiple origins for GnRH-containing cells in the developing embryo. We have shown, using zebrafish as a model system, that GnRH cells originate from precursors lying outside the olfactory placode: the region of the anterior pituitary gives rise to hypothalamic GnRH cells and the cranial neural crest gives rise to the GnRH cells of the terminal nerve and midbrain. Cells of both the forming anterior pituitary and cranial neural crest are closely apposed to the precursors of the olfactory epithelium during early development. Disruption of *kallmann* gene function results in loss of the hypothalamic but not the terminal nerve GnRH cells during early development. The GnRH proteins are expressed early in development and this expression is mirrored by the onset of GnRH receptor (GnRH-R) expression during early development. Thus the signaling of the GnRH neuronal circuitry is set up early in development laying the foundation for the GnRH network that is activated at puberty leading to reproductive function in the mature animal.

---

[2] Whitlock KE, Illing N, Brideau NJ, Smith KM, Twomey S. (2006) Development of GnRH cells: setting the stage for puberty. *Molecular and Cellular Endocrinology*, 254-255, 39-50.

V.C.2 Introduction

The neuroendocrine decapeptide gonadotropin-releasing hormone (GnRH) is not only an essential reproductive hormone but it also acts as a neuromodulator within the nervous system. Much effort has been invested in the study of GnRH as it relates to the control of puberty in vertebrate animals. At the onset of puberty GnRH activates the pituitary-gonadal axis, but this is not a *de novo* activation. In a species-specific manner the GnRH system is active during both the pre-natal and post-natal period (Plant, 2001, Ebling, 2005 and Trudeau, 1997). This early development of GnRH cells is crucial for establishing the GnRH systems that will be later activated at onset and progression of puberty. GnRH has many structural variants with a minimum of 16 variants described to date in vertebrates (Somoza et al., 2002 and Yamamoto, 2003) and these forms are found in a diverse group of tissues including mesodermally derived gonadal, placental, mammary and immune tissues and neurectodermally derived peripheral and central nervous system (Gore, 2002). The GnRH cells of the nervous system include those found in the terminal nerve, a cranial nerve associated with the olfactory nerve, the midbrain which have an apparent neuromodulatory function, and those of the hypothalamic system that are crucial to the control of puberty. Within a vertebrate species two and more generally three forms of GnRH are present and between species these forms can vary in their location of expression within the brain. For the purpose of clarity the terminology for naming GnRH forms based on their location in the brain, regardless of their amino acid or nucleotide sequence will be used. The population of GnRH cells in the hypothalamus responsible for hypophysiotropic function is referred to as

GnRH1, that of the midbrain is referred to as GnRH2 and the GnRH cells of the terminal nerve/ventral telencephalon as GnRH3 (Fernald and White, 1999). Of these three populations, the molecular form found in the midbrain (*GnRH2*) is unique in that it is conserved across taxa. The hypophysiotropic form (*GnRH1*) shows greater sequence variation as well as variation in amino acid structures (Montaner et al., 1998 and Montana et al., 2002) and the terminal nerve contains either the form originally isolated in salmon (*sGnRH*/*GnRH3*), or the hypophysiotropic form. The sGnRH form is almost exclusively found in fishes although there are recent reports in mammals (Montaner et al., 1998 and Parhar et al., 2005). Understanding the developmental origins of the GnRH cells is essential to diagnosis of early birth defects as well as predicting subsequent difficulties in the onset of puberty. Kallmann syndrome in humans represents a developmental defect affecting both the olfactory system and the GnRH system, suggesting a developmental link between these sensory and reproductive axes (MacColl et al., 2002b). In the late 1980s the GnRH cells of the hypothalamus (GnRH1) and terminal nerve (GnRH1/GnRH3) were proposed to originate from the medial olfactory placode (Schwanzel-Fukuda and Pfaff, 1989, Wray et al., 1989a and Wray et al., 1989b). Subsequent studies proposed that these cells have multiple embryonic origins including the ventral diencephalon (Parhar et al., 1998, Quanbeck et al., 1997 and Tobet et al., 1996), neural crest and anterior pituitary placode (Whitlock et al., 2003 and Whitlock, 2005). Unlike those of the forebrain, the GnRH cells of the midbrain were proposed to originate outside the olfactory system within the germinal zone of the third ventricle (Northcutt and Muske, 1994) and neural crest (Whitlock et al., 2005). Here we will review the data supporting multiple, non-olfactory origins for the GnRH

cells, analyze the defects observed in Kallmann syndrome in light of these non-olfactory origins and investigate possible roles for GnRH in the early embryo as reflected by the expression of GnRH receptors.

D.3 Timing of development

In order to understand the development of the GnRH cells of the hypothalamus, terminal nerve, and midbrain one must investigate and visualize the dramatic cell movements that underlie the development of the neural tube including the neural crest-derived structures of the head. The sensory organs of the vertebrate head are almost wholly derived from sensory placodes which are neurectodermal/ectodermal thickenings that will give rise to the olfactory sensory epithelium, anterior pituitary (or adenohypophysis), lens of the eye (but not the underlying retinal ganglia neurons), otic sensory epithelium, and parts of the cranial nerves. The neural crest cells, which are in essence a stem cell-like population, will migrate from the dorsal neural tube and contribute to neurons, glia, pigment cells, connective tissues and in the head skeletal elements such as the bones of the jaw and frontal mass (for review see Le Douarin and Kalcheim, 1999). The nervous system of all vertebrates develops from the neural ectoderm which starts out as a plate, the neural plate (Figure D.1A). The neural plate will form a tube either by primary neurulation which is essentially bringing the edges of the plate together to form a hollow tube, as in mouse and chick embryos, or secondary neurulation where cells coalesce along the midline to form a solid core which will hollow through cavitation, as is seen in fish embryos. As these cell movements take place, the cells at the edge of the neural plate become specialized to form the pre-placode domain (Figure D.1, red, orange) and pre-migratory neural crest

cells (Figure D.1, purple) which will end up localized to the dorsal neural tube (Figure D.1B). The cells giving rise to the olfactory placodes, which are flanked posteriorly by the forming neural crest domain (Figure D.1A and B, purple) and anteriorly by the field of cells giving rise to the adenohypophysis (anterior pituitary) (Figure D.1A and B, orange), will move rostrally (Figure D.1C, red) and converge (Whitlock and Westerfield, 2000 and Streit, 2002). Concurrent with the rostral migration of the olfactory field (Figure D.1C, red arrow) the cranial neural crest cells move rostrally both dorsal (Langille and Hall, 1988) and ventral (Schilling and Kimmel, 1994), to the forming eye (Figure D.1C, purple arrows). These movements will bring cranial neural crest cells into association with the olfactory placode (Figure D.1D). During this same time window the adenohypophyseal (Rathkes pouch) precursors coalesce on the midline (Figure D.1C, orange) and move caudally to fuse with the neurohypophysis (Figure D.1D, orange arrow). Thus by the time one can clearly identify the olfactory placodes in the developing embryo (Figure D.1D), cells have already moved great distances, changed neighbors, and formed tissues. It is this fantastic choreography of cell movements that will generate our face and aid in the differentiation of underlying neuronal structures including GnRH cell precursors within the developing nervous system.

D.4 Mixing of cells at borders

The olfactory organ is composed of a placodally derived sensory epithelium surrounded by neural crest-derived olfactory capsule, which has a different embryonic origin from that of the olfactory epithelium. Combining data on embryonic origin of the olfactory placodes using morphological analysis in

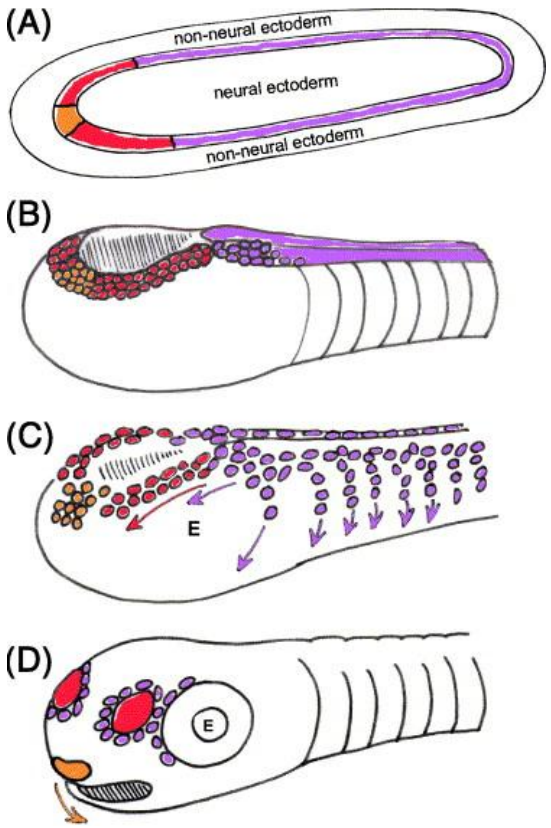

Figure D.1 Development of the neural tube, olfactory placodes, pituitary and neural crest in the vertebrate embryo. Orange = anterior pituitary (adenohypophysis), red = olfactory placode cells, purple = neural crest cells. (A) Neural plate stage showing domain lying at the interface of neural and non-neural ectoderm that will give rise neural crest and sensory placodes. (B) The neural plate forms a neural tube and cells at the edge become localized to the dorsal side. (C) Cells that will form the olfactory placodes (red arrow) and cranial neural crest derivatives (purple arrows) migrate rostrally. E = eye. (D) Olfactory placodes are formed and surrounded by neural crest cells as the anterior pituitary (Rathkes pouch) migrates caudally (orange arrow) to fuse with the posterior pituitary.

mouse (Verwoerd and Oostrom, 1979), quail-chick chimeras (Couly and Le Douarin, 1985), and single cell lineage tracing in zebrafish (Figure D.2A; Whitlock and Westerfield, 2000), we can conclude that the olfactory placodes arise within the edge of the neural plate of the developing embryo (Figure D.1 and Figure D.2A, red). Our analysis in the zebrafish has demonstrated that the olfactory placodes arise through the anterior convergence a large field of cells (Figure D.1 and Figure D.2) and this morphogenesis occurs in the absence of cell division (Whitlock and Westerfield, 2000). The olfactory placode fields (Figure D.2A) are initially contiguous with those giving rise to the adenohypophysis (Whitlock and Westerfield, 2000 and Whitlock, 2004b) which arises from a field of cells located on the midline at the anterior end of the neural plate (Figure D.2A, orange: Herzog et al., 2003, Karlstrom et al., 1999 and Sbrogna et al., 2003). These precursors must segregate through cell movements (Figure D.1) thus giving rise to adult tissues. A recent study used a line of transgenic fish with the proopiomelanocortin (POMC) gene promoter linked to green fluorescent protein (GFP) to visualize the development of pituitary lineages. This study reports that a cluster of POMC–GFP expressing cells at 22 h post-fertilization (hpf) is closely associated with the medial edge of each olfactory placode. We have used this transgenic line (POMC–GFP; Liu et al., 2003) to examine the development of these adenohypophyseal-derived cells in the early embryo. In this case one can use the expression of GFP as a *de facto* lineage tracer. Because the GFP has a longer perdurance than the endogenous protein, the GFP is maintained beyond the time when the endogenous protein is no longer expressed. In the POMC–GFP zebrafish there are cells within the olfactory placode (Figure D.2B and C, arrowhead)

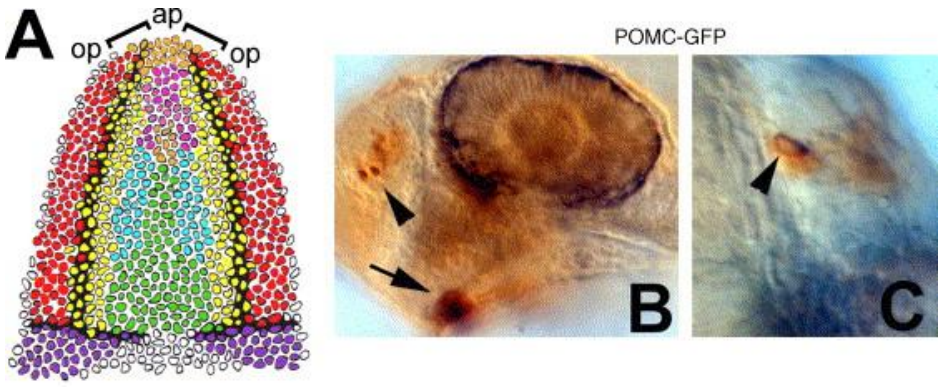

Figure D.2 Borders separating precursors of anterior pituitary and olfactory placodes are not strict. (A) Schematic representing the anterior end of the developing neural plate. Fields of cells in red are olfactory placode precursors, orange are anterior pituitary precursors, and magenta are hypothalamic precursors. (B and C) Cells labeled with an antibody recognizing green fluorescent protein (GFP) in 26 hpf POMC–GFP embryos. The anterior pituitary clearly expresses POMC–GFP in (B, arrow). In addition there are POMC–GFP cells in the olfactory placode (B and C, arrowhead).

that express GFP well after the formation of the anterior pituitary (Figure D.2B, arrow). If these POMC–GFP cells are monitored past 24 hpf they down-regulate GFP as they presumably incorporate into the olfactory epithelium. The transient appearance of the POMC–GFP cells in the olfactory placode demonstrates that there is an association of endocrine tissue with the olfactory placode. The POMC–GFP cells in the olfactory placode most likely result from low-level mixing of the cells as the adenohypophyseal and olfactory fields sort to form their respective placodes.

D.5 Embryonic origins GnRH cells

Late in 1980 two separate laboratories reported that the GnRH cells of the ventral forebrain appeared to arise from the olfactory placode in the mouse. In these studies the GnRH cells were those that migrate to the preoptic area/hypothalamus and those of the terminal nerve. Using *in situ* hybridization and immunocytochemistry, it was shown that GnRH positive cells were first seen in association with the olfactory placode, and then, based on observations in staged fixed tissue, appeared to migrate through the nasal septum into the forebrain along the terminal nerve-vomeronasal nerves (Schwanzel-Fukuda and Pfaff, 1989, Wray et al., 1989a and Wray et al., 1989b). Thus it was proposed that the olfactory placode generated not only olfactory sensory neurons and support cells, but also neuroendocrine cells containing the GnRH decapeptide. Subsequent investigations using axolotl (*Ambystoma mexicanum*, a salamander) demonstrated that olfactory placode removal resulted not only in the expected loss of the olfactory epithelium, nerve and bulb but also in the loss of the GnRH cells (Northcutt and Muske, 1994). However in rat ablation of the olfactory placode does not result in loss

of the GnRH cells (Daikoku and Koide, 1998 and Daikoku-Ishido et al., 1990). Because the placode ablations were done after the olfactory placodes had formed (Figure D.1D) the ablation of the placode may inadvertently remove precursors of the GnRH cells that were transiently associated with the placode at the time of removal. Genetic removal of the olfactory placode has also been reported. Animals heterozygous for mutations in the *Pax6* gene result in the mouse the *small-eye* (*Sey*) phenotype and animals homozygous for the *Pax6* gene are missing both the olfactory placodes and GnRH cells (Dellovade et al., 1998). These animals have extreme frontal mass defects including a disrupted pituitary (Kioussi et al., 1999), thus the loss of GnRH cells in the *Pax6* mutant could result from the disrupted development of any number of tissues.

D.5.1 Alternate origins for GnRH cells

Studies using chick as well as fish (medaka, zebrafish) embryos have suggested that the origin of the GnRH cells is not shared with the olfactory placode. Using ablations in the neural plate stage chick embryo (see Figure D.1A) it was demonstrated that loss of the region giving rise to the olfactory sensory neurons did not result in loss of the forebrain GnRH cells. However, loss of the respiratory epithelium, which arises from a region more anterior in the neural plate, did result in loss of forebrain GnRH cells (El Amraoui and Dubois, 1993). Thus GnRH cells in chick appear to arise from the most anterior limits of the neural fold which is the region giving rise to the precursors of the anterior pituitary placode (Figure D.1 and Figure D.2A, orange). In addition, in chick the *GnRH1* gene is first expressed along the neural fold, becomes localized to the anterior neural folds, and subsequently is expressed

in bilateral clusters of cells within the most anterior neural folds (Witkin et al., 2003). Therefore it appears that the anterior neural fold, which contains precursors of anterior pituitary lying adjacent to hypothalamic precursors (Figure D.2A; Le Douarin and Kalcheim, 1999) is a good candidate for the source of *GnRH1* cells in chick. In medaka, a species-specific form of *GnRH1* has been cloned (Parhar et al., 1998) and it is expressed in the hypothalamus. The differences in timing between the onset of GnRH1 and GnRH3 gene expression led to the proposal that the terminal nerve and hypothalamic GnRH cells do not share a common origin in the olfactory placode but have separate origins (Dubois et al., 2002 and Parhar et al., 1998). Thus, while intriguing, an olfactory origin for GnRH cells does not appear to be universal across vertebrates.

D.5.2 Forebrain gonadotropin-releasing hormone cells

We have shown that endocrine and neuromodulatory GnRH cells arise from two separate regions of the developing neural plate. Specifically, the neuromodulatory GnRH cells of the terminal nerve (Figure D.3, purple, #3) arise from the cranial neural crest, and the endocrine GnRH cells of the hypothalamus (Figure D.3, orange, #1) arise from the adenohypophyseal region of the developing anterior neural plate (Whitlock et al., 2003). We uncovered this developmental relationship by first creating a fate map of the domain giving rise to the olfactory placodes in early embryo (Figure D.3, red, #2). Our fate map was created by labeling single cells in the region of the neural plate giving rise to the olfactory placodes and showing that this domain gives rise to only olfactory cell types (Figure D.2A), and not to GnRH cells (Whitlock and Westerfield, 2000, Whitlock, 2004b and Whitlock, 2004c). This

is the equivalent of marking cells when the embryo is at a developmental stage pictured in Figure D.1B. The majority of experiments investigating the origin of GnRH cells were done at a developmental stage equivalent to Figure D.1D or later. Investigations using chick suggested that the GnRH cell origin might lie in the very anterior region of the neural plate (El Amraoui and Dubois, 1993) in the region of the adenohypophyseal precursors. Using the *you-too* and *detour* mutants (Karlstrom et al., 1999) we showed that the loss of the pituitary results in the loss of the GnRH cells of the hypothalamus but not the GnRH cells of the terminal nerve (Whitlock et al., 2003). Because the olfactory organs develop normally in these mutants, the loss of GnRH cells cannot be due to loss of the olfactory placode. Subsequently, using several forms of lineage tracer dyes to mark cells in the forming neural tube and labeling the resulting clones with an anti-GnRH antibody, we demonstrated that the cranial neural crest gives rise to the GnRH3 cells of the terminal nerve (Figure D.3, purple, #3) (Whitlock et al., 2003, Whitlock et al., 2005 and Whitlock, 2004c K.E. Whitlock, Development of the nervus terminalis: origin and migration, *Microsc. Res. Tech.* 65 (2004) (1–2), pp. 2–12.

D.5.3 Transient forebrain GnRH cells

Analysis of GnRH cells in transgenic mice expressing the LacZ reporter gene driven by GnRH promoter (GnRH-LacZ) revealed a population of LacZ-positive GnRH cells that were not previously described by immunocytochemical or *in situ* hybridization studies (Skynner et al., 1999 and Spergel et al., 2001). In addition to the preoptic area these GnRH-LacZ cells were found in lateral and septal nuclei, and septofimbrial nuclei. Subsequent analysis demonstrated that the GnRH-LacZ cells expressed GnRH but only

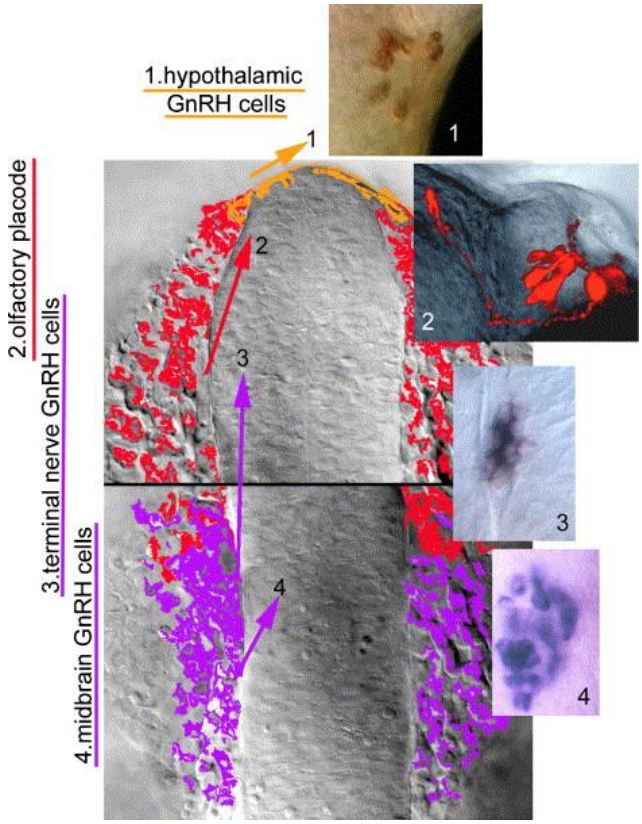

Figure D.3 Summary of embryonic origins of GnRH cells in the zebrafish embryo. Background photo is a Nomarski image of the forming neural tube in a living zebrafish embryo, a dorsal view with anterior toward the top. Image is pseudo colored as in Figure D.1: orange = anterior pituitary field, red = olfactory placode field, purple = cranial neural crest field. Hypothalamic GnRH cells (1) arise from the anterior pituitary field which converges along the midline (1, orange arrow), olfactory sensory neurons (2) arise within the olfactory placode generated by the anterior convergence (2, red arrow) of cells, terminal nerve GnRH cells (3) arise from cranial neural crest as it migrates anteriorly (3, purple arrow) and midbrain GnRH cells (4) also arise from cranial neural crest as it migrates in the lateral neural tube (4, purple arrow).

during embryogenesis (Skynner et al., 1999). In addition to the ectopic GnRH populations reported in the transgenic mice, immunocytochemical analysis supports a transient population of GnRH cells in the tectum of the developing mouse (Wu et al., 1995). Studies in rhesus monkeys indicate that there are two populations of forebrain GnRH cells that express immunocytochemically distinct forms of GnRH and migrate at different times (Quanbeck et al., 1997 and Terasawa et al., 2001). Our studies in zebrafish (Whitlock et al., 2003) as well as studies in chick (Mulrenin et al., 1999) have shown that a subset of GnRH cells divide during their migration into the central nervous system.These cells may in fact not be “migrating” but dividing as the tissue differentiates and undergoes morphogenesis, thus giving the impression that the GnRH cells are migrating. Furthermore by immunocytochemical studies in developing zebrafish we see GnRH cells ectopic to those expressing *GnRH2* or *GnRH3* (Gopinath et al., 2004 and Whitlock et al., 2005). Taken together, observations in transgenic mice coupled with immunocytochemical analyses in a variety of animals provide evidence supporting a non-uniform population of GnRH cells in the developing forebrain. Because of the apparent developmental regulation of GnRH expression in these varied populations it is tempting to propose that this dynamic expression pattern reflects an organizational role for GnRH prior to puberty.

D.5.4 Midbrain gonadotropin-releasing hormone cells

In our further analysis of embryonic origins of GnRH cells we examined the development of the midbrain GnRH2 cells. GnRH2 containing cells of the midbrain are proposed to arise locally from within the neural tube, but no definitive data exists to support or refute this origin. Because we had

previously shown that neuromodulatory GnRH3 cells arise from cranial neural crest, we investigated the neural crest as the origin of the neuromodulatory GnRH2 cells of the midbrain (Figure D.3, purple, #4). To determine whether loss of neural crest cells results in loss of midbrain GnRH2 cells we used modified oligonucleotide technology (morpholinos: Nasevicius and Ekker, 2000 and Ekker, 2000) to knock-down function of two genes, *sox10* and *foxd3*, important for the survival and differentiation of neural crest cells (Mollaaghababa and Pavan, 2003 and Sasai et al., 2001). We have shown that the loss of either the Sox10 or Foxd3 proteins results in a reduction in the number of midbrain *GnRH2* and terminal nerve *GnRH3* (*sGnRH*) expressing cells, and that reduction of both Sox10 and Foxd3 proteins results in the loss of both these GnRH cell populations (Whitlock et al., 2005). Our data support a model where the neuromodulatory GnRH2 cells of the midbrain share a common neural crest origin with the neuromodulatory GnRH3 cells. This provides additional support of commonalities between the neuromodulatory cells of the terminal nerve and midbrain for they have been shown to contain molecularly similar forms of GnRH (Lethimonier et al., 2004) and both populations have larger cell bodies (Whitlock, personal observation; Yamamoto, 2003) when compared to the hypothalamic GnRH cells. In contrast, we have shown previously that GnRH1 cells of the hypothalamus arise from the anterior pituitary region. Thus, this suggests that the hypothalamic GnRH1 cells differ from GnRH2/GnRH3 cells in function, origin and molecular events controlling their differentiation.

D.6 Kallmann syndrome and GnRH

D.6.1 Defects observed in Kallmann syndrome patients

Kallmann syndrome is a form of hypogonadic hypogonadism (deficits in GnRH) associated with anosmia (loss of sense of smell). In addition to having olfactory dysfunction and GnRH deficits, Kallmann patients can have a variety of additional defects such as renal abnormalities, dental agenesis, and cleft palate (Hardelin, 2001). Analysis of human pedigrees has shown X-linked, autosomal dominant, and autosomal recessive transmission of Kallmann syndrome. The gene responsible for the X-linked form of Kallmann, KAL-1 (MacColl et al., 2002a and MacColl et al., 2002b), was cloned in humans (Legouis et al., 1991) and encodes a 95 kDa extracellular matrix protein, anosmin-1, which is expressed in multiple embryonic tissues including the developing olfactory sensory system (Soussi-Yanicostas et al., 1996). In contrast the autosomal dominant form of Kallmann syndrome (KAL2) has recently been shown to result from mutations in the *fibroblast growth factor receptor-1* (*fgfr1*) gene (Dode et al., 2003 and Sato et al., 2004). The *fgfr1* gene is a member of a family of transmembrane tyrosine kinases containing four fibroblast growth factor receptors (FGFR1-4) that serve as high affinity receptors for FGF ligands (Coumoul and Deng, 2003). Loss of function of the *fgfr1* in mouse is lethal but use of conditional mutants has shown that the *fgfr1* gene is necessary for proper formation of the olfactory bulb; animals lacking *fgfr1* gene in the forebrain have severely reduced olfactory bulbs (Hebert et al., 2003). Analysis of a human Kallmann (KAL1) fetus has shown that the olfactory nerve fails to grow into the forebrain during development resulting in arrested migration of the GnRH cells (Schwanzel-Fukuda et al., 1989). This suggests that in KAL1 and KAL2 patients the GnRH neurons differentiate but

fail to migrate to their target in the hypothalamus because their migratory route along the olfactory nerve is disrupted.

D.6.2. Expression of kal and fgfr1 genes in early development

Prior to the migration of the GnRH cells to the hypothalamus there are extensive cell movements within the forming neural tube that generate not only the olfactory nerve, but also the pituitary (joining of anterior and posterior) and hypothalamus (Figure D.1 and Figure D.2A). Analysis of the Kallmann phenotypes suggests a complex disruption of developmental events beyond the formation of the olfactory nerve and bulb, and subsequent migration of GnRH cells. In fact Kallmann patients exhibit phenotypes characteristic of defects in neural crest migration such as cleft lip and dental agenesis (Sato et al., 2004 and Iovane et al., 2004). Furthermore defects have also been reported in the formation of the anterior pituitary (Madan et al., 2004), a structure that arises from the tissues lying between the forming olfactory placodes, and rostral to the precursors of the hypothalamus (Figure D.1 and Figure D.2A). The developmental mechanisms controlling the sorting of cells giving rise to the anterior pituitary and hypothalamus are complex and poorly understood. Studies in zebrafish have isolated both the *kal1.1* and *kal1.2* genes (Ardouin et al., 2000) and the *fgfr1* gene (Scholpp et al., 2004). Both the *kallmann* genes and the *fgfr1* gene are expressed in the developing hypothalamic and olfactory regions of the brain in the first 2 days of development (Ardouin et al., 2000; Kim and Whitlock unpublished; Figure VI.D.4). In zebrafish temporal expression differs between the *fgfr1* and *kal* genes where *fgfr1* has a broad expression pattern at 1-day post-fertilization (Figure D.4A) and *kal* maintains a broad expression domain in the second day

post-fertilization (Figure D.4B). The *fgfr1* is required for initial olfactory bulb development in mouse (Hebert et al., 2003). The FGFR-1 protein is detectable by immunocytochemistry in 30% of embryonic and 60% of post-natal forebrain GnRH neurons in mouse (Gill et al., 2004) but very few GnRH cells show FGFR-1 immunoreactivity in the juvenile rat (Voigt et al., 1996). In mouse the expression of a dominant negative *fgfr* mutant results in a reduction in the number of GnRH cells in the migratory route (Tsai et al., 2005). Thus development of the migratory route, encompassing at the very least the olfactory nerve, requires *fgfr1* gene function, and at least a subset of the GnRH cells also appear to require FGF receptors for normal development.

D.7 Do GnRH cells arise from hypothalamic precursors?

We have used morpholino gene knock-down techniques (Ekker, 2000) to block the translation of the *kal1.1*, *kal1.2*, and *fgfr1* genes in developing zebrafish. In examining the resulting embryos for defects in GnRH cell development we have observed that in the *kal1.1* gene knock-down the hypothalamic GnRH cells are lost but those of the terminal nerve remain (Whitlock et al., 2005). Furthermore the structure of the olfactory bulb and hypothalamus is abnormal showing disorganization of tissues and limited necrosis 2 days post-fertilization (Kim and Whitlock, unpublished). These data suggest that defects observed in Kallmann patients may also be extend to the developing hypothalamus. The adenohypophyseal placode in vertebrate animals arises from precursors located on the midline (Chapman et al., 2005). Mutations such as the *you-too* and *detour* mutants in zebrafish have missing or disrupted adenohypophyseal formation resulting from mutations in the *gli1* and *gli2* genes important in midline signaling (Karlstrom et al., 1999).

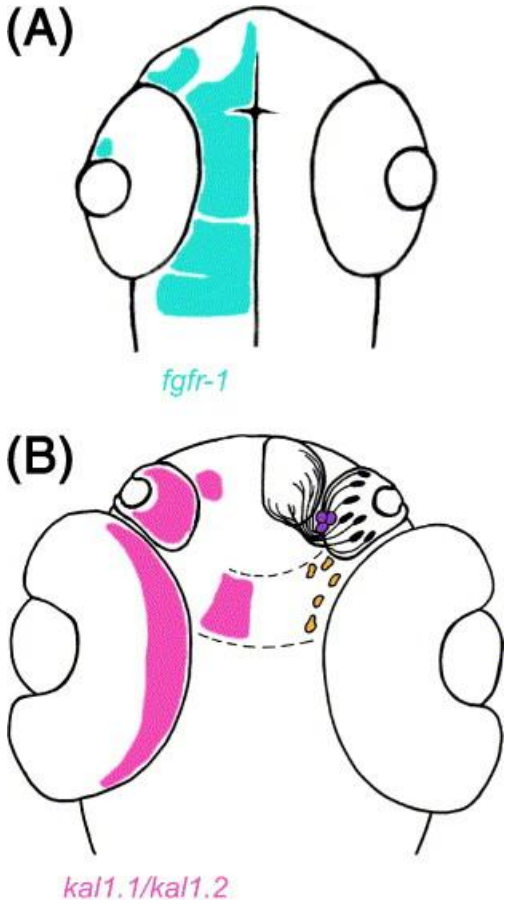

Figure D.4 Expression of *fgfr1* and *kal1.1*/*1.2* genes in the migratory route for hypothalamic GnRH cells in the developing zebrafish embryo. (A) Summary of *fgfr1* expression (blue) at 24 hpf (Whitlock and Kim, unpublished data; Scholpp et al., 2004), showing expression in olfactory placode and forebrain. (B) Summary of *kal1.1*/*1.2* expression (pink) at 56 hpf (Ardouin et al., 2000) showing expression in olfactory organ, bulb and ventral diencephalon. Terminal nerve cells are in purple and hypothalamic cells in orange. Black cells are sensory neurons of the olfactory epithelium with axons extending into the developing olfactory bulb.

Previously we have shown that the *you-too* mutant lacks not only adenohypophysis but also GnRH1 cells of the hypothalamus. Strikingly the GnRH cells of the terminal nerve were normal in this mutant (Whitlock et al., 2003). Based on the phenotype of missing adenohypophysis but reportedly normal hypothalamus we proposed that the GnRH cells originated from the region of the embryo giving rise to the adenohypophysis. In examining data presented in a subsequent analysis of the *you-too* mutant it appears that there are defects in ventral diencephalon, and possibly the hypothalamus (Kondoh et al., 2000). Thus the lack of GnRH cells observed in the *you-too* mutant (Whitlock et al., 2003) may result from disruption of either anterior pituitary and/or hypothalamus development. This is an intriguing possibility because fate maps of the neural plate in chick embryos have demonstrated that the precursors of the hypothalamus lie between the adenohypophyseal and neurohypophyseal precursors and these regions are flanked by the olfactory precursors Figure D.2A (Le Douarin and Kalcheim, 1999). Therefore loss of *kallmann* and/or *fgfr1* genes most likely results in a disruption in early patterning and development of the hypothalamus as well as the anterior pituitary and olfactory system.

D.7 Function of GnRH in the developing animal

Clearly GnRH plays a crucial role in the onset and maintenance of puberty. Yet prior to puberty GnRH is synthesized and released within the developing animal and its role during this period in life is poorly understood. The onset of GnRH expression during development has been studied most intensively in fishes (for review see Yamamoto, 2003) where the populations of the terminal nerve, hypothalamus and midbrain can be discerned with ease because the

embryos develop outside the mother. The presence of GnRH in the developing embryo argues that it plays a role prior to and is most likely necessary for the later onset of pulsatile GnRH secretion. In order to understand the role of GnRH in the early embryos the sites of action can be inferred from the expression of the GnRH receptors in the developing embryos. Much like their ligands, GnRH receptors come in a variety of forms with a bewildering nomenclature that is somewhat inconsistent across groups of animals. GnRH receptors (GnRH-R) are G-protein coupled receptors of the rhodopsin family and are reported to consist of three types: Type I, first isolated from mammalian pituitary, Type II, the cognate receptor for GnRH2, and Type III, isolated in bullfrogs (Wang et al., 2001), and is highly related to the Type II receptor (Millar et al., 2004). It has been proposed that there are three GnRH-R types in fishes to accompany the three ligands (Okubo et al., 2003 and Millar, 2003). More recent phylogenetic analyses suggest that there are three subtypes, by splitting the mammalian Type II GnRH-R into two different groups (Levavi-Sivan and Avitan, 2005 and Millar et al., 2004). But in some reports the Type II and Type III are not clearly divisible phylogenetically and thus fishes are considered to have two GnRH-R types (Moncaut et al., 2005 and Lethimonier et al., 2004). In humans the Type II receptor has a frame shift and internal stop codon making it non-functional, thus it appears that the Type I receptor can bind both ligands (GnRH1 and GnRH2) (Millar et al., 2004). Therefore, for any given receptor multiple GnRH ligands exist (Illing et al., 1999) suggesting a complex regulatory mechanism underlying their activation. In order to determine possible site of action for GnRH decapeptide during early development we examined developmental onset of GnRH-R expression by immunocytochemical and *in situ* hybridization (Figure D.5).

We refer to the GnRH receptors in zebrafish according to Lethimonier (Lethimonier et al., 2004) in which four receptors (one apparently truncated) are present: two Type I (GnRH-R2/GnRH-R4) and two Type II (GnRH-R1/GnRH-R3) receptors. We cloned these GnRH receptors from the zebrafish and analysis of the putative receptors confirms that there are four receptors: two type I receptors (*GnRH-R2*, *GnRH-R4*) and two type II receptors (*GnRH-R1*, *GnRH-R3*; Illing and Whitlock, unpublished data). Using digoxygenin labeled mRNA probes generated against these sequences we were able to detect signal for putative receptor *GnRH-R3* (Type II) and *GnRH-R4* (Type I) at 56 hpf (Figure C.5E and F). Our semi-quantitative PCR data indicate that all four forms of the receptors are expressed starting around 36 hpf (Illing and Whitlock, unpublished data) suggesting that perhaps that the levels of *GnRH-R1* and *GnRH-R2* mRNA are too low to be detected by digoxygenin labeled probes at 56 hpf. This is the first report of *GnRH-R* expression during early development. This onset of *GnRH-R* expression in the developing zebrafish is temporally coincidental with that of the GnRH peptide expression and suggests that the GnRH decapeptides are acting in the early embryo. We also used the ISPR3 antibody reported to recognize medaka GnRH-R Type III (Parhar et al., 2002) but also striped bass/medaka GnRH-R Type I [=GnRH-RIII, in tilapia] (Soga et al., 2005). The ISPR3 antibody recognizes the CLEGKVSHSL motif in extracellular loop 3 which is not conserved in the zebrafish receptors GnRH-R1 and GnRH-R3 (Type II), but does have a related motif in GnRH-R4. Thus, GnRH-R4 is most similar to the motif that was used to raise the antibody. The ISPR3 antibody first recognizes GnRH-R protein at 56 hpf (Figure D.5A–D). The ISPR3 antibody recognizes cells in the pituitary (Figure D.5A and B, arrowheads), clusters of cells lying lateral to

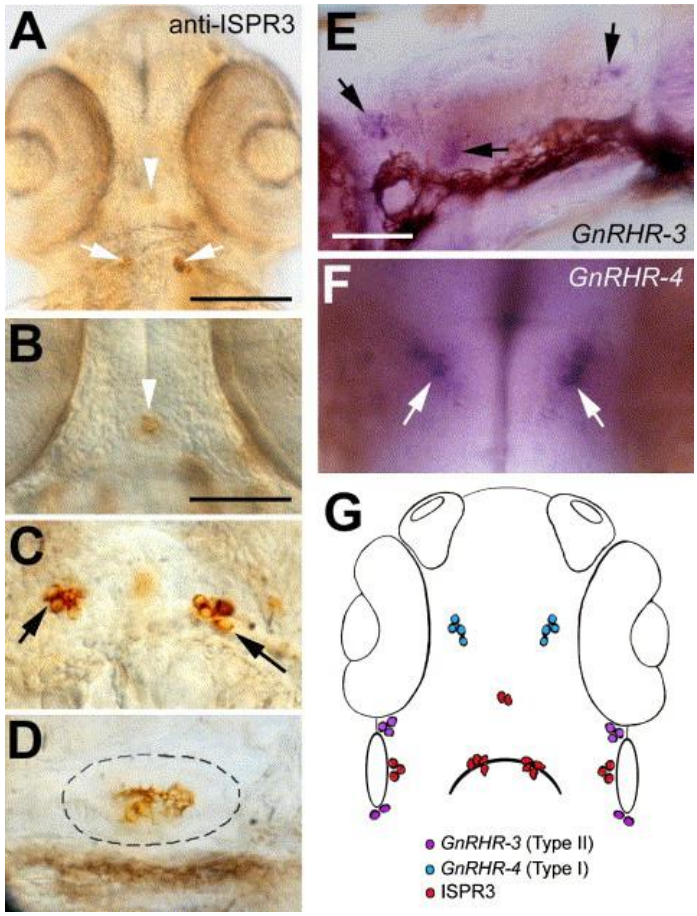

Figure D.5 Expression of GnRH receptors at 56 h post-fertilization: (A–D) Cells labeled with the antibody (ISPR3); (A–C and G) Ventral view with anterior toward the top of the page; (D and E) lateral view with anterior to the left; (F) dorsal view with anterior to the top of the page. By immunocytochemistry cells are lightly labeled in the pituitary (A and B, arrowhead). Cells lying lateral to the developing heart (A and C, arrows), as well as cells associated with the ear (D, dashed line) are labeled. (E and F) *In situ* hybridization with probes against *GnRH-R3* (E) with expression in cranial ganglia, black arrows, and *GnRH-R4* (F) with expression in the putative midbrain tegmentum (F, white arrows). (G) Summary of GnRH-R expression and antibody labeling at 56 hpf. Scale bars: A = 100 μm, B–D = 50 μm, E and F = 50 μm.

the forming heart (Figure D.5A and C, arrows) and cells in the cranial ganglia (Figure D.5D). The pituitary expression was visualized in animals partially lacking pigment (*golden* mutant) and protein expression was very low. In contrast the antibody labeling in the cell lateral to the heart was very strong (Figure D.5A and C, arrows). The labeling in the cranial ganglia was strongest adjacent to the developing otic capsule (Figure D.5D, dashed line). We were not able to detect expression in these tissues during the first 3 days post-fertilization by *in situ* hybridization using the *GnRH-R4* probe suggesting that the message may be too low to detect in these cells or that there may be a fifth GnRH-R as has been reported in *Fugu* (Moncaut et al., 2005). The antibody recognizing the GnRH-R (ISPR3) has previously been reported to label the olfactory epithelium in the cichlid fish (Soga et al., 2005). This we found to be true for zebrafish as well although the labeling was more restricted and specific (Figure D.6). In the adult animal we were able to identify two cell types, large diameter cells in the respiratory epithelium (Figure D.6B, arrow) and smaller, apparently neuron cells in the sensory epithelium (Figure D.6C, arrow). In the reported expression of this receptor protein in the developing olfactory epithelium of cichlid fish there was no apparent division of cell types. Thus the specific expression of the GnRH-R proteins in these cells within the respiratory and sensory epithelia may be a characteristic of the adult animal. Whether the expression of the receptors is functional is hinted at by a recent study using morpholinos to knock-down gene function of *GnRH2* and *GnRH3*. In this study the patterning of midbrain-hindbrain boundary, eye, and pigment are disrupted (Sherwood and Wu, 2005). These results are difficult to interpret because the effects are evident at 24 and 48 hpf, times before any of the GnRH proteins are expressed in zebrafish

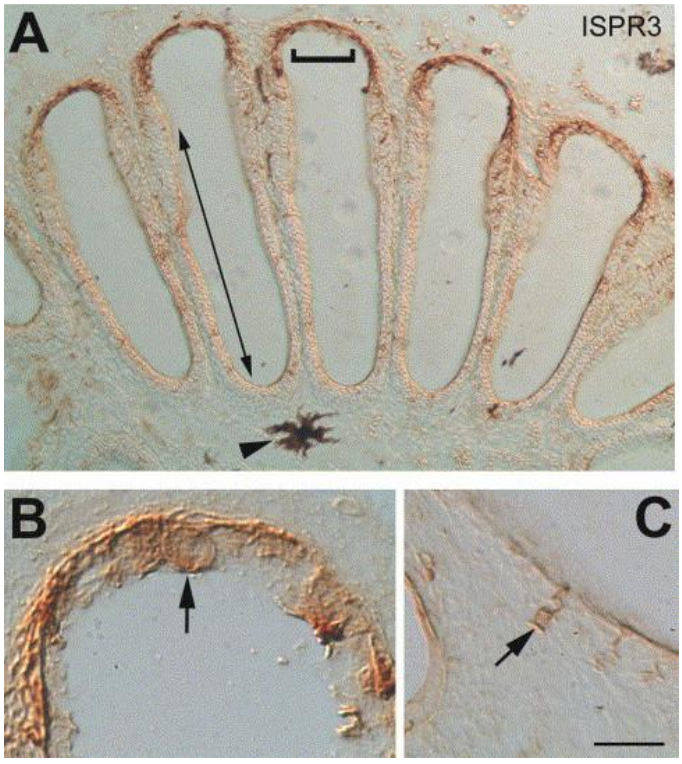

Figure D.6 Antibody labeling of putative of GnRH-R (Type I) in the adult olfactory epithelium. (A) Cross-section of adult olfactory epithelium labeled with ISPR3 antibody. Double-headed arrow indicates the sensory epithelium and bracket the respiratory epithelium. Arrowhead indicates a pigment cell. (B) High magnification view of large diameter (20–25 μm) cells (arrow) in respiratory epithelium. (C) High magnification view of small diameter (10–12 μm) cells (arrow) in sensory epithelium. Scale bar = 25 μm.

(Whitlock et al., 2003 and Gopinath et al., 2004). Additionally the limited distribution of both the GnRH peptides and receptors during early development would suggest such gross defects in morphology may be due to pleiotrophic effects of the morpholinos.

D.8 Endocrine disruptors

To date few investigations have examined the effects of endocrine disruptors on the development of the GnRH systems within vertebrate animals. A recent study in frogs suggests that animals collected from the wild and having abnormal limb formations also had disrupted endocrine profiles. Specifically, relative to the normal appearing animals, the levels of GnRH and androgens were decreased in male frogs with deformed limbs (Sower et al., 2000). Because zebrafish develop outside the mother, have large clutch sizes, readily accessible transparent embryos and have a characterized pattern of GnRH cell development, they hold great potential as a model system to study the effects of endocrine disruptors on early development of the GnRH system in vertebrate embryos.

D.9 Conclusions

The cellular and molecular mechanisms underling the differentiation and migration of GnRH cells in the early embryo are poorly understood. In zebrafish the GnRH cells arise from anterior pituitary and cranial neural crest, regions closely apposed to the precursors of the olfactory placode. Clearly in the case of POMC expressing cells there is mixing across the border separating the anterior pituitary from olfactory placodes hinting at the intimacy of their prior association. This intimate association can be extended to the

precursors of the hypothalamus a field of cells that, like the anterior pituitary, forms through dramatic morphogenesis. In order to better understand the development of GnRH cells we have to work within the context of the dynamic cellular movements that generate the forebrain structures. This type of analysis will allow us to more accurately diagnose GnRH deficits in early development by understanding associated phenotypes. Furthermore the expression of GnRH-Rs during early development suggests that these decapeptides are acting before the brain is terminally differentiated and most likely contributing to the formation of the neural circuits on which GnRH acts during the onset of puberty.

D.10 Acknowledgements

We thank members of the Whitlock lab for helpful discussions, Dr. R. Millar for sending us the lSPR3 antibody, and the organizers of the meeting "*Puberty: A Sensor of Genetic and Environmental Interactions Throughout Development*" for the opportunity to share our work with the larger scientific community. Support: NIH/DC0421801, NIH/HD050820, and New York State Hatch Grant (KEW).

REFERENCES

Aagaard, L, G Laible, P Selenko, et al. 1999. Functional mammalian homologues of the *Drosophila* PEV-modifier Su(var)3-9 encode centromere-associated proteins which complex with the heterochromatin component M31. EMBO J 18:1923-1938.

Aasland, R, AF Stewart. 1995. The chromo shadow domain, a second chromo domain in heterochromatin-binding protein 1, HP1. Nucleic Acids Res 23:3168-3173.

Aruna, S, HA Flores, DA Barbash. 2009. Reduced fertility of *Drosophila* melanogaster *hybrid male rescue (Hmr)* mutant females is partially complemented by *Hmr* orthologs from sibling species. Genetics 181:1437-1450.

Bachtrog, D. 2008. Positive selection at the binding sites of the male-specific lethal complex involved in dosage compensation in *Drosophila*. Genetics. 180:1123-1129.

Bannister, AJ, P Zegerman, JF Partridge, EA Miska, JO Thomas, RC Allshire, T Kouzarides. 2001. Selective recognition of methylated lysine 9 on histone H3 by the HP1 chromo domain. Nature 410:120-124.

Barbash, DA. 2007. Nup96-dependent hybrid lethality occurs in a subset of species from the simulans clade of *Drosophila*. Genetics 176:543-552.

Barbash, DA. 2009. Genetic Testing of the Hypothesis That Hybrid Male Lethality Results From a Failure in Dosage Compensation. Genetics.

Barbash, DA, M Ashburner. 2003. A novel system of fertility rescue in *Drosophila* hybrids reveals a link between hybrid lethality and female sterility. Genetics 163:217-226.

Barbash, DA, P Awadalla, AM Tarone. 2004. Functional divergence caused by ancient positive selection of a *Drosophila* hybrid incompatibility locus. PLoS Biol 2:e142.

Barbash, DA, JG Lorigan. 2007. Lethality in *Drosophila melanogaster*/*Drosophila simulans* species hybrids is not associated with substantial transcriptional misregulation. J Exp Zool B Mol Dev Evol 308:74-84.

Barbash, DA, J Roote, M Ashburner. 2000. The *Drosophila melanogaster* H*ybid male rescue* gene causes inviability in male and female species hybrids. Genetics 154:1747-1771.

Barbash, DA, DF Siino, AM Tarone, J Roote. 2003. A rapidly evolving MYB-related protein causes species isolation in *Drosophila*. Proc Natl Acad Sci USA 100:5302-5307.

Bayes, JJ, HS Malik. 2009. Altered Heterochromatin Binding by a Hybrid Sterility Protein in *Drosophila* Sibling Species. Science.

Belgareh, N, G Rabut, SW Bai, et al. 2001. An evolutionarily conserved NPC subcomplex, which redistributes in part to kinetochores in mammalian cells. J Cell Biol 154:1147-1160.

Belyaeva, ES, LV Boldyreva, EI Volkova, RA Nanayev, AA Alekseyenko, IF Zhimulev. 2003. Effect of the *Suppressor of Underreplication (SuUR*) gene on position-effect variegation silencing in *Drosophila melanogaster*. Genetics 165:1209-1220.

Betancourt, AJ, DC Presgraves. 2002. Linkage limits the power of natural selection in *Drosophila*. Proceedings of the National Academy of Sciences, U.S.A 99:13616-13620.

Bhaskar, V, AJ Courey. 2002. The MADF-BESS domain factor Dip3 potentiates synergistic activation by Dorsal and Twist. Gene 299:173-184.

Biggs, WH, 3rd, KH Zavitz, B Dickson, A van der Straten, D Brunner, E Hafen, SL Zipursky. 1994. The Drosophila *rolled* locus encodes a MAP kinase required in the sevenless signal transduction pathway. EMBO J 13:1628-1635.

Bischof, J, RK Maeda, M Hediger, F Karch, K Basler. 2007. An optimized transgenesis system for *Drosophila* using germ-line-specific φC31 integrases. Proc. Natl. Acad. Sci. U.S.A. 104:3312-3317.

Bolkan, BJ, R Booker, ML Goldberg, DA Barbash. 2007. Developmental and cell cycle progression defects in *Drosophila* hybrid males. Genetics 177:2233-2241.

Brand, AH, N Perrimon. 1993. Targeted gene expression as a means of altering cell fates and generating dominant phenotypes. Development 118:401-415.

Brasher, SV, BO Smith, RH Fogh, D Nietlispach, A Thiru, PR Nielsen, RW Broadhurst, LJ Ball, NV Murzina, ED Laue. 2000. The structure of mouse HP1 suggests a unique mode of single peptide recognition by the shadow chromo domain dimer. EMBO J 19:1587-1597.

Brideau, NJ, HA Flores, J Wang, S Maheshwari, X Wang, DA Barbash. 2006. Two Dobzhansky-Muller genes interact to cause hybrid lethality in *Drosophila*. Science 314:1292-1295.

Cabot, EL, AW Davis, NA Johnson, C-I Wu. 1994. Genetics of reproductive isolation in the *Drosophila simulans* clade: Complex epistasis underlying hybrid male sterility. Genetics 137:175-189.

Carvajal, AR, MR Gandarela, HF Naveira. 1996. A three-locus system of interspecific incompatibility underlies male inviability in hybrids between *Drosophila buzzatii* and *D. koepferae*. Genetica 98:1-19.

Cattani, MV, DC Presgraves. 2009. Genetics and lineage-specific evolution of a lethal hybrid incompatibility between *Drosophila mauritiana* and its sibling species. Genetics 181:1545-1555.

Chatterjee, RN, P Chatterjee, A Pal, M Pal-Bhadra. 2007. *Drosophila simulans Lethal hybrid rescue* mutation (*Lhr*) rescues inviable hybrids by restoring X chromosomal dosage compensation and causes fluctuating asymmetry of development. J Genet. 86:203-215.

Chen, J, J Ding, Y Ouyang, et al. 2008. A triallelic system of *S5* is a major regulator of the reproductive barrier and compatibility of indica-japonica hybrids in rice. Proc Natl Acad Sci U S A. 105:11436-11441.

Christie, P, MR MacNair. 1984. Complementary lethal factors in two North American populations of the yellow monkey flower. J. Hered. 75:510-511.

Cleard, F, M Delattre, P Spierer. 1997. SU(VAR)3-7, a *Drosophila* heterochromatin-associated protein and companion of HP1 in the genomic silencing of position-effect variegation. EMBO J 16:5280-5288.

Cleard, F, P Spierer. 2001. Position-effect variegation in *Drosophila*: the modifier Su(var)3-7 is a modular DNA-binding protein. EMBO Rep 2:1095-1100.

Coyne, JA, B Charlesworth. 1986. Location of an X-linked factor causing sterility in male hybrids of *Drosophila simulans* and *D. mauritiana*. Heredity 57 (Pt 2):243-246.

Coyne, JA, HA Orr. 1989. Patterns of speciation in *Drosophila*. Evolution 43:362-381.

Coyne, JA, HA Orr. 2004. Speciation. Sunderland, MA: Sinauer.

Craig, DaD, NJ. 1998. E. coli ß-galactosidase is heterogeneous with respect to the activity of individual molecules. Can. J. Chem. 76:623-626.

Crosby, MA, JL Goodman, VB Strelets, P Zhang, WM Gelbart. 2007. FlyBase: genomes by the dozen. Nucleic Acids Res. 35:D486-491.

Darwin, C. 1859. On the origin of species by means of natural selection. London,: J. Murray.

de Wit, E, F Greil, B van Steensel. 2005. Genome-wide HP1 binding in *Drosophila*: developmental plasticity and genomic targeting signals. Genome Res 15:1265-1273.

Devlin, RH, B Bingham, BT Wakimoto. 1990. The organization and expression of the *light* gene, a heterochromatic gene of *Drosophila melanogaster*. Genetics 125:129-140.

Dobzhansky, T. 1937. Genetics and the Origin of Species. New York: Columbia University Press.

Dorer, DR, S Henikoff. 1997. Transgene repeat arrays interact with distant heterochromatin and cause silencing in *cis* and *trans*. Genetics 147:1181-1190.

Dover, G. 1982. Molecular drive: a cohesive mode of species evolution. Nature 299:111-117.

Eissenberg, JC, SC Elgin. 2000. The HP1 protein family: getting a grip on chromatin. Curr. Opin. Genet. Dev. 10:204-210.

Eissenberg, JC, TC James, DM Foster-Hartnett, T Hartnett, V Ngan, SC Elgin. 1990. Mutation in a heterochromatin-specific chromosomal protein is associated with suppression of position-effect variegation in *Drosophila melanogaster*. Proc Natl Acad Sci U S A 87:9923-9927.

Estojak, J, R Brent, EA Golemis. 1995. Correlation of two-hybrid affinity data with in vitro measurements. Mol Cell Biol 15:5820-5829.

Fanti, L, M Berloco, L Piacentini, S Pimpinelli. 2003. Chromosomal distribution of heterochromatin protein 1 (HP1) in *Drosophila*: a cytological map of euchromatic HP1 binding sites. Genetica 117:135-147.

Fanti, L, G Giovinazzo, M Berloco, S Pimpinelli. 1998. The heterochromatin protein 1 prevents telomere fusions in *Drosophila*. Mol Cell 2:527-538.

Fanti, L, S Pimpinelli. 2008. HP1: a functionally multifaceted protein. Curr Opin Genet Dev 18:169-174.

Farkas, G, BA Leibovitch, SC Elgin. 2000. Chromatin organization and transcriptional control of gene expression in *Drosophila*. Gene 253:117-136.

Ferree, PM, DA Barbash. 2009. Species-specific heterochromatin prevents mitotic chromosome segregation to cause hybrid lethality in *Drosophila*. PLoS Biol 7:e1000234.

Fields, S, O Song. 1989. A novel genetic system to detect protein-protein interactions. Nature 340:245-246.

Fishman, L, A Saunders. 2008. Centromere-associated female meiotic drive entails male fitness costs in monkeyflowers. Science. 322:1559-1562.

Gatti, M, S Pimpinelli. 1992. Functional elements in *Drosophila melanogaster* heterochromatin. Annu Rev Genet 26:239-275.

Gauhar, Z, Ghanim, M., Herreman, T., Lambert, D.D., Li, T.R., Mason, C., Rifkin, S., Lun, L., White, K.P., Costello, J.C., Andrews, J.R. 2008. *Drosophila melanogaster* life-cycle gene expression dataset and microarray normalisation protocols. Personal Communication to Flybase.

Gietz, DR, RA Woods. 2002. Transformation of yeast by lithium acetate/single-stranded carrier DNA/polyethylene glycol method. Methods in Enzymology: Academic Press. p. 87-96.

Giot, L, JS Bader, C Brouwer, et al. 2003. A Protein Interaction Map of *Drosophila melanogaster*. Science 302:1727-1736.

Girton, JR, KM Johansen. 2008. Chromatin structure and the regulation of gene expression: the lessons of PEV in *Drosophila.* Adv Genet 61:1-43.

Gong, WJ, KG Golic. 2003. Ends-out, or replacement, gene targeting in *Drosophila*. Proc Natl Acad Sci U S A 100:2556-2561.

Good, JM, MD Dean, MW Nachman. 2008. A complex genetic basis to X-linked hybrid male sterility between two species of house mice. Genetics 179:2213-2228.

Graze, RM, LM McIntyre, BJ Main, ML Wayne, SV Nuzhdin. 2009. Regulatory divergence in *Drosophila melanogaster* and *D. simulans*, a genomewide analysis of allele-specific expression. Genetics 183:547-561, 541SI-521SI.

Greil, F, E de Wit, HJ Bussemaker, B van Steensel. 2007. HP1 controls genomic targeting of four novel heterochromatin proteins in *Drosophila*. EMBO J 26:741-751.

Greil, F, I van der Kraan, J Delrow, JF Smothers, E de Wit, HJ Bussemaker, R van Driel, S Henikoff, B van Steensel. 2003. Distinct HP1 and Su(var)3-9 complexes bind to sets of developmentally coexpressed genes depending on chromosomal location. Genes Dev 17:2825-2838.

Groth, AC, M Fish, R Nusse, MP Calos. 2004. Construction of transgenic *Drosophila* by using the site-specific integrase from phage phiC31. Genetics 166:1775-1782.

Grumbling, G, V Strelets, TF Consortium. 2006. FlyBase: anatomical data, images and queries. Nucleic Acids Res. 34: D484-D488; doi:410.1093/nar/gkj1068. http://flybase.org/.

Hadorn, E. 1961. Zur Autonomie und Phasenspezifität der Letalität von Bastarden zwischen *Drosophila melanogaster* und *Drosophila simulans*. Rev. Suisse Zool. 68:197-207.

Heitz, E. 1928. Das Heterochromatin der Moose. Jahrb. Wiss. Bot. 69:762-818.

Heitz, E. 1930. Der Bau der somatischen Kerne von *Drosophila melanogaster*. Z. Indukt. Abstamm. Vererb. 54:248-249.

Henikoff, S, K Ahmad, HS Malik. 2001. The centromere paradox: stable inheritance with rapidly evolving DNA. Science 293:1098-1102.

Hines, KA, DE Cryderman, KM Flannery, H Yang, MW Vitalini, T Hazelrigg, CA Mizzen, LL Wallrath. 2009. Domains of heterochromatin protein 1 required for *Drosophila melanogaster* heterochromatin spreading. Genetics 182:967-977.

Hollocher, H, C-I Wu. 1996. Genetics of reproductive isolation in the *Drosophila simulans* clade: *X vs*. autosomal effects and male *vs*. female effects. Genetics 143:1243-1255.

Huang, Y, MP Myers, RM Xu. 2006. Crystal structure of the HP1-EMSY complex reveals an unusual mode of HP1 binding. Structure 14:703-712.

Hueber, SD, I Lohmann. 2008. Shaping segments: Hox gene function in the genomic age. BioEssays 30:965-979.

Hutchinson, JB. 1932. The genetics of cotton. VII. "Crumpled": a new dominant in Asiatic cottons produced by complementary factors. J. Genet. 25:281-291.

Hutter, P, M Ashburner. 1987. Genetic rescue of inviable hybrids between *Drosophila melanogaster* and its sibling species. Nature 327:331-333.

Hutter, P, J Roote, M Ashburner. 1990. A genetic basis for the inviability of hybrids between sibling species of *Drosophila*. Genetics 124:909-920.

Inoue, A, J Hyle, MS Lechner, JM Lahti. 2008. Perturbation of HP1 localization and chromatin binding ability causes defects in sister-chromatid cohesion. Mutat Res 657:48-55.

Ivanova, AV, MJ Bonaduce, SV Ivanov, AJ Klar. 1998. The chromo and SET domains of the Clr4 protein are essential for silencing in fission yeast. Nat Genet 19:192-195.

Jacobs, SA, S Khorasanizadeh. 2002. Structure of HP1 chromodomain bound to a lysine 9-methylated histone H3 tail. Science 295:2080-2083.

James, TC, SC Elgin. 1986. Identification of a nonhistone chromosomal protein associated with heterochromatin in *Drosophila melanogaster* and its gene. Mol Cell Biol 6:3862-3872.

Jaquet, Y, M Delattre, A Spierer, P Spierer. 2002. Functional dissection of the *Drosophila* modifier of variegation Su(var)3-7. Development 129:3975-3982.

Jenuwein, T, G Laible, R Dorn, G Reuter. 1998. SET domain proteins modulate chromatin domains in eu- and heterochromatin. Cell Mol Life Sci 54:80-93.

Jones, DO, IG Cowell, PB Singh. 2000. Mammalian chromodomain proteins: their role in genome organisation and expression. BioEssays 22:124-137.

Joppich, C, S Scholz, G Korge, A Schwendemann. 2009. Umbrea, a chromo shadow domain protein in *Drosophila melanogaster* heterochromatin, interacts with Hip, HP1 and HOAP. Chromosome Res 17:19-36.

Josefsson, C, B Dilkes, L Comai. 2006. Parent-dependent loss of gene silencing during interspecies hybridization. Curr Biol. 16:1322-1328.

Kalderon, D, BL Roberts, WD Richardson, AE Smith. 1984. A short amino acid sequence able to specify nuclear location. Cell 39:499-509.

Karpen, GH, AC Spradling. 1990. Reduced DNA polytenization of a minichromosome region undergoing position-effect variegation in *Drosophila*. Cell 63:97-107.

Kazianis, S, H Gutbrod, RS Nairn, et al. 1998. Localization of a *CDKN2* gene in linkage group V of *Xiphophorus* fishes defines it as a candidate for the *DIFF* tumor suppressor. Genes Chromosomes Cancer 22:210-220.

Kellum, R, BM Alberts. 1995. Heterochromatin protein 1 is required for correct chromosome segregation in *Drosophila* embryos. J Cell Sci 108 (Pt 4):1419-1431.

Kellum, R, JW Raff, BM Alberts. 1995. Heterochromatin protein 1 distribution during development and during the cell cycle in *Drosophila* embryos. J. Cell Sci. 108:1407-1418.

Kumar, S, K Tamura, M Nei. 2004. MEGA3: Integrated software for Molecular Evolutionary Genetics Analysis and sequence alignment. Briefings in Bioinformatics 5:150-163.

Lachaise, D, JR David, F Lemeunier, L Tsacas, M Ashburner. 1986. The reproductive relationships of *Drosophila sechellia* with *Drosophila mauritiana*, *Drosophila simulans* and *Drosophila melanogaster* from the Afrotropical region. Evolution 40:262-271.

Lazzaro, BP, AG Clark. 2001. Evidence for recurrent paralogous gene conversion and exceptional allelic divergence in the *Attacin* genes of *Drosophila melanogaster*. Genetics. 159:659-671.

Le, MH, D Duricka, GH Karpen. 1995. Islands of complex DNA are widespread in *Drosophila* centric heterochromatin. Genetics 141:283-303.

Lee, H-Y, J-Y Chou, L Cheong, N-H Chang, S-Y Yang, J-Y Leu. 2008. Incompatibility of nuclear and mitochondrial genomes causes hybrid sterility between two yeast species. Cell 135:1065-1073.

Lewis, EB. 1950. The phenomenon of position effect. Adv Genet 3:73-115.

Liu, LP, JQ Ni, YD Shi, EJ Oakeley, FL Sun. 2005. Sex-specific role of *Drosophila melanogaster* HP1 in regulating chromatin structure and gene transcription. Nat Genet 37:1361-1366.

Lohe, AR, PA Roberts. 1988. Evolution of satellite DNA sequences in *Drosophila*. In: RS Verma, editor. Heterochromatin: Molecular and Structural Aspects. Cambridge: Cambridge University Press.

Lu, BY, PC Emtage, BJ Duyf, AJ Hilliker, JC Eissenberg. 2000. Heterochromatin protein 1 is required for the normal expression of two heterochromatin genes in *Drosophila*. Genetics 155:699-708.

Luijsterburg, MS, C Dinant, H Lans, et al. 2009. Heterochromatin protein 1 is recruited to various types of DNA damage. J Cell Biol 185:577-586.

Maheshwari, S, J Wang, DA Barbash. 2008. Recurrent positive selection of the *Drosophila* hybrid incompatibility gene Hmr. Mol Biol Evol 25:2421-2430.

Mallet, J. 2006. What does *Drosophila* genetics tell us about speciation? Trends in Ecology and Evolution 21:386-393.

Maside, XR, JP Barral, HF Naveira. 1998. Hidden effects of *X* chromosome introgressions on spermatogenesis in *Drosophila simulans* x *D. mauritiana* hybrids unveiled by interactions among minor genetic factors. Genetics 150:745-754.

Masly, JP, CD Jones, MA Noor, J Locke, HA Orr. 2006. Gene transposition as a cause of hybrid sterility in *Drosophila*. Science. 313:1448-1450.

Mayr, E. 1963. Animal Species and Evolution: Belknap Press.

McDonald, JH, M Kreitman. 1991. Adaptive protein evolution at the *Adh* locus in *Drosophila*. Nature 351:652-654.

Mihola, O, Z Trachtulec, C Vlcek, JC Schimenti, J Forejt. 2009. A mouse speciation gene encodes a meiotic histone H3 methyltransferase. Science. 323:373-375.

Moyle, LC, EB Graham. 2005. Genetics of hybrid incompatibility between *Lycopersicon esculentum* and *L. hirsutum*. Genetics. 169:355-373.

Mukai, M, Y Hayashi, Y Kitadate, S Shigenobu, K Arita, S Kobayashi. 2007. MAMO, a maternal BTB/POZ-Zn-finger protein enriched in germline progenitors is required for the production of functional eggs in *Drosophila.* Mech Dev 124:570-583.

Muller, H. 1930. Types of visible variatons induced by X-rays in *Drosophila*. J. Genet. 22.

Muller, HJ. 1942. Isolating mechanisms, evolution and temperature. Biol. Symp. 6:71-125.

Nagai, T, K Ibata, E Park, M Kubota, K Mikoshiba, A Miyawaki. 2002. A variant of yellow fluorescent protein with fast and efficient maturation for cell-biological applications. Nat Biotechnol 20:87-90.

Naisbit, RE, CD Jiggins, M Linares, C Salazar, J Mallet. 2002. Hybrid sterility, Haldane's rule and speciation in *Heliconius cydno* and *H. melpomene*. Genetics 161:1517-1526.

Naveira, H, A Fontdevila. 1986. The Evolutionary History of DROSOPHILA BUZZATII. Xii. the Genetic Basis of Sterility in Hybrids between D. BUZZATII and Its Sibling D. SERIDO from Argentina. Genetics 114:841-857.

Nei, M. 1987. Molecular Evolutionary Genetics. New York: Columbia University Press.

Oikemus, SR, N McGinnis, J Queiroz-Machado, H Tukachinsky, S Takada, CE Sunkel, MH Brodsky. 2004. *Drosophila* atm/telomere fusion is required for telomeric localization of HP1 and telomere position effect. Genes Dev 18:1850-1861.

Orr, HA. 1995. The population genetics of speciation: the evolution of hybrid incompatibilities. Genetics 139:1805-1813.

Orr, HA, S Irving. 2000. Genetic analysis of the *Hybrid male rescue* locus of *Drosophila.* Genetics 155:225-231.

Orr, HA, LD Madden, JA Coyne, R Goodwin, RS Hawley. 1997. The developmental genetics of hybrid inviability: a mitotic defect in *Drosophila* hybrids. Genetics 145:1031-1040.

Pal Bhadra, M, U Bhadra, JA Birchler. 2006. Misregulation of sex-lethal and disruption of male-specific lethal complex localization in *Drosophila* species hybrids. Genetics. 174:1151-1159.

Pantazidis, AC, VK Galanopoulos, E Zouros. 1993. An autosomal factor from *Drosophila arizonae* restores normal spermatogenesis in *Drosophila mojavensis* males carrying the *D. arizonae* Y chromosome. Genetics 134:309-318.

Paro, R, DS Hogness. 1991. The Polycomb protein shares a homologous domain with a heterochromatin-associated protein of *Drosophila*. Proc Natl Acad Sci U S A 88:263-267.

Phadnis, N, HA Orr. 2009. A single gene causes both male sterility and segregation distortion in *Drosophila* hybrids. Science 323:376-379.

Pontecorvo, G. 1943. Viability interactions between chromosomes of *Drosophila melanogaster* and *Drosophila simulans*. J. Genet. 45:51-66.

Powers, JA, JC Eissenberg. 1993. Overlapping domains of the heterochromatin-associated protein HP1 mediate nuclear localization and heterochromatin binding. J. Cell Biol. 120:291-299.

Presgraves, DC. 2003. A fine-scale genetic analysis of hybrid incompatibilities in *Drosophila*. Genetics 163:955-972.

Presgraves, DC, L Balagopalan, SM Abmayr, HA Orr. 2003. Adaptive evolution drives divergence of a hybrid inviability gene between two species of *Drosophila*. Nature 423:715-719.

Quackenbush, LS. 1910. Unisexual broods of *Drosophila*. Science 32:183-185.

Ranz, JM, K Namgyal, G Gibson, DL Hartl. 2004. Anomalies in the expression profile of interspecific hybrids of *Drosophila melanogaster* and *Drosophila simulans*. Genome Res. 14:373-379.

Rea, S, F Eisenhaber, D O'Carroll, et al. 2000. Regulation of chromatin structure by site-specific histone H3 methyltransferases. Nature 406:593-599.

Reuter, G, M Giarre, J Farah, J Gausz, A Spierer, P Spierer. 1990. Dependence of position-effect variegation in *Drosophila* on dose of a gene encoding an unusual zinc-finger protein. Nature 344:219-223.

Richards, S, Y Liu, BR Bettencourt, et al. 2005. Comparative genome sequencing of *Drosophila pseudoobscura*: chromosomal, gene, and cis-element evolution. Genome Res. 15:1-18.

Rifkin, SA, J Kim, KP White. 2003. Evolution of gene expression in the *Drosophila melanogaster* subgroup. Nature Genetics 33:138-144.

Rodriguez, MA, D Vermaak, JJ Bayes, HS Malik. 2007. Species-specific positive selection of the male-specific lethal complex that participates in dosage compensation in *Drosophila.* Proc Natl Acad Sci U S A. 104:15412-15417.

Rozas, J, JC Sánchez-DelBarrio, X Messegyer, R Rozas. 2003. DnaSP, DNA polymorphism analyses by the coalescent and other methods. Bioinformatics 19:2496-2497.

Sanchez, L, A Dübendorfer. 1983. Development of imaginal discs from lethal hybrids between *Drosophila melanogaster* and *Drosophila mauritiana*. Roux Arch. Dev. Biol. 192:48-50.

Sawamura, K, T Taira, TK Watanabe. 1993. Hybrid lethal systems in the *Drosophila melanogaster* species complex. - I. The *maternal hybrid rescue* (*mhr*) gene of *Drosophila simulans*. Genetics 133:299-305.

Sawamura, K, M-T Yamamoto. 1997. Characterization of a reproductive isolation gene, *zygotic hybrid rescue*, of *Drosophila melanogaster* by using minichromosomes. Heredity 79:97-103.

Sawamura, K, M-T Yamamoto, TK Watanabe. 1993. Hybrid lethal systems in the *Drosophila melanogaster* species complex. - II. The *Zygotic hybrid rescue* (*Zhr*) gene of *Drosophila melanogaster*. Genetics 133:307-313.

Schotta, G, A Ebert, R Dorn, G Reuter. 2003. Position-effect variegation and the genetic dissection of chromatin regulation in *Drosophila.* Semin Cell Dev Biol 14:67-75.

Schotta, G, A Ebert, V Krauss, A Fischer, J Hoffmann, S Rea, T Jenuwein, R Dorn, G Reuter. 2002. Central role of *Drosophila* SU(VAR)3-9 in histone H3-K9 methylation and heterochromatic gene silencing. EMBO J 21:1121-1131.

Schotta, G, G Reuter. 2000. Controlled expression of tagged proteins in Drosophila using a new modular P-element vector system. Mol Gen Genet 262:916-920.

Schulze, SR, LL Wallrath. 2007. Gene regulation by chromatin structure: paradigms established in *Drosophila melanogaster.* Annu Rev Entomol 52:171-192.

Schwartz, BE, JK Werner, JT Lis. 2003. Indirect Immunofluorescent Labeling of *Drosophila* Polytene Chromosomes: Visualizing Protein Interactions with Chromatin *In Vivo*. Methods in Enzymology 376:393-404.

Schwendemann, A, T Matkovic, C Linke, A Klebes, A Hofmann, G Korge. 2008. Hip, an HP1-interacting protein, is a haplo- and triplo-suppressor of position effect variegation. Proc Natl Acad Sci U S A 105:204-209.

Seum, C, E Reo, H Peng, FJ Rauscher, 3rd, P Spierer, S Bontron. 2007. *Drosophila* SETDB1 is required for chromosome 4 silencing. PLoS Genet 3:e76.

Singh, PB, SD Georgatos. 2002. HP1: facts, open questions, and speculation. J Struct Biol 140:10-16.

Slotman, M, A Della Torre, JR Powell. 2004. The genetics of inviability and male sterility in hybrids between *Anopheles gambiae* and *An. arabiensis.* Genetics 167:275-287.

Smothers, JF, S Henikoff. 2000. The HP1 chromo shadow domain binds a consensus peptide pentamer. Curr Biol 10:27-30.

Spierer, A, F Begeot, P Spierer, M Delattre. 2008. SU(VAR)3-7 links heterochromatin and dosage compensation in *Drosophila.* PLoS Genet. 4:e1000066.

Spierer, A, C Seum, M Delattre, P Spierer. 2005. Loss of the modifiers of variegation Su(var)3-7 or HP1 impacts male X polytene chromosome morphology and dosage compensation. J Cell Sci. 118:5047-5057.

Stephens, GE, EE Slawson, CA Craig, SC Elgin. 2005. Interaction of Heterochromatin protein 2 with HP1 defines a novel HP1-binding domain. Biochemistry 44:13394-13403.

Stolc, V, Z Gauhar, C Mason, et al. 2004. A gene expression map for the euchromatic genome of *Drosophila melanogaster.* Science 306:655-660.

Sturtevant, AH. 1920. Genetic studies of *Drosophila simulans*. I. Introduction. Hybrids with *Drosophila melanogaster*. Genetics 5:488-500.

Sturtevant, AH. 1925. The Effects of Unequal Crossing over at the *Bar* Locus in *Drosophila.* Genetics 10:117-147.

Sun, S, C-T Ting, C-I Wu. 2004. The normal function of a speciation gene, *Odysseus*, and its hybrid sterility effect. Science 305:81-83.

Sweigart, AL, L Fishman, JH Willis. 2006. A simple genetic incompatibility causes hybrid male sterility in *mimulus*. Genetics. 172:2465-2479. Epub 2006 Jan 2416.

Tang, S, DC Presgraves. 2009. Evolution of the Drosophila nuclear pore complex results in multiple hybrid incompatibilities. Science. 323:779-782.

Tao, Y, Z-B Zeng, J Li, DL Hartl, CC Laurie. 2003. Genetic Dissection of Hybrid Incompatibilities Between *Drosophila simulans* and *D. mauritiana*. II. Mapping Hybrid Male Sterility Loci on the Third Chromosome. Genetics 164:1399-1418.

Thompson, JD, DG Higgins, TJ Gibson. 1994. CLUSTAL W: improving the sensitivity of progressive multiple sequence alignment through sequence weighting, position-specific gap penalties and weight matrix choice. Nucleic Acids Res. 22:4673-4680.

Ting, C-T, S-C Tsaur, M-L Wu, C-I Wu. 1998. A rapidly evolving homeobox at the site of a hybrid sterility gene. Science 282:1501-1504.

True, JR, BS Weir, CC Laurie. 1996. A genome-wide survey of hybrid incompatibility factors by the introgression of marked segments of *Drosophila mauritiana* chromosomes into *Drosophila simulans*. Genetics 142:819-837.

Tschiersch, B, A Hofmann, V Krauss, R Dorn, G Korge, G Reuter. 1994. The protein encoded by the *Drosophila* position-effect variegation suppressor gene *Su(var)3-9* combines domains of antagonistic regulators of homeotic gene complexes. EMBO J 13:3822-3831.

Vermaak, D, HS Hayden, S Henikoff. 2002. Centromere targeting element within the histone fold domain of Cid. Mol Cell Biol 22:7553-7561.

Vermaak, D, HS Malik. 2009. Multiple roles for Heterochromatin protein 1 genes in *Drosophila.* Annu Rev Genet 43:467-492.

Vieira, C, D Lepetit, S Dumont, C Biemont. 1999. Wake up of transposable elements following *Drosophila simulans* worldwide colonization. Mol Biol Evol 16:1251-1255.

Watanabe, TK. 1979. A gene that rescues the lethal hybrids between *Drosophila melanogaster* and *Drosophila simulans*. Japanese Journal of Genetics 54:325-331.

Weiler, KS, BT Wakimoto. 1995. Heterochromatin and gene expression in *Drosophila.* Annu Rev Genet 29:577-605.

Wittbrodt, J, D Adam, B Malitschek, W Maueler, F Raulf, A Telling, SM Robertson, M Schartl. 1989. Novel putative receptor tyrosine kinase encoded by the melanoma-inducing *Tu* locus in *Xiphophorus*. Nature 341:415-421.

Wittkopp, PJ, BK Haerum, AG Clark. 2004. Evolutionary changes in *cis* and *trans* gene regulation. Nature. 430:85-88.

Wittrup, KD, JE Bailey. 1988. A single-cell assay of beta-galactosidase activity in *Saccharomyces cerevisiae.* Cytometry 9:394-404.

Yamamoto, M-T. 1992. Inviability of hybrids between *D. melanogaster* and *D. simulans* results from the absence of simulans X not the presence of simulans Y chromosome. Genetica 87:151-158.

Yamamoto, M-T, M Kamo, S Yamamoto, TK Watanabe. 1997. Cytogenetic mapping of the *Lethal hybrid rescue* gene of *Drosophila simulans*. Genes Genet. Systems 72:297-301.

Yang, Z. 1997. PAML: a program package for phylogenetic analysis by maximum likelihood. CABIOS 13:555-556.

Zhimulev, IF. 1998. Polytene chromosomes, heterochromatin, and position effect variegation. Adv Genet 37:1-566.